

UNIVERSITY OF SÃO PAULO  
INSTITUTE OF ARCHITECTURE AND URBANISM OF SÃO CARLOS

MICHELE MARTA ROSSI

Regression models to assess the thermal performance of Brazilian low-cost  
houses: consideration of natural ventilation

São Carlos

2016



MICHELE MARTA ROSSI

Regression models to assess the thermal performance of Brazilian low-cost houses: consideration of natural ventilation

Thesis submitted to the Institute of Architecture and Urbanism of São Carlos of University of São Paulo in partial fulfillment of the requirements for the degree of Master of Science.

Concentration Area:  
Architecture, Urbanism and Technology

Advisor:  
Prof. Dr. Karin Maria Soares Chvatal

Sponsors Agencies:  
Fundação de Amparo à Pesquisa do Estado de São Paulo – FAPESP.

Conselho Nacional de Desenvolvimento Científico e Tecnológico – CNPq.

“Versão corrigida”

São Carlos

2016

I AUTHORIZE TOTAL OR PARTIAL REPRODUCTION OF THIS WORK BY ANY CONVENTIONAL OR ELECTRONIC MEANS, FOR RESEARCH PURPOSES, SO LONG AS THE SOURCE IS CITED.

R867r Rossi, Michele Marta  
Regression models to assess the thermal performance of Brazilian low-cost houses : consideration of natural ventilation / Michele Marta Rossi ; advisor Karin Maria Soares Chvatal. - São Carlos, 2016.

Thesis (MA) - Graduate Program in Architecture and Urbanism and Concentration Area in Architecture, Urbanism and Technology - Institute of Architecture and Urbanism of São Carlos University of São Paulo, 2016.

1. Building performance simulation. 2. Regression model (meta-models). 3. Brazilian low-cost house (LCH). 4. Natural ventilation strategies. 5. Thermal comfort. I. Title.

**FOLHA DE JULGAMENTO**

Candidato(a): Arquiteto e Urbanista Michele Marta Rossi

Título da dissertação: "Regression models to assess the thermal performance of Brazilian low-cost houses: consideration of natural ventilation"

Data da defesa: 28/01/2016

**Comissão Julgadora:**

**Resultado:**

**Profa. Dra. Karin Maria Soares Chvatal (Orientador)**  
(Instituto de Arquitetura e Urbanismo/USP)

APROVADA

**Prof. Dr. Victor Figueiredo Roriz**  
(Faculdade Dom Pedro II)

APROVADA

**Prof. Dr. S. Ranji Ranjithan**  
(North Carolina State University)

APROVADA

Coordenadora e Presidente da Comissão de Pós-Graduação do Programa de Pós-Graduação em Arquitetura e Urbanismo: Profa. Dra. **Cibele Saliba Rizek.**



*To my parents, Laécio Rossi  
and Jussara Rossi, my fortress.*





## ACKNOWLEDGEMENTS

Firstly, I would like to thank **God**, the architect of the universe, for giving me wisdom, strength and faith for I never gave up on my dreams and goals.

To my parents, **Laércio Rossi** and **Jussara Rossi**, for loving me unconditionally, for providing the enough support and also for making me believe that anything is impossible when you have willpower and courage.

To my brother, **Lucas Rossi** who has always shown me that life can be mild and beautiful.

To my grandparents, **Emílio Rossi**, **Jandira Rossi**, **María Ester da Costa** (in memoriam) and **Benedicto da Costa** (in memoriam) for having always encouraged me. To all relatives and close friends who helped me in this journey and also comprehend my absence at some moments.

To **Marcos Almeida**, for believing me and for encouraging me to never give up and also for providing the love and the necessary humour for me complete this work. Thank you for always being by my side!

To **University of São Paulo (USP)** for the structure to develop this research. To **Institute of Architecture of São Carlos (IAU-USP)** where I graduated and also finished this Masters, I would like to thank all the professors who contributed for my academic foundation. To **Marcelo Suzuki** for allowing architectural designs samples and to **Kellen Dornelles** for giving important contributions along this research. To all the staff from IAU-USP and also from USP who help me to complete this work, especially **Pedro Mattia**, **Jose Renato Dibo**, **Marcelo Celestini**, **Mara Lino** and **Marcelo Brocco**.

To my advisor, **Karin Chvatal** for trusting in my work since the college years. For all your dedication, patience, aid and encouragement that were essential for achieving the proposed objectives. No words to thank you!

To **Victor Roriz** who also gave significant improvements in this research and for being always ready to discuss a result. Thank you!

To **North Carolina State University**. For all the staff who worked in the visa documentation. To the professors **S. Ranji Ranjithan**, **David Hill**, **Joseph F. DeCarolis** and **Soolyeon Cho** for receiving me so well, for trusting in my work, for giving significant support and contributions and also for being very involved with this work every single meeting. To the PhD and Master students: **Yifan Yang**, for working hard to develop the programming code in Python, to **Jeffrey Thomas** for also working hard in multivariate regression analyses to develop and to validate the meta-models. To Sedighehsadat (**Nasim**) Mirianhosseinabadi for contributing in early stages of this research. And, finally to **Janelle Hygh** for helping to solve doubts about the methodological process and the parameters selection since the early stages of this research.

I would like to thank all friends and very special people that I met in Raleigh, NC, USA for providing special memories from this internship.

To **Marcelo Suzuki Arquitetura, Boldarini Arquitetos Associados, MMBB Arquitetura e Urbanismo, Lotufo Engenharia, Companhia de Habitação Popular (COHAB) of Curitiba/ PR** in the person of **Roberta Gehr, Caixa Econômica Federal – MT** in the person of **Kátia Alves Barcelos**, and **Sirlene Cheriato** for collaborating with data collection which was very important to develop the base model geometry.

To Professor **Fernando Marques da Silva** for contributing significantly with some natural ventilation issues during the beginning of this research. To **Lefícia Neves** for helping to solve some EnergyPlus doubts. To **Michele Fossati** and **Ana Paula Melo** from CB3E for explaining some questions about natural ventilation modeling on EnergyPlus.

To **Ana Paula Oliveira Favretto** and **Camila Anchieta** for joining with me this meta-model challenge. Working with you was a great experience!

To my close friends **Simone** and **Márcio** for always being by my side!

To all **Pura Ideia Arquitetura team**, especially for **Talita Costa** to be always present in my trajectory.

To my college friends **Paula Jareta, Camila Teixeira, Camila Rocha, Maiara Nicolau, Chen Chien Lin, Tamiris Ferreira, Inah Prado, Yara Bragatto**, and **Amanda Mitre** to be my second family.

To my ArqTeMa family: **Rosilene Brugnera, Ana Paula Favretto, Carol Santesso, Kamila Mendonça, Marieli Lukiantchuki, Héctor Castaño, Pilar Gil** for suggestions, improvements, discussions and the humor that were essential for complete this work. You all are very important to me!

To **Igor Vida** for being a great funny friend and for the English classes and reviews.

To **São Paulo Research Foundation (FAPESP)** for providing the National and International Master scholarships (grant #2013/16768-5 and grant #2014/09225-8, respectively) that provided me enough financial support to conclude this research.

And last, but not least, I would also like to thank the **Conselho Nacional de Desenvolvimento Científico e Tecnológico (CNPq)** for providing a scholarship to financially support the first six months of this research.

## ABSTRACT

ROSSI, M.M. **Regression models to assess the thermal performance of Brazilian low-cost houses: consideration of natural ventilation.** Thesis (Master). Institute of Architecture and Urbanism of São Carlos, University of São Paulo, São Carlos, 2016.

Building performance simulations [BPS] tools are important in all the design stages, mainly in the early ones. However, some barriers such as time, resources and expertise do not contribute to their implementation in architecture offices. This research aimed to develop regression models (meta-models) to assess the thermal discomfort in a Brazilian low-cost house [LCH] during early design. They predicted the degree-hours of discomfort by heat and/or by cold as function of the design parameters' changes for three Brazilian cities: Curitiba/PR, São Paulo/SP, and Manaus/AM. This work focused on using the meta-models to evaluate the impact of the parameters related to natural ventilation strategies on thermal performance in LCH. The analyzed Brazilian LCH consisted in a naturally ventilated representative unit developed based on the collected data. The most influential parameters in thermal performance, namely as key design parameters, were building orientation, shading devices' positions and sizes, thermal material properties of the walls and roof constructive systems as well as window-to-wall ratios (WWR) and effective window ventilation areas (EWVA). The methodology was divided into: (a) collecting projects of Brazilian LCH, and based on that a base model that was able to represent them was proposed, (b) defining the key design parameters and their ranges, in order to compose the design space to be considered, (c) simulating thermal performance using EnergyPlus coupled with a Monte Carlo framework to randomly sample the design space considered, (d) using the greater part of the simulation results to develop the meta-models, (e) using the remaining portion to validate them, and (f) applying the meta-models in a simple design configuration in order to test their potential as a support design tool. Overall, the meta-models showed  $R^2$  values higher than 0.95 for all climates. Except for the regression models to predict discomfort by heat for Curitiba ( $R^2 = 0.61$ ) and São Paulo ( $R^2 = 0.74$ ). In their application, the models showed consistent predictions for WWR variations, but unexpected patterns for EWVA.

**KEYWORDS:** Building performance simulation, Regression models (meta-models), Brazilian Low-cost house [LCH], Natural ventilation strategies, Thermal Comfort.



## RESUMO

ROSSI, M.M. **Modelos de regressão para avaliação do desempenho térmico de habitações de interesse social brasileiras: consideração da ventilação natural.** Dissertação (Mestrado). Instituto de Arquitetura e Urbanismo de São Carlos, Universidade de São Paulo, São Carlos, 2016.

Simulações do desempenho de edificações são ferramentas importantes em todo processo de desenvolvimento do projeto, especialmente nas etapas iniciais. No entanto, barreiras como tempo, custo e conhecimento especializado impedem a implementação de tais ferramentas nos escritórios de arquitetura. A presente pesquisa se propôs a desenvolver modelos de regressão (meta-modelos) para avaliar o desconforto térmico em uma habitação de interesse social [HIS] brasileira. Estes meta - modelos predizem os graus-hora de desconforto por calor ou por frio em função de alterações nos parâmetros de projeto para três cidades brasileiras: Curitiba/PR, São Paulo/SP e Manaus/AM. O foco deste trabalho é o uso dos meta-modelos para avaliar o impacto de parâmetros relacionados com estratégias de ventilação natural no conforto térmico em HIS. A HIS brasileira analisada consistiu em uma unidade representativa, naturalmente ventilada e desenvolvida baseada em dados coletados. Os parâmetros que mais influenciam o conforto térmico, nomeados parâmetros-chave de projeto foram: orientação da edificação, posição e tamanho das proteções solares, propriedades térmicas dos sistemas construtivos das paredes e do telhado, assim como, áreas de janela nas fachadas e áreas efetiva de abertura. A metodologia foi dividida em: (a) coleta de projetos de HIS brasileiras que embasaram a proposição de um modelo-base que os representassem, (b) definição dos parâmetros – chave de projeto e suas faixas de variação, a fim de compor o universo de projeto a ser explorado, (c) simulações térmicas usando o EnergyPlus acoplado com uma ferramenta de Monte Carlo para variar aleatoriamente o universo de projeto considerado, (d) uso da maior parte dos resultados das simulações para o desenvolvimento dos meta-modelos,(e) uso da porção remanescente para a validação dos meta-modelos e (f) aplicação dos meta-modelos em uma simples configuração de projeto, visando testar o seu potencial como ferramenta de suporte de projeto. De modo geral, os meta-modelos apresentaram  $R^2$  superiores a 0,95 para todos os climas, exceto os meta-modelos para prever desconforto por calor para Curitiba ( $R^2 = 0,61$ ) e São Paulo ( $R^2 = 0,74$ ). Na fase de aplicação, os modelos mostraram previsões consistentes para variações na área de janela na fachada, mas incoerências para variações nas áreas efetiva de abertura.

**PALAVRAS-CHAVE:** Simulações do desempenho de edificações, modelos de regressão (meta-modelos), habitações de interesse social [HIS] brasileiras, estratégias de ventilação natural, conforto térmico.



## LIST OF FIGURES

Figure 1: Dissertation outline.....	31
Figure 2: Relationship between the buildings' life cycle and the effectiveness of design decision.....	34
Figure 3: Pressure distribution derived by wind action in buildings.....	44
Figure 4: Wind-driven ventilation.....	44
Figure 5: Cross-ventilation and single-sided ventilation examples.....	46
Figure 6: Influence of Wind Profile and Terrain Characteristics on Local Wind Speed. ....	47
Figure 7: Brazilian Bioclimatic Zones.....	51
Figure 8: AirflowNetwork scheme model in EnergyPlus. ....	56
Figure 9: Relationship between the indoor operative temperature and prevailing mean outdoor air temperature proposed by Adaptive Thermal Comfort Approach of ASHRAE 55 – 2013 for naturally conditioned spaces.....	57
Figure 10: Base model and their variable design parameters. ....	62
Figure 11: Base model geometry with the selected windows distribution.....	66
Figure 12: Qualitative analysis of the selected windows distribution, considering the natural ventilation efficacy by changing the building orientation. ....	67
Figure 13: Building orientations. ....	68
Figure 14: MZM and SZM. ....	68
Figure 15: Annual Air temperature difference between SZM and MZM (each long-stay room) .....	70
Figure 16: Distribution of hourly absolute differences between the predictions of operative temperatures by the different modeling approaches along the year.....	71
Figure 17: Average difference during the year between SZM and MZM in hourly discomfort by heat (A) and by cold (B) .....	71
Figure 18: Building North Axis.....	72
Figure 19: Azimuth Angle of Long Axis of Building.....	72
Figure 20: Roof and walls' systems structures.....	74
Figure 21: Geometric factors of the openings (windows and doors). ....	86
Figure 22: Distribution of number of hours along the year that both models (LOCCp and AVCp) are venting (Case A), none are venting (Case B) and when one is venting and other is not (Case C).....	89
Figure 23: Annual average hourly air changes per hour rate differences between each long-stay room of LOCCp and AVCp models.....	90
Figure 24: Annual average hourly air temperature differences between each long-stay room of LOCCp and AVCp models.....	90

Figure 25: Annual average hourly operative temperature differences between each long-stay room of LOCCp and AVCp models.....	91
Figure 26: Generated IDF files.....	96
Figure 27: Example of a domain file.....	97
Figure 28: Degree hours of discomfort.....	98
Figure 29: Validation of the regression models to predict discomfort by heat and by cold for three Brazilian locations.....	106
Figure 30: Validation of the NZ regression models to predict discomfort by heat for Curitiba and São Paulo, considering all 10 000 data points.....	107
Figure 31: Impact of variation in Window-to-Wall ratios and Effective window ventilation area (ewva) in discomfort by heat in a LCH in Curitiba.....	109
Figure 32: Impact of variation in Window-to-Wall ratios and Effective window ventilation area (ewva) in discomfort by heat in a LCH in São Paulo.....	109
Figure 33: Impact of variation in Window-to-Wall ratios and Effective window ventilation area (ewva) in discomfort by cold in a LCH in Curitiba.....	110
Figure 34: Impact of variation in Window-to-Wall ratios and Effective window ventilation area (ewva) in discomfort by cold in a LCH in São Paulo.....	110
Figure 35: Impact of variation in Window-to-Wall ratios and Effective window ventilation area (ewva) in total discomfort in a LCH in Curitiba.....	110
Figure 36: Impact of variation in Window-to-Wall ratios and Effective window ventilation area (ewva) in total discomfort in a LCH in São Paulo.....	110
Figure 37: Impact of variation in Window-to-Wall ratios and Effective window ventilation area (ewva) in discomfort by heat in Manaus.....	111



## LIST OF TABLES

Table 1: Terrain types roughness coefficients ( $\alpha$ and $\delta$ ) .....	48
Table 2: Window types and the maximum areas for ventilation .....	50
Table 3: Windows sizing to ventilation according to NBR 15220-3.....	52
Table 4: Minimum window areas to ventilation according to NBR 15 575 .....	53
Table 5: Minimum percentages for long-stay rooms' window areas proposed by RTQ-R .....	54
Table 6: Overview of Curitiba/PR climate. ....	59
Table 7: Overview of São Paulo/SP climate.....	60
Table 8: Overview of Manaus/AM climate. ....	61
Table 9: Variable design parameters and their respectively ranges and units. ....	63
Table 10: Base model geometry characteristics.....	64
Table 11: Best solar orientations for Curitiba/PR, São Paulo/SP, and Manaus/AM. ....	66
Table 12: Analyzed simulation cases.....	69
Table 13: Metrics applied to evaluate the results. ....	69
Table 14: Wind Speed Coefficients and description according to terrain type definition .....	73
Table 15: Roof virtual material structures and their properties. ....	75
Table 16: Walls (external and internal) virtual material structures and their properties. ....	75
Table 17: Fixed building materials and constructions systems in simulations.....	76
Table 18: Shading devices characteristics to be considered in simulations. ....	76
Table 19: Occupancy routine for weekdays and weekends in long-stay rooms.....	77
Table 20: Metabolic Rates for each activity and the minimum occupation pattern per room. .....	77
Table 21: Adjustments on occupancy routine for weekdays and weekends in long-stay rooms. .....	78
Table 22: Electric Equipment internal gains. ....	78
Table 23: Lights routines for weekend and weekdays in long-stay rooms and the applied power. ....	79
Table 24: Description of fixed and variable fenestrations. ....	80
Table 25: Description of Window-to-Wall Ratios for the Long-Stay Rooms. ....	80
Table 26: Values for rectangular windows and doors established by RTQ-R for modeling the parameters related with infiltration .....	81
Table 27: Overview of Airflow Network Inputs : Simulation Control.....	82
Table 28: Overview of Airflow Network Inputs: Multizone: Zone.....	83
Table 29: Overview of Airflow Network Inputs: Multizone: Surface.....	83
Table 30: Overview of Airflow Network Inputs: MultiZone: Component: Detailed Opening.....	84
Table 31: Summary of the input data.....	88
Table 32: Input data summary.....	91
Table 33: Output data summary. ....	93
Table 34: Parameter Domain file example. ....	98
Table 35: Performance Metric file example.....	99
Table 36: Original key design parameters.....	102
Table 37: Result Error Analysis. ....	105
Table 38: Fixed and variable parameters for meta-models' application.....	108
Table 39: Frequency of parameters related with natural ventilation in the final regression models.....	111



**LIST OF EQUATIONS**

Equation 1 .....	45
Equation 2 .....	47
Equation 3 .....	57
Equation 4 .....	57
Equation 5 .....	99
Equation 6 .....	99
Equation 7 .....	102



## LIST OF ABBREVIATIONS AND SYMBOLS

°Ch	Degree-Hour
ABNT	Associação Brasileira de Normas Técnicas
ach	air change per hour
AIVC	Air Infiltration Ventilation Centre
AM	Amazonas
ArqTeMa	Architecture, Technology and Materials
AV	Surface-average pressure coefficient values
AVCp	Model with surface-average pressure coefficient
Avg % Error	average percent error
BATH	Bathroom
BDR_1	Bedroom 1
BDR_2	Bedroom 2
BPS	Building Performance Simulation
Cd	Discharge Coefficient
CFD	Computational fluid dynamics
CNPq	Conselho Nacional de Desenvolvimento Científico e Tecnológico
Cp	Pressure Coefficient
C <sub>q</sub>	Air mass flow coefficient
CSV	Comma separated variable
CV (RMESE)	coefficient of variation of root mean square error
DHC	Degree-hours of discomfort by cold
DHH	Degree-hours of discomfort by heat
$D_{c,i}^{M,room}$	Multi Zone Model hourly discomfort by cold for each long-stay room
$D_{c,i}^S$	Single Zone Model hourly discomfort by cold
$D_{h,i}^{M,room}$	Multi Zone Model hourly discomfort by heat for each long-stay room
$D_{h,i}^S$	Single Zone Model hourly discomfort by heat
EERE	Department of Energy Efficiency and Renewable Energy
ENCE	National Energy Conservation Label
EP	EnergyPlus
EPW	EnergyPlus weather file

EWVA	Effective Window Ventilation Area
FAPESP	Fundação de Amparo à Pesquisa do Estado de São Paulo
H	wall height;
HC	Heat Capacity
HIS	Habitação de interesse social
H <sub>met</sub>	height of meteorological station, generally 10 m above the ground;
IDF	Input data file
INMETRO	National Institute of Metrology, Quality and Technology
LCH	Low-cost house
LOC	local pressure coefficient values
LOCCp	Model with local pressure coefficient
Low	Lower comfort limit calculated according ASHRAE 55-2013
LR_KIT	Living room and kitchen
MZM	Multi Zone Model
n	Air mass flow exponent
N	North Axis
NCSU	North Carolina State University
NMBE	normalized mean bias error
NZ	non-zero
PBE	Brazilian Labeling Program
P <sub>d</sub>	dynamic pressure
P <sub>o</sub>	static reference pressure
PR	Paraná
P <sub>x</sub>	static pressure at a determine point on the building façade
R <sup>2</sup>	Coefficient of determination
RMSE	Root mean square error
RTQ-C	Technical Regulation for Energy Efficiency Labelling of Commercial Buildings
RTQ-R	Technical Regulation for Energy Efficiency Labelling of Residential Buildings
SP	São Paulo
SRC	Standardized regression coefficient
SZM	Single Zone Model

$T_{a,i}^{M,room}$	Multi Zone Model hourly air temperature for each long-stay room
$T_{a,i}^S$	Single Zone Model hourly air temperature
$T_{o,i}^{M,room}$	Multi Zone Model hourly operative temperature for each long-stay room
$T_{o,i}^S$	Single Zone Model hourly operative temperature
$T_o$	hourly operative temperature
$T_{OUTDOOR}$	Outdoor air temperature
$T_{pma} (out)$	prevailing mean outdoor air temperature
TPU	Tokyo Polytechnic University
$T_{SETPOINT}$	Set point air temperature
$T_{ZONE}$	Zone air temperature
$U_h$	wind speed
$U_{met}$	the hourly wind speed from a nearby meteorological station;
$U_p$	Upper comfort limit calculated according ASHRAE 55-2013
USP	University of São Paulo
U-value	Thermal Transmittance
WWR	Window-to-Wall Ratio
$\alpha$	exponent for the local building terrain.
$\alpha$	Azimuth Angle of Long Axis of Building
$\alpha$	Solar Absorptance
$\alpha_{met}$	Exponent for the meteorological station;
$\delta$	wind boundary layer thickness for the local building terrain;
$\Delta D_{C^{room}}$	Average difference in discomfort by cold prediction between Single Zone Model and each long-stay room of Multi Zone Model
$\Delta D_{h^{room}}$	Average difference in discomfort by heat prediction between Single Zone Model and each long- stay room of Multi Zone Model
$\delta_{met}$	wind boundary layer thickness for the meteorological station;
$\Delta T_{a^{room}}$	Average difference in air temperature prediction between Single Zone Model and each long-stay room of Multi Zone Model
$\Delta T_{o^{room}}$	Average difference in operative temperature prediction between Single Zone Model and each long-stay room of Multi Zone Model
$\rho$	air density
$\phi$	airflow rate





## SUMMARY

<b>1</b>	<b>INTRODUCTION .....</b>	<b>27</b>
1.1	OBJECTIVES .....	30
1.1.1	General/Overall .....	30
1.1.2	Specifics.....	30
1.2	METHOD OVERVIEW AND DISSERTATION STRUCTURE .....	30
<b>2</b>	<b>LITERATURE REVIEW .....</b>	<b>33</b>
2.1	BUILDING PERFORMANCE SIMULATION TOOLS IN THE BUILDING DESIGN PROCESS .....	33
2.2	MODELS IN BUILDING PERFORMANCE PREDICTION .....	34
2.2.1	Regression Models .....	35
2.2.1.1	Regression Models as Building Performance Prediction Alternative .....	37
2.3	NATURAL VENTILATION IN BUILDINGS: DEFINITION, FUNCTIONALITIES AND REQUIREMENTS....	42
2.3.1	Building Indoor Air Quality .....	43
2.3.2	Thermal Comfort of the Users .....	43
2.3.3	Building Structural Cooling.....	43
2.4	BASIC PRINCIPLES ABOUT WIND DRIVEN NATURAL VENTILATION .....	44
2.4.1	Natural Ventilation Systems: Cross Ventilation and Single-Sided Ventilation .....	46
2.4.2	Building and Environmental Factors Affecting the Wind Driven Ventilation.....	46
2.4.2.1	Openings .....	49
2.5	NATURAL VENTILATION IN BRAZILIAN BUILDING THERMAL PERFORMANCE STANDARDS AND REGULATIONS.....	51
2.5.1	NBR 15220: Thermal Performance in Buildings .....	51
2.5.2	NBR 15575- Residential Buildings – Performance .....	52
2.5.3	RTQ-R: Technical Regulation for Energy Efficiency Labelling of Residential Buildings ...	53
<b>3</b>	<b>DESIGN PROBLEM DEFINITION .....</b>	<b>55</b>
3.1	OVERALL DEFINITIONS .....	55
3.1.1	Simulation Program .....	55
3.1.2	Natural Ventilation Simulation in Energyplus .....	56
3.1.3	Thermal Comfort Evaluation Method .....	56

3.1.4	Weather Analysis .....	58
3.1.4.1	Curitiba/Paraná (Bioclimatic Zone - 01) .....	59
3.1.4.2	São Paulo/São Paulo (Bioclimatic Zone - 03) .....	60
3.1.4.3	MANAUS/AM (BIOCLIMATIC ZONE – 08) .....	61
3.2	BASE MODEL SET-UP AND DESIGN PARAMETER RANGES .....	62
3.2.1	Geometry .....	63
3.2.2	Windows Distribution Definition .....	65
3.2.3	Thermal Zone Definition .....	68
3.2.4	North Axis/ Orientation in the Terrain .....	72
3.2.5	Terrain Type .....	73
3.2.6	Ground Temperature .....	73
3.2.7	Materials Thermal Properties and Construction Systems of Building Opaque Envelope .....	73
3.2.8	Shading Devices .....	76
3.2.9	Internal Gains .....	76
3.2.9.1	Occupancy .....	77
3.2.9.2	Electric Equipment .....	78
3.2.9.3	Lights .....	78
3.2.10	Fenestrations .....	79
3.2.10.1	Window-to-Wall Ratio .....	80
3.2.10.2	Infiltration through Windows Cracks Analysis .....	81
3.2.10.3	Effective Window Ventilation Area .....	81
3.3	NATURAL VENTILATION MODELING .....	81
3.3.1	Airflow Network Inputs .....	82
3.3.2	Impact of Using Surface-Average Instead of Local Wind Pressure Coefficients on the Thermal Comfort Analyses .....	86
3.4	INPUT AND OUTPUT DATA SUMMARY .....	91
<b>4</b>	<b>MONTE CARLO SIMULATION .....</b>	<b>95</b>
4.1	INTRODUCTION .....	95
4.2	MONTE CARLO SIMULATION APPLICATION .....	95

4.2.1	Parameter Files .....	96
4.2.2	Sampling and Substitution Routines and Energyplus Simulations.....	97
4.2.3	Parameter Domains .....	98
4.2.4	Performance Metric .....	98
<b>5</b>	<b>MULTIVARIATE REGRESSION .....</b>	<b>101</b>
5.1	INTRODUCTION.....	101
5.2	REGRESSION MODELS' DEVELOPMENT.....	101
5.3	REGRESSION MODELS' RESULTS AND VALIDATION.....	105
5.4	REGRESSION MODELS' APPLICATION .....	107
<b>6</b>	<b>CONCLUSIONS .....</b>	<b>113</b>
6.1	FURTHER WORK.....	114
<b>7</b>	<b>REFERENCES.....</b>	<b>117</b>
	<b>APPENDIX A - Collected Architectural Designs Classification.....</b>	<b>125</b>
	<b>APPENDIX B - Solar Charts.....</b>	<b>127</b>
	<b>APPENDIX C - Wind Wheels (Seasons) .....</b>	<b>129</b>
	<b>APPENDIX D - Windows and Door Distribution Possibilities in Base Model Geometry .....</b>	<b>131</b>
	<b>APPENDIX E - Ground Temperatures .....</b>	<b>133</b>
	<b>APPENDIX F - Curitiba/PR Meta-model coefficients – Degree-hours of discomfort by cold (standard approach with regression floor) .....</b>	<b>135</b>
	<b>APPENDIX G - Curitiba/PR Meta-model coefficients – Degree-hours of discomfort by heat (standard approach with regression floor) .....</b>	<b>141</b>
	<b>APPENDIX H-Curitiba/PR Meta-model coefficients – Degree-hours of discomfort by heat (Non-zero approach with regression floor) .....</b>	<b>143</b>
	<b>APPENDIX I - São Paulo/SP: Meta-model coefficients – Degree-hours of discomfort by cold (standard approach with regression floor) .....</b>	<b>145</b>
	<b>APPENDIX J - São Paulo/SP: Meta-model coefficients – Degree-hours of discomfort by heat (standard approach with regression floor) .....</b>	<b>149</b>
	<b>APPENDIX K- São Paulo/SP: Meta-model coefficients – Degree-hours of discomfort by heat (Non-zero approach with regression floor) .....</b>	<b>153</b>
	<b>APPENDIX L- Manaus/AM: Meta-model coefficients – Degree-hours of discomfort by heat (standard approach with regression floor) .....</b>	<b>157</b>



## 1 INTRODUCTION

---

Energy resources scarcity is a recurring theme in global actual scenario. For this reason, the architects and engineers' challenge is to emphasize the use of natural resources instead of non-renewable energy sources since the early design stages. Hence, there is a gradual attempt to adapt the buildings to sustainability proposes.

Thermal comfort is a key sustainability aspect that may be incorporated in low-cost houses in developing countries, like Brazil. However, this aspect has been often overlooked in the Brazilian process of housing production for low-income population. The results are standardized houses located in different climate conditions (MONTEIRO; VELOSO; PEDRINI, 2012).

According to Monteiro, Veloso and Pedrini (2012), the design plays an important role in scenarios which the budget is limited. Bittencourt and Cândido (2008) emphasize that low-income population depend on an elaborated design for the thermal comfort maintenance in their respective houses. Therefore, the adoption of bioclimatic strategies during early design as, for example, natural ventilation strategies or constructive systems with good thermal performances may result in greater gains in the final design of low-cost houses [LCH] (MONTEIRO; VELOSO; PEDRINI, 2012).

Bittencourt and Cândido (2008) outline natural ventilation in buildings as an important and social bioclimatic strategy. Once, it is a free resource that ensures thermal comfort for users in urban and architectural spaces. Also, it enables the replacement of the indoor air by fresh air, the buildings' internal and external surfaces cooling as well as the energy savings. As a result, natural ventilation is a significant strategy to ensure good indoor air quality and thermal comfort for users (ALLARD, 2002).

Federal laws and regulations<sup>1</sup> describe construction guidelines and methods to evaluate buildings thermal and energy performances, otherwise these documents show some limitations and also discrepancies among them (BOGO, 2008; CÓSTOLA, 2006; BASTOS; BARROSO-KRAUSE; BECK, 2007; SORGATO, 2009; QUEIROZ et al., 2011 RORIZ, 2012 (a) (b); CHVATAL; RORIZ, 2015). According to NBR 15220: Thermal Performance in Buildings (ABNT, 2005), natural ventilation is indicated as a design strategy in seven of eight bioclimatic zones in which the Brazilian territory is divided. However, there are limitations associated with the recommendations to guarantee this strategy. Furthermore, according to Sorgato (2009) the number of references that discuss building thermal performance simulation of air-conditioned

---

<sup>1</sup> According to the parameters established by NBR 15220: Thermal Performance in Buildings (ABNT, 2005), NBR 15575: Residential Buildings – Performance (ABNT, 2013), and the Technical Regulation for Energy Efficiency Labelling of Residential Buildings (RTQ-R) (INMETRO, 2012).

buildings is notable higher than the naturally ventilated ones. The same author highlights the importance of studying this passive strategy in Brazilian reality, because of the climate, and also the significant amount of buildings that depend strictly on it.

According to Bittencourt and Cândido (2008) natural ventilation consists in the air displacement through the building due pressure differences. Such differences may be generated by the buildings' interior and exterior air temperature differences, the wind impact in buildings' surfaces or also by the coupled processes.

Natural ventilation is a complex phenomenon and hard to be captured by the drawing, which is the traditional way to represent a design (KOWALTOWSKI et al., 1998). This cooling strategy is often characterized by arrows that not represent properly the air movement. Simulation tools are indicated to overcome these limitations (KOWALTOWSKI et al., 2005). However, simulation of natural ventilation is complex and demands, sometimes, computational fluid dynamics knowledge and expensive tools.

Overall, building performance simulation requires time and expertise knowledge to prepare the virtual model, to run the simulations, and also to understand the results. For these reasons, simulation tools are not often applied in design offices (WESTPHAL, 2007). Such tools are frequently used by architects and engineers in the final design to verify an alternative or to evaluate a project that is already concluded (CATALINA; VIRGONE; BLANCO, 2008; HENSEN et al., 2004; HYGH et al., 2012; WESTPHAL, 2007). At this moment, the design changes are remote due the advanced level of buildings' constructive systems and components development (PEDRINI; SZOKOLAY, 2005).

Therefore, it is notable the importance of building performance simulation tools integrate all design phases, mainly in early ones in order to guide the designer's choices for the development of more efficient strategies, providing economic, energy efficiency and thermal comfort gains (MARQUES; REGOLÃO; CHVATAL, 2011; MORBITZER, 2003; SCHLUETER; THESELING, 2009; WESTPHAL, 2007). For this reason, the decision-making process needs to be aware (PETERSEN; SVENDSEN, 2010).

Practical alternatives are the application of simplified simulation methods or simplified user interface (HYGH, 2011). Westphal and Lamberts (2007) argue that sensitivity analysis of parameters and regression equations (generally obtained through numerous simulations) can be very useful in the decision-making process.

The work of Hygh et al. (2012) is an example of regression models developed to aid in the decision-making during the initial phase of the design process. In this work, the EnergyPlus software was coupled with the statistical method of Monte Carlo in order to develop multivariate linear regression models, based on 27 parameters considered relevant during the conceptual design. The geometry modelled was an artificially conditioned office building,

medium-sized, rectangular shape, simulated for four different American bioclimatic zones. In almost all cases, the resulting models presented, for the same input data, a significant match between the results obtained from their application to those obtained by means of robust simulations on EnergyPlus. Other studies pointed the regression analysis as a viable and accurate alternative in prediction of buildings' performances (LAM; HUI; CHAN, 1997; SIGNOR; WESTPHAL; LAMBERTS, 2001; CARLO, 2008; CATALINA; VIRGONE; BLANCO, 2008; LAM et al., 2010; CATALINA; IORDACHE; CARACALEANU, 2013).

In national sphere the prescriptive methods<sup>2</sup> of Technical Regulation for Energy Efficiency Labelling of Commercial Buildings (RTQ-C) (INMETRO, 2009) and Technical Regulation for Energy Efficiency Labelling of Residential Buildings (RTQ-R) (INMETRO, 2012) were generated based on regression analyses in simulation results, regarding the building type. Such equations classify the building energy efficiency level on a scale from A to E, the highest and the lowest efficiency levels, respectively. Both regulations include the natural ventilation in their analyses. While in the first regulation, such strategy is represented as an independent factor in general equation and this data is obtained through simulation, the second one considered simulations of naturally ventilated and artificially air-conditioned buildings in equations' development.

Facing the lack of practical tools in assessing the building thermal performance of naturally ventilated LCH without cooling or heating systems, the presented study proposed to develop regression models (meta-models) to be applied during early design in order to guide designer's choices. Based on Hygh et al. (2012) methodology, such meta-models consisted in regression equations created by a huge amount of simulations ran through the software EnergyPlus. The models' accuracy was verified by comparing, for the same input values, the predictions provided by the regression models and EnergyPlus simulations.

Finally, these regression models may be very important because they are equations and, therefore, can be easily used by designers during the conceptual design stage, offering a more realistic quantitative analysis of the thermal comfort predictions of natural ventilation parameter variation in buildings. As a result, they can be a first step towards to improve the thermal comfort levels in LCH and also to reduce the use of artificial air conditioning in this type of building in Brazil.

---

<sup>2</sup> Prescriptive methods, which assess thermal performance of building envelope.

## 1.1 OBJECTIVES

### 1.1.1 General/Overall

- To develop a set of regression models (meta-models) that are able to evaluate low-cost houses' thermal performance at early design stages adapted to three Brazilian cities (Curitiba/PR, São Paulo/SP, and Manaus/AM), focusing on natural ventilation strategies.

### 1.1.2 Specifics

- To promote and simplify the thermal performance of a Brazilian artificially non-conditioned LCH during the early design stages, focusing on natural ventilation strategies.
- To develop a method to aid in the creation of a meta-model for naturally ventilated Brazilian LCH.
- To contribute to the quality improvement of Brazilian LCH and to the reduction of air conditioning use in this type of building.

## 1.2 METHOD OVERVIEW AND DISSERTATION STRUCTURE

The ultimate goal of this research is to develop a set of regression models for three Brazilian cities – Curitiba/PR, Manaus/AM, and São Paulo/SP – based on EnergyPlus simulation data of a representative naturally ventilated Brazilian LCH. Therefore, these models can be applied independently of the computational program utilized in their development to assess the LCH's thermal discomfort levels during the early design, giving a significant support in decision-making to architects and engineers. Figure 1 illustrates the dissertation outline and its seven chapters.

The first chapter consists in the Introduction that sets the context to the discussion in this research.

The second chapter comprehends the Literature Review. First of all, it presents the limitations and benefits of applying building performance simulation tools during the design process, especially in the early stages. Time, resources and expertise knowledge are highlighted as the biggest barriers for the real implementation of these tools in actual design scenario. Facing these obstacles, the regression models are given as an alternative to building performance predictions in early design. Additionally, national and international studies that applied such models are approached. However, the major part of them refers to air-conditioned instead



of naturally ventilated buildings. The identified gap can be related with the complexity that rules the natural ventilation phenomena and the lack of knowledge by architects and engineers to deal with that rules. As a result, a brief explanation about the natural ventilation definitions, functionalities, and requirements is given, emphasizing the aspects from the building and the environment which most impact the effectiveness of this passive strategy. Finally, natural ventilation evaluation through Brazilian standards and regulations– NBR 15 220, NBR 15 575 and RTQ-R –is shown.

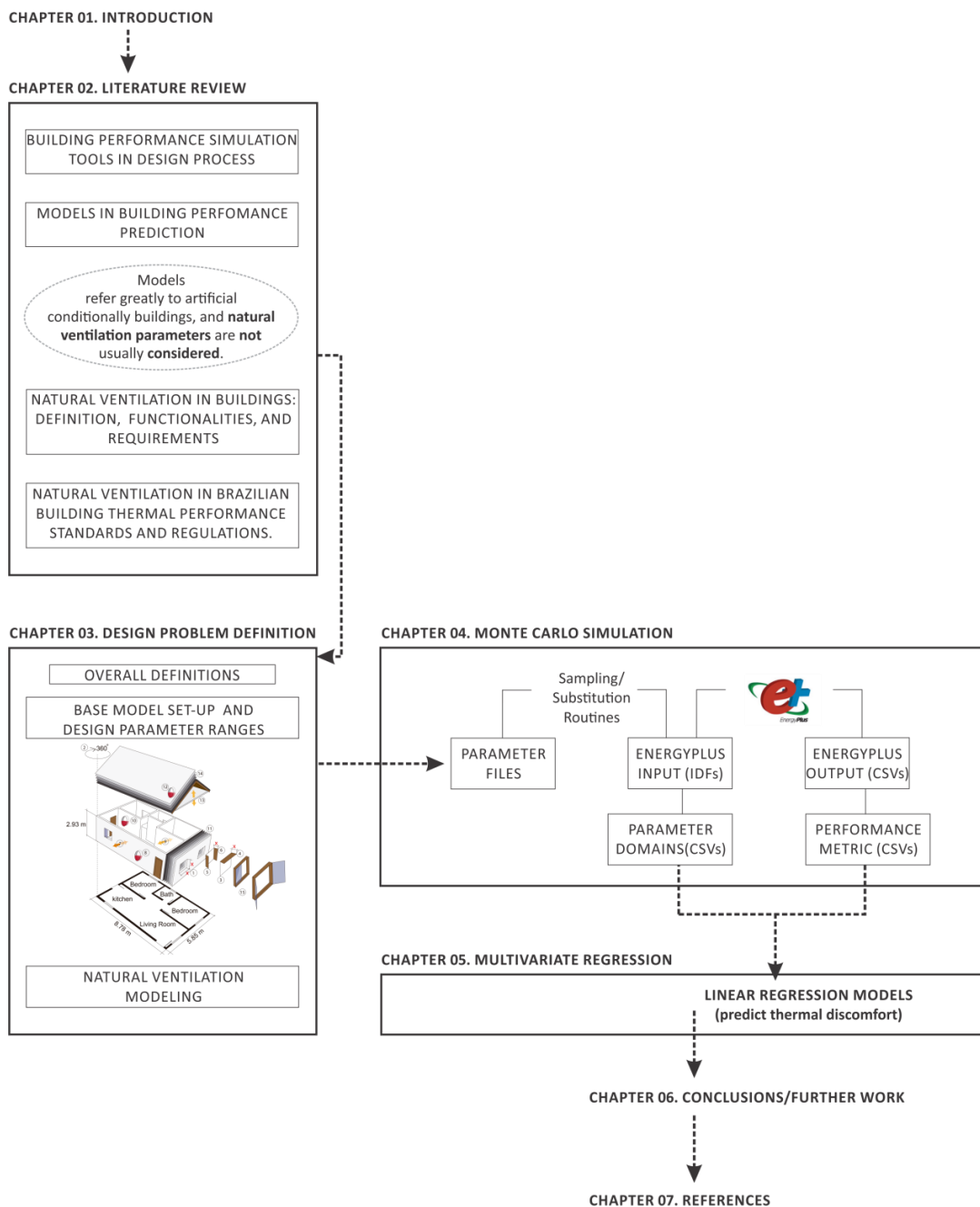


Figure 1: Dissertation outline.

The following three chapters, (3) Design Problem Definition, (4) Monte Carlo Simulation, and (5) Multivariate Regression address the methodology to achieve the research objectives. At the first, Design Problem Definition presents overall definitions such as simulation program, thermal comfort evaluation method and the analyzed climates. It also shows the base model set-up and design parameter ranges, which comprehends the definition of all fixed and variable parameters and their ranges necessary to run an annual building performance simulation. Following, natural ventilation modelling is approached in details.

The chapter 04 comprises the coupling of Monte Carlo (statistical method) to EnergyPlus simulation process, in which the base model and the key design parameter ranges defined – in the previous chapter – are the input of the simulations and their outputs will be based on the following stage namely as Multivariate Regression.

The Multivariate Regression, chapter 05, brings the regression models' development, and their validation. In order to test the regression models' potential as a support tool during the decision-making process, an application is done, regarding common design features. The results and the identified limitations in the meta-models' assessing are described.

Finally, the sections: (6) conclusions and further work, (7) references and appendices are shown.

## 2 LITERATURE REVIEW

---

### 2.1 BUILDING PERFORMANCE SIMULATION TOOLS IN THE BUILDING DESIGN PROCESS

Building Performance Simulation [BPS] tools are an efficient technique to assess the performance of design alternatives (STRUCK; HENSEN, 2007). The application of these tools by the design team can contribute to improve building performance as well as to aid the development and the refinement of guidelines, regulations and standards that guide the new buildings constructions. Hensen et al.(2004) highlight that great improvement in indoor conditions and energy consumption levels could be achieved from an integrated understanding about all systems associated to the building. For this reason, BPS is indicated by these authors as an ideal tool for that approach.

It is observed in current panorama of design practice a concentration of BPS in the final design stages to verify an alternative or to evaluate a design that is already concluded. However, greater gains in costs as well as thermal performance are achieved during the early stages. According to Struck and Hensen (2007), the decision-making are often based on designers' experience or intuition rather than quantitative prediction indicators, as for example, thermal comfort.

Venâncio and Pedrini (2011) emphasize that, although the close relationship between design decisions and building thermal and energy performances are recognized, such decisions have been selected essentially in qualitative information. The architects' choices are based on their own experiences, previously analyzed solutions or generalized recommendations about a determined aspect. Even though these information may result in a quality design, quantitative assessment methods could increase the design support and, consequently, the building performance. Therefore, when BPS is applied in design process, it seeks to improve the information quality that supports the decision-making.

According to Morbitzer (2003) the reality that BPS is used to verification proposes (in the final design stages) instead of a decision-making support (during the early stages) triggers two implications: (a) the flexibility in parameters changes becomes limited, and (b) the impact of decisions in building quality design is reduced (Figure 2).

It is fact that the use of BPS tools in current design practice is limited. This reality is justified by many barriers faced by designer teams for the effective implementation of such tools in the design process. There are among these difficulties: (a) time and knowledge required to characterize the energy model which demands experts, resulting in outsourcing service or in the concentration of these simulation tools in the academic field; (b) high complexity due the innumerous inputs and outputs inconsistent with early design stages when many points have not been defined yet; (c) interoperability difficulties between the process and simulation

programs and the conceptual design; (d) increase in design costs; and (e) difficulties by the designers to understand the results provided by simulation programs (ATTIA et al., 2012; HENSEN et al., 2004; HYGH et al., 2012; PEDRINI; SZOKOLAY, 2005; SCHLUETER; THESSELING, 2009; WESTPHAL; LAMBERTS, 2007). Attia et al. (2012) also recognized that besides the proliferation of BPS in last decade the barriers to integrate them in early design in architectural practice are still high. The majority tools focus on evaluation the design alternatives rather than decision-making supported.

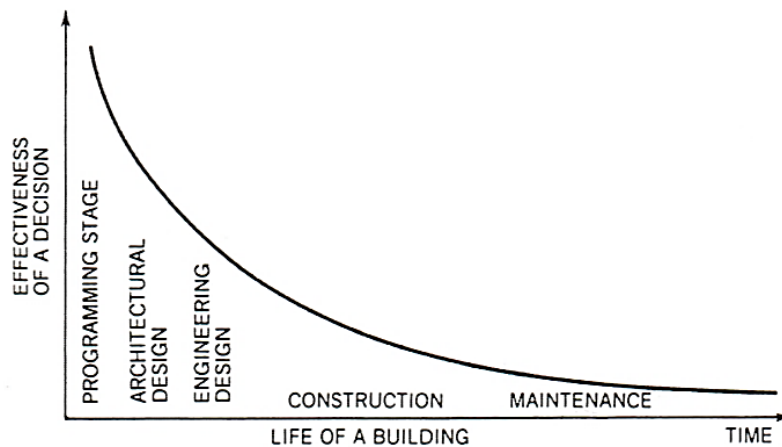


Figure 2: Relationship between the buildings' life cycle and the effectiveness of design decision.  
Source: LECHNER, 2009.

Facing that reality, Hygh (2011) outlines that simplified simulation methods or user interface for detailed simulation software are addressed to enable the building performance analysis during early design. However, while such tools and methods could help the design process by seeking to simplify the building performance simulation, the simplified tools do not capture the whole thermal interactions along the year. They reduce the complex physical processes that governing the building interaction with its environment, and also the input data that describes the building construction characterization and its use (HYGH et al., 2012). Therefore, to recognize how to simplify the methods or the physics processes is a hard task and their simplifications need to be aware and also to keep the accuracy.

## 2.2 MODELS IN BUILDING PERFORMANCE PREDICTION

"Models are entities that represent other entities" (MAHDAVI, 2004, p. 1). Therefore, reduced models could describe highly complex entities, allowing to users to predict and also to explore, in an efficient manner, the original entity's features and behaviors (MAHDAVI, 2004).

Overall, according to Cui et al. (2016) the models may be classified in three groups: physics-based models, data-driven models and hybrid models. The first category consists in models that simulate the individual behavior of a real system's components and also their interactions based on the fundamental physics. Besides describing in fidelity the analyzed system, their development requires a significant computational effort and an expertise knowledge domain. The hybrid modeling combines the physic-based model and statistical tools in order to predict the model's parameters (KRISTENSEN; MADSEN; JØRGENSEN, 2004<sup>3</sup> *apud* Cui et al.; 2016). Finally, the data-driven models, also namely as meta-models, are an approach that permits to model a system based strictly on the data available. The meta-models may be applied for exploring the design space, optimizing the design, what-if analysis, sensitivity analysis, and real-time decisions.

Meta-modeling consists in a modeling of a model and "Meta" means an abstraction from the original concept in order to add or complement it (CUI et al., 2016). Kleijnen; Burg and Ham (1979) outlines that real systems may be modeled using a simulation program. In addition, the relationship between simulations' inputs and outputs can be also modeled in a linear regression model. Therefore, a regression model generated by simulation model may be namely a meta-model (KLEIJNEN, 1992). As regression models may function as an auxiliary model or as a meta-model, the results of simulations can be generalized (KLEIJNEN; BURG; HAM, 1979).

According to Hygh et al. (2012), regression equations may be applied as a meta-model in order to optimize building design. In addition, in an optimization framework they may contribute to reduce the computational effort by replacing the time-consuming and robust simulations.

### 2.2.1 Regression Models

Regression models are examples of reduced models that could aid in building performance prediction. Lam, Hui and Chan (1997) highlight the need of simplified approaches during the early design stages when several design alternatives are considered what making not viable the building performance simulation [BPS] application due costs, time and complexity.

Hygh et al.(2012) proposed reduced models using regression methods and considering parameters commonly explored during conceptual design. The models are an alternative to overcome the barriers caused by the directly work with BPS tools, making the process simpler and easier for designers not experts in simulation. In addition, they can provide a fast quantitative feedback about the analyzed variables and then, be a suitable tool to the early design stages dynamic process.

---

3 KRISTENSEN, N. R.; MADSEN, H.; JØRGENSEN, S.B. A method for systematic improvement of stochastic grey-box models. **Computers and Chemical Engineering**, v.28, p. 1431–1449, 2004.

The rapid feedback about the building performance assessment provided by regression equations could aid architects in the decision-making process since the first design draft definition (WESTPHAL, 2007). According to Catalina, Virgone and Blanco (2008) different prediction models developed from mathematical methods such as Fourier series, regression models and neural network have been proposed by researchers along the years to predict a building's temperature based on weather data. However, those authors emphasize that regression analysis are applied when the objective is to predict a dependent variable (thermal comfort, for example) by independent variables used as input data of the function (e.g. shape factor, window-to-wall ratio, etc.).

Usually, in statistical models there is one variable, the response (or dependent) and the interest is to identify in which manner the explanatory variables (or independent variables) explain the first one (SEBER; LEE, 2003). Therefore, the regression analysis consists in a statistical method applied to relate variables (LAM; HUI; CHAN, 1997) and the main objective is to develop a mathematical model, which better explains those relations. Such models are characterized as simple or multivariate, depending on the number of variables involved, two and more than two, respectively. In addition, these relationships may be linear, when the resulted equation is a line or a plane, or nonlinear, when the equations are exponential, geometric, among others (TORRES, 2007).

In comparison with other methods, as for example, neural networks, regression analysis may be satisfactory when applied to a significant database which is ruled by a constant pattern, resulting in a good fit between the analyzed and predicted data (CATALINA; VIRGONE; BLANCO, 2008). However, the biggest challenge during the models' development consists in identifying the key parameters that will be in the equation (CATALINA; IORDACHE; CARACALEANU, 2013; CATALINA; VIRGONE; BLANCO, 2008; LAM et al., 2010). According to Lam, Hui and Chan (1997), it is essential to have a great knowledge about the physical and operable features of the building for the adequate energy model characterization.

The regression equations could be obtained from regression analysis of a large amount of robust and detailed simulations. Least squares estimates are widely employed when the errors have a normal distribution to impartial estimates of the regression coefficients (SEBER; LEE, 2003). Therefore, the least squares estimation method can be applied to result sets to define a regression trend in which the sum of the squared distances between simulated and analyzed points present a minimum value (TORRES, 2007).

The regression models accuracy may be evaluated by the coefficient of determination ( $R^2$ ) and standard error. The  $R^2$  value means the percentage of the variance in the dependent variable that is explained by the independent variables. As a result, if the  $R^2$  is closer to 1 proves that the equation represents in a reliable manner the dependent variable in function of independent variables and if the values come towards 0, it shows the non-effectiveness of

this equation in translating the relationships between such variables (STAT TREK, s/d). On the other hand, the standard error computes the average amount of overpredicts or underpredicts by the regression equation. In conclusion, it is interesting to have the lowest value for standard error and the highest value for the coefficient of determination (STAT TREK, s/d).

Consequently, after testifying the models accuracy – by comparing the model results to the simulation, for the same input data – they may be used independently of simulation programs applied in their development.

### 2.2.1.1 Regression Models as Building Performance Prediction Alternative

Many scientific studies indicate regression models as a viable and accurate alternative in the building performance predictions (LAM; HUI; CHAN, 1997; SIGNOR; WESTPHAL; LAMBERTS, 2001; CARLO, 2008; CATALINA; VIRGONE; BLANCO, 2008; LAM et al., 2010; HYGH et al., 2012; EISENHOWER et al., 2012; CATALINA; IORDACHE; CARACALEANU, 2013; ASADI; AMIRI; MOTTAHEDI, 2014; AL GHARABLY; DE CAROLIS; RANJITHAN, 2015). The most relevant studies to this research are shown further in a chronological order. It is presented in details the work of Hygh et al. (2012), once it based the methodology applied in this present research.

Lam, Hui and Chan (1997) applied linear and non-linear multiple regression techniques to develop an assessment tool to support the decision-making in early design stages, which predicted the annual energy consumption of a generic and air-conditioned office building in Hong Kong. Over than 300 energy simulations were performed on DOE-2 and the results analysis correlated the energy consumption to 62 parameters used in initial simulations. Twenty-eight from these parameters related with internal gains, air-conditioning and cooling systems that impact in the annual building energy consumption were selected. Sensitivity analyses were conducted in these 28 parameters and 12 of them represented great influence on energy consumption and were include in the models' development. The resulted equations showed a good fit with  $R^2$  values higher than 0.92.

Signor, Westphal and Lamberts (2001) developed reduced models to predict energy consumption of artificially air-conditioned office buildings for 14 Brazilian cities. In previous studies (SIGNOR, 1994) the close relationship between energy consumption and buildings' architectural and constructive features had been verified<sup>4</sup>. Based on that, many variables were considered in VisualDOE2.6 simulations. The simulation results were the input for regression analyses. From those variables, eight were selected to be used in the equations:

---

<sup>4</sup> A reduction of about 30 % in energy consumption without, however, losses on thermal comfort to the users when bioclimatic strategies were considered during the conceptual design.

roof area/total area ratio, facade area/total area ratio, window-to-wall ratio, projecting factor of windows overhangs; roof transmittance; roof absorptance; shading coefficient of glazing, exterior wall transmittance, exterior wall absorptance; and finally internal load density. In general, the developed models showed a good fit between the simulated and predicted data with a  $R^2$  greater than 0.99 for most analyzed cities.

Catalina, Virgone and Blanco (2008) created regression models to predict the monthly heating demand of single-family house sector in temperate climates. The simulations were performed considering 16 French cities that illustrated different climate conditions. The input data for models' development were: the building shape factor, the envelope thermal transmittance, the climate, the building time constant and the window-to-wall ratio. A total of 270 scenarios were analysed and their results based the development of the equations. A maximum deviation of 5.1% when compared predicted and simulated data had proven the models' efficacy in predicting heating demand for this building type in complex scenarios. Those models can be an assessment tool for decision-making during early design in order to better define energy efficient solutions or to enable fast parametric studies for optimizing buildings' aspects.

Lam et al. (2010) elaborated regression models for five Chinese locations, – Harbin, Beijing, Shanghai, Kunming e Hong Kong – which covered a significant climatic variety. The models predicted energy performance of artificially air-conditioned office buildings. They were composed by 12 key design parameters identified<sup>5</sup> through parametric and sensitivity analyses. Such developed models showed a good fit between the data predicted by them against the ones provided by simulations in DOE-2.1 software. The  $R^2$  values varied from 0.89 to 0.97 among the Chinese locations. In conclusion, the authors indicated that these regression models could be used in energy performance comparative studies of the analyzed typology in early design when several alternatives are under consideration.

Motivated by the lack of practical tools on building energy assessment during the early design stages, Hygh et al.(2012) developed multivariate linear regression models utilizing EnergyPlus within a Monte Carlo framework. The models were based on 27 parameters relevant in conceptual design. The geometry was a rectangular, medium-sized, artificially air-conditioned office building. It was simulated for four different American cities: Albuquerque, Miami, Minneapolis and Winston-Salem. The key design parameters and their respective ranges were selected based on two criteria: (1) the parameter impact on energy consumption and (2) the architectural parameter relevance during the early design stages.

To randomly sample the building design space to be explored, Monte Carlo Simulation was applied to generate a statistically representative set of design cases by testing combinations

---

<sup>5</sup> The key design parameters were related to building load, HVAC system, HVAC refrigeration plant.



of parameter values within their established ranges. Perl Scripts updated the IDFs (Input Data Files), identifying the EnergyPlus objects – by name and type – and replaced them. As a result, a set of IDFs equal to the number of samples was generated. Annual simulations were performed on EnergyPlus for each model instance, totalizing 20000 runs. Monte Carlo Simulation results produced a rich database for the regression analyses. The results were divided in two portions: 80% of the samples were randomly selected to regression procedure and the remaining 20% were used to validate the regression equations.

The regression analyses provided approximated equations to estimate the consumption for heating, cooling and total energy. As aforementioned, 80% of the samples were considered in regression analyses in relation to the 27 key design parameters. Some additional terms, which were function of the original parameters, were included to increase the regression models reliability.

After that, Stepwise regressions were conducted to identify and retain which design parameters, considering the original and additional terms, make a contribution to decrease the error. A total of 63 parameters were considered, but 45, 37 and 51 variables to heating, cooling and total annual energy models were used, respectively. The remaining Monte Carlo Simulation results were applied in regression models' validation by comparing the regression model predictions with the simulation results, considering the same input data. The Root mean square error (RMSE),  $R^2$  and average percent error indicated the models' accuracy. A good fit was observed in almost all models – except for heating in Miami – with  $R^2$  higher than 0.96. The results showed the efficacy of these equations in promoting real-time quantitative energy consumption predictions for the base geometry to designers during the early design stages in place of direct simulations.

The Monte Carlo Simulation provided a global sensitivity analysis, however to quantify the individual parameter sensitive, standardized regression coefficients (SRCs)<sup>6</sup> were applied to normalize the coefficients, eliminating the scale parameter and allowing the parameter comparison. In addition, the standardized regression coefficients may provide important information about the individual impact of each parameter on energy consumption, guiding the design choices.

Eisenhower et al. (2012) encompassed in their study the energy models optimization and the benefits of considering this approach. The developed meta-model was based on parametric EnergyPlus simulations of a real high-rise artificially air-conditioned building. Once elaborated, this model had its parameters and scenarios varied without simulation aid and therefore, in a time-saving procedure. This study indicated that minimum energy consumption and the maintenance or improvement of thermal comfort levels may be achieved simultaneously

---

<sup>6</sup> By the standard deviation of the sample.

from adjustments on determining building parameters or scenarios identified by sensitivity analyses.

Asadi, Amiri and Mottahedi (2014), proposed a new model to be applied during the early design to predict energy consumption in commercial buildings. A typical office building in Houston, Texas, USA configured the base model. Occupant schedules, building envelope variables, building orientation and shape described the 17 variable design parameters taking under consideration. Also, this study identified the building's shape as a key parameter in consumption analysis, and for this reason changes were made in base model to develop seven different building geometries. Monte Carlo simulation techniques and the softwares eQUEST and DOE-2 were responsible to produce an amount of 70000 runs (10000 for each building shape). Multiple linear regressions were applied in the generated dataset. All models showed a good fitness with  $R^2$  between 0.94 and 0.95. Finally, standardized regression coefficients were used to identify the parameters that the most and the least influenced in energy consumption, regarding the geometric shape.

Al Gharably, De Carolis and Ranjithan (2015) based on a previous work (HYGH et al., 2012) proposed a model reformulation in order to face the geometric limitation identified in that previous work by including complex geometries. The authors hypothesized that non-rectangular geometries may influence on building heating and cooling loads by increasing the exposed surface area, changing the thermal zoning or producing self-shading effects. Therefore, in order to testify that hypothesis, the study considered three methodological steps. First of all, the original model was systematically tested in predictions of cooling and heating loads of non-rectangular geometries. Secondly, an updated model of Hygh et al. (2012) work was developed based on the original Monte Carlo simulations (HYGH et al., 2012), regarding 30 variable early design parameters derived from those results. Roof area and building wall area by cardinal direction were included as exploratory variables. Finally, the modified model was tested considering four different non-rectangular geometric cases, and after considering a non-rectangular geometry that synthesized all geometric characteristics explored individually in the early tests. In all cases, the model framework was used to predict the cooling and heating loads, regarding the four analyzed locations. Comparisons between EnergyPlus data and models' predictions showed a relative error usually less than 10%.

In the national sphere, in addition to the aforementioned study (SIGNOR; WESTPHAL; LAMBERTS, 2001) others have been developed considering the energy and thermal efficiency of buildings. In 2001, a significant supply crisis occurred in the national energy sector triggered the National Policy Conservation and Rational Use of Energy (BRAZIL, 2001). As consequence, the National Institute of Metrology, Quality and Technology (INMETRO) created the Brazilian Labeling Program (PBE), which was implemented by Technical Regulation for Energy Efficiency Labelling of Commercial Buildings (RTQ-C), and Technical Regulation for Energy

Efficiency Labelling of Residential Buildings (RTQ-R), published in 2009 and 2010, respectively. The last one was updated in 2012.

Both Brazilian Regulations to classify the building energy efficiency level in order to obtain the National Energy Conservation Label (ENCE) show two methods: prescriptive and simulation. In this classification, the systems are evaluated according to their energy efficiency level from A to E, the highest and the lowest efficiency levels, respectively. These Brazilian Regulations prescriptive methods were developed from regression analyses that considered the simulation<sup>7</sup> results, regarding the building type.

The RTQ-C (INMETRO, 2009) categorizes the energy efficient level of commercial buildings on a scale from A to E, considering the efficiency of the systems: envelope, air conditioning and lighting. Regarding envelope system, the RTQ-C shows two methods to evaluate it: the prescriptive and simulation. The prescriptive method to assess thermal performance of building's envelope consists in a set of equations derived by multiple regression analyses on simulation results of the analyzed building type. Three indicators of consumption are calculated by applying these equations: consumption indicator of the analyzed building, minimum and maximum consumption indicators referred to characteristics showed in tables in RTQ-C. Variables as floor area, envelope area, projection area of the building, projection area of the roof, vertical and horizontal shading angles, shape factor, height factor, solar factor, building volume and perceptual of openings in the total of facades characterize such equations. The ventilation integrates the general equation as a numerical equivalent; however it is only obtained through simulation, once the complexity of natural ventilation does not allow the development of general rules in order to evaluate the building thermal comfort (CARLO; LAMBERTS, 2010).

The RTQ-R (INMETRO, 2012) classifies the energy efficiency level of residential buildings<sup>8</sup> in Brazil. This classification evaluates the long-stay rooms (bedrooms and living room) of a unit, considering the thermal performance of the building envelope and the water heating system<sup>9</sup> on a scale from A to E<sup>10</sup>. The thermal performance of the building envelope can be assessed by two methods: the prescriptive and the simulation (SCALCO et al., 2012). The prescriptive method consists in multiple linear regression equations, which predict indicators as relative consumption for cooling and for heating, and cooling degree hours. More than 150000 cases (VERSAGE, 2011) were used to develop the equations. The simulation results consisted in naturally ventilated and artificially air-conditioned buildings, once the use of bioclimatic strategies as natural ventilation was encouraged by this regulation. Such

---

<sup>7</sup> The simulations were performed on EnergyPlus software.

<sup>8</sup> Autonomous housing units, multifamily residential buildings and its common areas.

<sup>9</sup> The water heating system classification was determined according to the evaluation of gas systems, heat pumps, solar heating systems, oil boilers, and electrical resistance.

<sup>10</sup> The systems are evaluated individually and also the overall rating range.

equations comprise four categories of influential parameters in building thermal performance: thermal variables (heat capacity of construction elements, thermal transmittance, solar absorptance), geometric variables (volume, ceiling height, glazed areas, etc.), construction variables (exposure of the roof, contact with soil, shading in the glazed areas, etc.), and finally combined variables that means a combination of geometric and thermal variables. Some limitations of these regression equations as high standard error associate with the method resulted in some imprecisions (SCALCO et al., 2012).

All the aforementioned studies describe regression models to assess the building's thermal comfort or energy consumption. However, such models refer greatly to artificial air-conditioned buildings. Natural ventilation parameters were not usually considered as input in their elaboration. This gap in the scientific literature may be explained by the complexity that governs the natural ventilation phenomenon and the difficulties in finding general rules to represent it.

Etheridge (2012) emphasizes the difficult task to translate the research findings in natural ventilation to design. For this reason, some approximations and assumptions are necessary and it is important that the designer understands the available techniques. Overall, selecting the adequate technique for a design problem demands knowing the important physical aspects considered, but also their limitations.

Therefore, facing these requirements the following section will approach the benefits and functionalities of natural ventilation in buildings.

### **2.3 NATURAL VENTILATION IN BUILDINGS: DEFINITION, FUNCTIONALITIES AND REQUIREMENTS**

Natural ventilation in buildings consists in the buildings' indoor air displacement through openings which may function as inlet or outlet (TOLEDO, 1999). According to Givoni (1976), the conditions to natural ventilation occurrence in indoor spaces are among the key factors that define the health, well-being and comfort of users.

This cooling passive strategy aims to maintain or provide three different aspects, such as: (a) building indoor air quality by ensuring – under all climate conditions – the minimum air indoor replacement by fresh air to guarantee indoor air quality, defining the named health ventilation; (b) thermal comfort of the users by increasing the heat loss from users' bodies to the environment, characterizing the called thermal comfort ventilation; and finally (c) building structure cooling when the indoor temperature is higher than the outdoor, identifying the structural cooling ventilation (GIVONI, 1976).

### 2.3.1 Building Indoor Air Quality

The health ventilation, according to Toledo (2006), seeks to assure the indoor air quality which is measured by the amounts of: oxygen, humidity and pollutants. This type of ventilation consists in ensuring minimum and permanent indoor air changes rates by outdoor fresh air, under all climate conditions, in order to guarantee requirements related to safety, health and well-being of the users (RUAS; LABAKI, 2001).

For these reasons, it is necessary to replace the vitiated air by living processes, occupancy and activities of the users (GIVONI, 1976), removing to exterior components as odours, carbon dioxide, smokes, water vapor, among others. High concentration levels of these components may develop disagreeable situations or even hazardous to the users' health.

Givoni (1976) points out that many countries have stipulated the minimum air changes per hour rates (or cubic meters per hour) for permanent ventilation; however the same author highlights that this minimum requirements in residential housings, in practice, are usually achieved by air infiltration through windows or doors cracks.

### 2.3.2 Thermal Comfort of the Users

The thermal comfort ventilation aims to increase heat loss (by convection or by evaporation) between users' bodies and the environment, removing from the indoor space the excessive heat derived from solar radiation or internal gains (lighting, electronic equipment, occupancy, among others).

Ruas and Labaki (2001) outline that the influence of the air motion in maintenance the users' thermal comfort may be positive or negative. The positive standpoint consists in the increment of heat loss processes between the users' bodies and the environment, improving the thermal comfort. On the other hand, the negative viewpoint occurs when the occupants' whole bodies or only one part of them are cooled excessively, promoting the effect internationally known as draught or when the air collides at high speed with the people, resulting in an undesired movement of clothes, materials, etc.

### 2.3.3 Building Structural Cooling

According to Lechner (2009), the building structural cooling may be achieved by the called night- flush cooling, which provides the introduction of the cool night air through the building, in order to flush out the heat of its surfaces and thereby, minimizing that heat gain to the building, by precooling it for the next day. Allard, Ghiaus and Mansouri (2003) outline that the

heat stored in building's structures during the daytime is function of the internal temperature swing and also the internal thermal inertia. Based on that, these authors indicate this technique application in locations where the outdoor air dew point and the outdoor temperatures are below comfort temperature.

## 2.4 BASIC PRINCIPLES ABOUT WIND-DRIVEN NATURAL VENTILATION

As was aforementioned, natural ventilation is the air displacement through the buildings by inlet and outlet openings (TOLEDO, 1999). The pressure differences – which may be derived from: (a) the wind effect; (b) the natural stack effect; or (c) the coupled effect – are the driven force to enable this behaviour.

The wind mechanical action on buildings generates the pressure differential, which enables the wind driven ventilation or dynamic ventilation as also called by some authors (RIVEIRO, 1985). The kinetic energy of wind that impacts in buildings' facades turns into potential energy (pressure) (ALLARD; GHIAUS; MANSOURI, 2003). According to Frota and Schiffer (2001), the wind is made of lamellar fillets that are moving parallel to the ground surface. When they find an obstacle, as for example a building, they deflect around and above it and after overtaking the building, the wind reassumes its initial direction.

Overall, the pressure differences created in a building by wind action happens as follows (Figure 3): the walls faced to the incoming wind (windward) present pressures over the atmospheric pressure, characterizing then positive pressure zones. On the other hand, the surfaces not exposed to the wind (roof and leeward) are subjected to negative outdoor-indoor pressure differential.

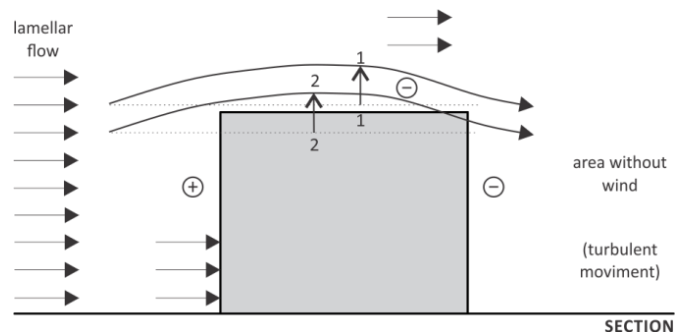


Figure 3: Pressure distribution derived by wind action in buildings. Source: Adapted from FROTA; SCHIFFER, 2001.

Once the pressures on them are lower than atmospheric pressure, they are represented as suction zones (GIVONI, 1976; ALLARD; GHIAUS; MANSOURI, 2003). Based on that, the air configuration through the interior spaces flows from the windward to leeward facades (FROTA; SCHIFFER, 2001).

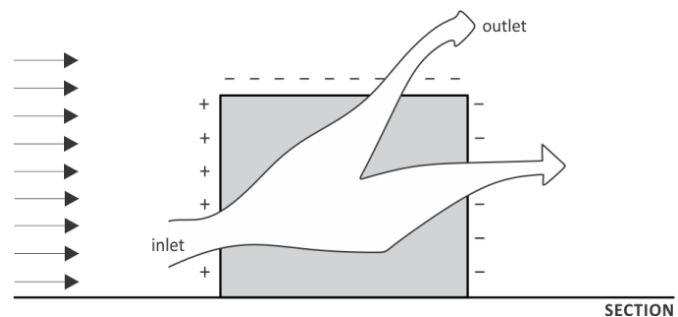


Figure 4: Wind-driven ventilation. Source: Adapted from FROTA; SCHIFFER, 2001.

Thus, the wind-driven ventilation in a space may occur more effectively, if the inlet openings are located in windward and the outlet ones in leeward walls (Figure 4) (OLGYAY, 1998). Consequently, the variations of the pressure distribution on buildings' envelopes are an essential point in this ventilation process (MARQUES DA SILVA, 2010).

According to Toledo (1999) the pressure differential distribution depends on the building shape and dimension and the wind direction, speed and also the angle of incidence. Furthermore, the neighbourhood features such as the proximity of obstacles and the terrain type where the building is located exert an important influence on ventilation by wind-driven.

The wind action on the envelope of the building is expressed by the local wind pressure coefficient ( $C_p$ ), which varies on the building surface. According to Cóstola et al. (2010) the mean (i.e. time-averaged) wind pressure coefficient ( $C_p$ ) is an important parameter in studies that consider ventilation and infiltration and the Equation 1 is often used to define this data:

$$C_p = \frac{P_x - P_o}{P_d} ;$$

$$P_d = \frac{\rho \cdot U_h^2}{2}$$

Where

Px: static pressure at a determine point on the building façade [Pa];

Po: static reference pressure [Pa];

Pd: dynamic pressure [Pa];

$\rho$ : air density [kg/m<sup>3</sup>]

Uh: wind speed [m/s].

Equation 1

Cóstola; Blocken and Hensen (2009) outline that the  $C_p$  data could be obtained by primary sources that are considered more accurate (full-scale measurements, wind-tunnel experiments or computational fluid dynamics programs); or by secondary sources, which are derived from the primary ones as databases (AIVC; ASHRAE) or analytical models (CpCal +, 1992; Swami and Chandra model, 1988; CpGenerator).

Cóstola et al. (2010) emphasize that building energy simulation and airflow network programs usually have a limited  $C_p$  database. For this reason according to those authors, a current assumption is to use surface-average wind pressure coefficient values in place of local pressure coefficients with a high resolution in space. Santamouris and Wouters (2006) emphasize that these coefficients are sensitive to small details of the building, which becomes essential the acquisition of these values for each analyzed case. Allard (2002) highlights the need for further investigations on this variable.

### 2.4.1 Natural Ventilation Systems: Cross Ventilation and Single-Sided Ventilation

When the natural ventilation is thoroughly considered in design, it is also important to verify how it may occur: cross ventilation and single-sided ventilation (Figure 5).

The cross ventilation occurs when the openings are positioned in different building's facades, being the inlet openings in the pressure zones and the outlet ones in the suction zones. On the other hand, the single-sided ventilation



Figure 5: Cross-ventilation and single-sided ventilation examples.

happens when there is only one opening for the air exchange or when the openings (inlet and outlet) are in the same façade; consequently, facing similar pressures or minimal difference (GIVONI, 1976; MELARAGNO, 1982<sup>11</sup> apud TOLEDO, 2001).

The cross ventilation may allow a better use by the wind-drive ventilation (TOLEDO, 1999). However, the single-sided ventilation may present some efficiency to ensure air changes per stack effect<sup>12</sup>, and poor performance for ventilation by wind action, especially when the openings are in low pressure areas (TOLEDO, 2006). According to Kleiven (2003), this ventilation system type has fewer benefits for indoor air quality and thermal comfort, once it presents low air changes values. As the user moves away from the opening, ventilation becomes barely noticeable, emphasizing a low efficiency for cooling in hot periods.

### 2.4.2 Building and Environmental Factors Affecting the Wind-Driven Ventilation

When the wind-driven ventilation strategies are thoroughly considered, direction, velocity, variation and diary and seasonal frequency are very important factors. In order to improve the design by the adoption of these strategies, it is necessary a study about the wind pattern in the analyzed location, its flow around the building. Additionally, the factors in the surrounding that may change the wind initial flow.

General and local, seasonal and momentary factors determine the wind regime. The general and seasonal ones result of the Earth's uneven heating due to the tilt axis relative to the sun, and the unequal distribution of water and land associated with its movement of rotation and translation. In contrast, local and momentary factors include: the topography, the distribution of waters and lands, vegetation and the built environment configuration that generate local

<sup>11</sup> MELARAGNO, M. G. **Wind in architectural and environment design**. U.S.A: Van Nostrand Reinhold, 1982.

<sup>12</sup> Natural stack effect ventilation consists in the air movement generated by the stack effect. It occurs when the temperatures of the ambient and the environment next to it are different, once such ventilation type depends on differences in air densities and also in openings heights. Therefore, the warm air rises and flows out of the ambient and the cooler air flows in (SANTAMOURIS, 2002; ALLARD; GHIAUS; MANSOURI, 2003).



wind regimes: breezes of land and sea, valley winds, slope, plain, and urban winds (TOLEDO, 2006).

Lechner (2009) outlines that air speed increases quickly with height above ground. Consequently, the increased air velocity that varies from zero on the analyzed surface to a velocity equals to the free-obstruction flow, generates the wind velocity gradient (BITTENCOURT; CÂNDIDO, 2008). Thus, this range bounded from air velocity equals to zero to free-obstruction flow is denominated as Atmospheric Boundary Layer (Figure 6) (MATSUMOTO; LABAKI; CARAM, 2011).

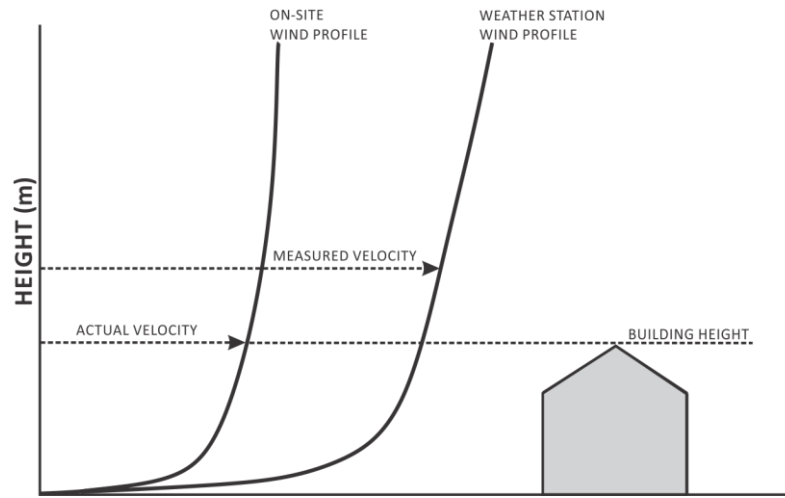


Figure 6: Influence of Wind Profile and Terrain Characteristics on Local Wind Speed. Source: LIDDAMENT, 1996.

Therefore, when natural ventilation strategies are taking under consideration in design process, it is worthwhile to consider the correction of wind speed data (by terrain roughness coefficients) to be used at a reference location (buildings' opening) under study, since the measurements standard are normally done at open field and 10m height above the ground.

To adjust the wind speed data measured in a weather station to the height of building's surfaces, considering the different terrain types, Equation 2 may be applied (ASHRAE, 2001):

$$U_H = U_{met} \left( \frac{\delta_{met}}{H_{met}} \right)^{\alpha_{met}} \left( \frac{H}{\delta} \right)^{\alpha} \quad \text{Equation 2}$$

Where:

- U<sub>H</sub>: Hourly average wind speed at wall height H;
- U<sub>met</sub>: the hourly wind speed from a nearby meteorological station;
- δ<sub>met</sub>: wind boundary layer thickness for the meteorological station;
- H<sub>met</sub>: height of meteorological station, generally 10 m above the ground;

$\alpha_{\text{met}}$ : Exponent for the meteorological station (Table 1);

H: wall height;

$\delta$ : wind boundary layer thickness for the local building terrain (Table 1);

$\alpha$ : exponent for the local building terrain.

Table 1: Terrain types roughness coefficients ( $\alpha$  and  $\delta$ )

TERRAIN COEFFICIENTS	Exponent, $\alpha$	Layer Thickness, $\delta$ (m)
Large city centers, in which at least 50% of buildings are higher than 21 m, over a distance of at least 2000 m or 10 times the height of the structure upwind, whichever is greater	0.33	460
Urban and suburban areas, wooded areas, or other terrain with numerous closely spaced obstructions having the size of single-family dwellings or larger, over a distance of at least 2000 m or 10 times the height of the structure upwind whichever is greater	0.22	370
Open terrain with scattered obstructions having heights generally less than 10 m, including flat open country typical of meteorological station surroundings	0.14	270
Flat, unobstructed areas exposed to wind flowing over water for at least 1.6 km, over a distance of 500 m or 10 times the height of the structure inland, whichever is greater	0.10	210

Source: ASHRAE, 2001.

Natural ventilation efficiency depends also on fixed and variable characteristics of the building. The fixed ones are: layout of the building, open spaces or obstacles in the immediate surroundings, building orientation, its shape, its geometric proportion, interior partitions, the placement of windows (vertical and horizontal), their sizes and types. On the other hand, the variable ones consist in: the wind direction, speed, and frequency and also the differences between interior and exterior air temperatures.

Bittencourt and Cândido (2008) delineate the factors affecting natural ventilation of buildings in two groups: a) buildings' outside factors, and (b) buildings' inside factors. The first ones comprehend the following items: the urban fabric configuration, the arrangement of the building set, the building shape and typology, the roof slope or eave, the presence of fences, walls, and vegetation outside the building. In contrast to that, the second group considers the size, shape, type and placement of the windows, the presence of vertical (fins, structural elements, extension of the walls) or horizontal (eaves, balconies, overhangs) elements, and internal partitions.

### 2.4.2.1 Openings

Bittencourt and Cândido (2008) highlight the window type has to be chosen according to the function of the space, environmental aspects (noise, rain, sun, ventilation and daylighting controls) and other aspects such as security, privacy, cost, aesthetics, and visibility.

The openings are key design parameters to determine the air flow pattern configuration in indoor spaces. However, to ensure their efficacy in natural ventilation systems, it is important to rightly place them, being, as aforementioned, the inlet openings in high-pressure area (windward) and the outlet openings in leeward (low-pressure areas) (OLGYAY, 1998).

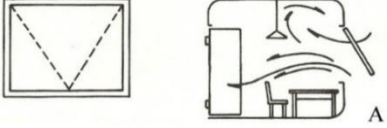
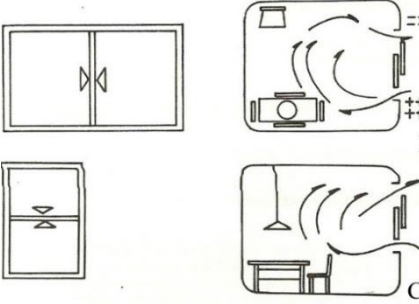
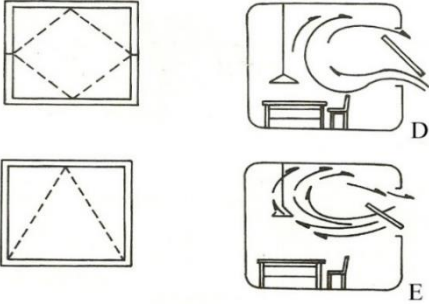
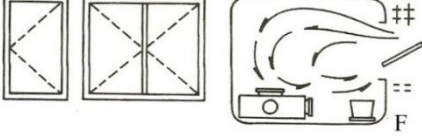
According Mascaró (1991) some key criteria are determined by the window type and its design, such as the effective window ventilation area, the tightness to air and rain, the possibility to split cool and warm air streams and also the possibility to be operable and controlled by the users. Neves (2006) also states that the operable facilities to manipulate these windows by the users as important features, once they promote the flexibility to the users to reduce, change the direction, and the intensity of the air stream when they desired. Based on the presented data, the Table 2 summarizes the windows' types and their effective window ventilation area.

Window shape resists to air stream in inlet and outlet openings, and this resistance is named as discharge coefficient.

In an ideal window all the pressure exerted by the wind is turned into air flow in the opening. On the other hand, a real window, its shape and its position in relation to external air flow may result in a dissipation of energy that hits it. A fraction of this energy is dissipated and another is used for ventilation. Based on that, the discharge coefficient ( $C_d$ ) – dimensionless value that varies from 0 to 1, being the commonly used value 0.6 – represents the useful energy fraction for ventilation (CÓSTOLA, 2006). Overall, Cóstola (2006) and Marques da Silva (2003) highlight the relevance to adopt an adequate value of  $C_d$  for each analyzed situation.

The definition of flow coefficient comprehends the leakage's geometrical characteristics and also the discharge effect. In the physically standpoint, it may be explained as the unitary pressure difference that causes the flow rate (ALLARD; ALVEREZ, 2002). Facing that, Santamouris (2002) highlights that the coefficient flow is related to opening geometry.

Table 2: Window types and the maximum areas for ventilation

WINDOW TYPE		MAXIMUM AREA FOR VENTILATION
	Awning (A)	Minimum
	Sliding and Double-hung (B e C)	50%
	Center Pivot and Hopper (D e E)	Up to 100%
	Casement (F)	Up to 100%

(A)- Awning / (B)- Sliding / (C)- Double-hung / (D)- Center Pivot / (E)- Hopper / (F)- Casement.  
Source: Adapted from ABCI, 1991.

The strong dependence of natural ventilation to environmental conditions as temperature and wind; and also the idea that it is hard to control as it is natural (ALLARD; GHIAUS; MANSOURI, 2003) results in a underestimation of natural ventilation strategies to ensure thermal comfort to the users, mainly in building in hot-humid climates. Facing this reason, Liddament (1996) states measurement data achieved by the application of calculation techniques and numerical models are primordial, once they guarantee means to designer develop and investigate an idea during any design process, before the final design.

## 2.5 NATURAL VENTILATION IN BRAZILIAN BUILDING THERMAL PERFORMANCE STANDARDS AND REGULATIONS

In National scenario there are three main documents – standards or regulations – to be referenced: (a) NBR 15220: Thermal Performance in Buildings (ABNT, 2005); (b) Residential Buildings - Performance (ABNT, 2013); and (c) The Technical Regulations for Energy Efficiency Labelling of Residential Buildings (RTQ-R) (INMETRO, 2012).

### 2.5.1 NBR 15220: Thermal Performance in Buildings

The Standard NBR 15 220: Thermal Performance in Buildings (ABNT, 2005) is divided into five parts<sup>13</sup> and it establishes guidelines and constructive details to improve the adoption of passive cooling strategies in order to optimize the thermal comfort in low-cost houses by adjusting them to the climate conditions, which they belong.

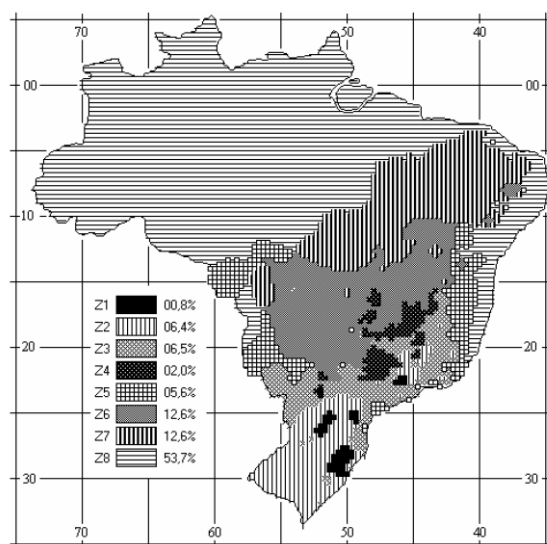


Figure 7: Brazilian Bioclimatic Zones. Source: ABNT, 2005-3.

Such guidelines refer to: (a) effective window ventilation area; (b) shading devices; (c) external walls and roofs systems thermal properties; and finally (d) passive cooling strategies (ABNT, 2005).

Considering an adapted version of Givoni's Bioclimatic Chart (1992), the Standard NBR 15220 (ABNT, 2005) in its third part – Part 3: Brazilian bioclimatic zones and building guidelines for low-cost houses – exhibits the national territory divided into eight bioclimatic zones that are classified by climatic similarities (Figure 7).

Natural ventilation, as aforementioned, is indicated as a passive cooling strategy in 7 of 8 zones that the country is divided (ABNT, 2005). The recommendations vary from permanent cross ventilation along the year, for zone 8; cross ventilation in Summer time, in the zones 2, 3, and 5; and selective ventilation, which means only during hot periods, when the outside temperature is lower than inside, in the zones 4, 6 and 7. Additionally, the referred Standard also indicates the effective window ventilation areas for each bioclimatic zone based on

<sup>13</sup> Part 1: Terminology, symbols and units; Part 2: Calculation methods of thermal transmittance, thermal capacity, thermal delay and solar heat factor of elements and components of buildings; Part 3: Brazilian bioclimatic zones and building guidelines for low-cost houses; Part 4: Measurements of the thermal resistance and thermal conductivity by the guarded hot plate apparatus; and Part 5: Measurement of the thermal resistance thermal conductivity in steady state by the fluximetric method.

floor area percentages, categorizing it in: small ( $10\% < A < 15\%$ ); medium ( $15\% < A < 25\%$ ); and big ( $A > 40\%$ ).

Table 3 summarizes the information of the Standard NBR 15220-3 relates with natural ventilation according to constructive guidelines and strategies.

Table 3: Windows sizing to ventilation according to NBR 15220-3

BIOCLIMATIC ZONES	WINDOWS SIZING TO VENTILATION	PASSIVE COOLING STRATEGIES
01	Medium ( $15\% < A < 25\%$ ) <sup>(1)</sup>	-
02		
03		Cross ventilation during Summer time
04		Selective ventilation
05		Cross ventilation during Summer time
06		
07	Small ( $10\% < A < 15\%$ ) <sup>(1)</sup>	Selective ventilation
08	Big ( $A > 40\%$ ) <sup>(1)</sup>	Permanent cross ventilation

**(1)** The effective window ventilation areas indicated by NBR 15220-3 were calculated based on floor area percentages.

Source: Adapted from ABNT, 2005

### 2.5.2 NBR 15575- Residential Buildings – Performance

The Standard NBR 15575 – Residential Buildings – Performance (ABNT, 2013) was written in 2010, however, only in June 2013, an update version came into force after an extensive review process. Such normative document is divided into six parts<sup>14</sup> and categorizes the building performance according to the following levels: minimum, intermediate, and superior.

The referred Standard is not a prescriptive normative, once it does not inform how the building needs to be built, but establishes a set of qualitative and quantitative requirements to ensure an adequate building performance (CHVATAL; RORIZ, 2015). It does not consider building with air conditioning systems (cooling and heating).

The thermal performance evaluation – considered in parts 1, 4, and 5 of that document – may be done through two methods: simplified or simulation. First of all, it is necessary to check the concordance of building features to the bioclimatic zone that it belongs, according to Brazilian bioclimatic zones proposed by the Standard NBR 15220 (Part 3). After that, the simplified method is applied to evaluate the exterior walls and roof thermal properties (thermal transmittance (U), heat capacity (CT), and solar absorptance (a)) according to the

<sup>14</sup> Part 1: General Requirements; Part 2: Requirements for Structural Systems; Part 3: Requirements for Floor Systems; Part 4: Requirements for Internai and Externai Wall Systems; Part 5: Requirements for Roofing Systems; and Part 6: Requirements for Hydrosanitary Systems.

requirements specified in this document. Also, the effective area to ventilation in the long-stay rooms (bedrooms and living room) may be observed according to Table 4.

Table 4: Minimum window areas to ventilation according to NBR 15 575

PERFORMANCE LEVEL	A= Effective area for ventilation/ floor area x 100 (%)	
	Bioclimatic Zones from 1 to 7	Bioclimatic Zone 8
Minimum	A ≥ 7 %	A ≥ 12 % - Northern region of Brazil A ≥ 8 % - Northeast and Southeast regions of Brazil

Note: In bioclimatic zones from 1 to 6 the window area designated to ventilation must permit to be closed during the cold period.

Source: Adapted from ABNT, 2013.

In the simulation method, the software has to be validated by ASHRAE Standard 140 (ASHRAE, 2014). The geometry must represent reliably the building, with one thermal zone for each room, the constructive systems with their respective thermal properties and the climatic characteristics to enable the evaluation of a typical summer day (for all bioclimatic zones) and a typical winter day (only for the zones from 1 to 5).

Some requirements are given to perform the simulation of natural ventilation, such as: the openings may be considered without obstructions that impact the wind pattern or solar incidence; the ventilation rate should be adjusted to one (1) air change per hour and, if the building thermal performance is below the minimum level during summer time, new simulations must be conducted with a new ventilation rate of five (5) air changes per hour.

### 2.5.3 RTQ-R: Technical Regulation for Energy Efficiency Labelling of Residential Buildings

Technical Regulation for Energy Efficiency Labelling of Residential Buildings (RTQ-R) – published in 2010 and updated in 2012 – proposes classification methods of residential units (single-family, multi-family and common areas of buildings) according to their respective energy consumption labels. It is evaluated by two systems: the building envelope's thermal performance and the water heating systems efficiency. The analyzed buildings receive a National Energy Conservation Label of Brazilian Labelling Program of INMETRO, in a range from A to E, most and least efficient, respectively (INMETRO, 2012). This classification takes under consideration the evaluation of the individual systems and also the overall rating. At the moment, this Label is still optional in the country.

In natural ventilation standpoint, the Regulations indicate minimum effective window ventilation areas for long-stay rooms. Such areas are percentages related with floor areas (Table 5):

Table 5: Minimum percentages for long-stay rooms' window areas proposed by RTQ-R

ROOM	EFFECTIVE WINDOW VENTILATION AREAS (PERCENTAGES RELATED WITH FLOOR AREA (A))		
	Bioclimatic Zones from 1 to 6	Bioclimatic Zone 7	Bioclimatic Zone 8
LONG-STAY ROOMS (bedrooms and living room)	A $\geq$ 8 %	A $\geq$ 5 %	A $\geq$ 10 %

**Note:** In Bioclimatic Zones from 1 to 7 and in the cities that show average monthly of minimum temperatures lower than 20°C, the openings for ventilation must be subject to close during the cold period (except in places where ventilation ensuring the security as gas installations areas).

Source: Adapted from INMETRO, 2012.

The building performance evaluation may be conducted by two procedures: the prescriptive method and the simulation. In both methods only the long-stay rooms are analyzed. Thus, the cooling degree hours and the energy consumption for heating and cooling are the indicators to classify the building's thermal performance and energy efficiency on a scale of A to E. In the prescriptive method the building envelope's performance is calculated based on a numerical equivalent (EqNumEnv), developed through multiple regression analyses (INMETRO, 2012). In computer simulation method, the unit must be modelled with reliable features of construction systems elements, internal gains, natural ventilation occurrence as well as weather conditions.

To simulate naturally ventilated houses, the Regulation recommends to use the EnergyPlus group called AirflowNetwork. It is counselled to model all openings and to adjust the wind speed profile exponent ( $\alpha$ ) to 0.33, which characterizes an urban terrain type; the discharge coefficients ( $C_d$ ) of rectangular doors and windows to 0.6; the air mass flow coefficient when opening is closed ( $C_Q$ ) to 0.001 kg/s.m; and the air mass flow exponent ( $n$ ) to 0.65. Finally, if a ventilation control mode is desired, it is indicated to adopt a control by temperature or enthalpy (INMETRO, 2012).



### 3 DESIGN PROBLEM DEFINITION

---

This chapter is divided in four subparts: (a) Overall definitions; (b) Base Model Set-Up and Design Parameter Ranges, (c) Natural Ventilation Modeling, and finally (d) Input and Output Data Summary.

#### 3.1 OVERALL DEFINITIONS

This part comprises the simulation program features, including natural ventilation modeling, the thermal comfort evaluation method, and finally a weather analysis of the selected cities.

##### 3.1.1 Simulation Program

EnergyPlus [EP] 8.1 (EERE, 2014a) was the selected simulation program. This software is developed and distributed by U.S. Department of Energy and validated by ASHRAE 140 (ASHRAE, 2014). EP is a robust and accurate tool, which avoids additional uncertainties introduced by simple algorithms and for this reason can be applied in a more detailed conception (HYGY, 2011). This software simulates the heat exchanges of the analyzed building. Also, it allows the modeling of conditioning systems (heating or cooling), lighting (natural or artificial), ventilation (natural or mechanical), among others (EERE, 2014b).

Its advantages include a significant documentation, the availability to use it in different computer operating systems and the use of input and output data in text format, which facilitates an automated work flow (HYGY, 2011). It has as options the EP-Launch and the IDF Editor in order to facilitate this interface to users not familiar with programming language and also with the software. The input files can be created and edited in IDF Editor. The files are automatically generated as .idf (input data file). The EP-Launch manages the simulations, permitting the user to select one idf file and one weather file .epw (EnergyPlus weather file). Brazil has a significant climate database with EPWs generated, recently, for 411 cities (RORIZ, 2013 c).

Considering the output files, the software presents a sort of them; however the main ones are the thermal loads, the interior temperature and the energy consumption of the analyzed building. The results could come in CSV (comma separated variable) files that may be easily open as a workbook in Excel®.

### 3.1.2 Natural Ventilation Simulation in Energyplus

Natural ventilation was modeled in Airflow Network group in EnergyPlus<sup>15</sup>. It permits to simulate airflows due to wind action or forced by any air distribution system (EERE, 2014b). The Airflow Network model can be considered simple when compared to CFD (computational fluid dynamics) ones. It consists in a grid that is formed by pressure nodes that represent the simulated zones and the exterior environment (Figure 8) (SANTAMOURIS, 2002).

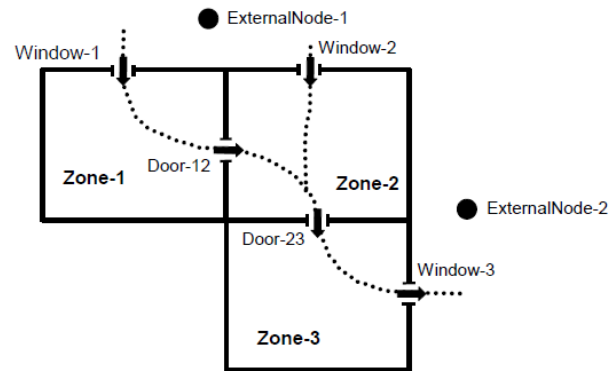


Figure 8: AirflowNetwork scheme model in EnergyPlus. Source: EERE, 2014 b.

The interaction between the nodes occurs by flow paths such as windows, doors and cracks, which determine the airflow. The external nodes pressures are known based on calculations using the wind data from the Energy Plus Weather file (EPW). And, the interaction between external and internal nodes allows the calculation of unknown pressures by applying the mass balance equation at each node. Therefore, the airflow rate may be determined, once it is function of pressure differences (SANTAMOURIS, 2002).

Also, this group enables to define a ventilation control mode to rule the thermal zones and openings surfaces (windows and doors) and to describe in details the parameters that influence the natural ventilation pattern for each linkage surface.

Main outputs are: the number of air changes per hour and heat losses or gains due to ventilation.

### 3.1.3 Thermal Comfort Evaluation Method

Thermal comfort evaluation method was based on the Adaptive approach of American Standard ASHRAE 55 – 2013<sup>16</sup> (ASHRAE, 2013), which comprises acceptable thermal conditions for naturally ventilated buildings.

The adaptive model gives an important role to factors beyond physics and physiological in determining the thermal preferences of the building's users (DE DEAR; BRAGER, 2002). An "adaptive theory" assumes that outdoor temperature variations rule the thermal comfort

<sup>15</sup> EnergyPlus airflow network model was based on AIRNET (WALTON, 1989) and COMIS (FUESTEL et al., 1990).

<sup>16</sup> Applicable to naturally ventilated spaces that meet the following requirements: (a) there is not air conditioning system (cooling or heating); (b) users have metabolic rates between 1 and 1.3 met; (c) users with free clothing choices with variations between 0.5 and 1.0 clo and (d) mean outdoor temperature between 10° C a 33.5° C (50°F a 92.5°F, respectively) (ASHRAE, 2013).

expectations of the users inside the buildings and then, the indoor temperature may be altered facing the regular season's temperature differences (FIGUEIREDO; FROTA, s/d). Consequently, the adaptive approach consists in recognizing that population from hotter regions may tolerate higher temperatures comparing with populations originated from cooler locations and vice versa (RORIZ; CHVATAL; CAVALCANTI, 2009). Figure 9 illustrates the relationship between the buildings' operative temperature<sup>17</sup> and the prevailing mean outdoor air temperature (tpma (out))<sup>18</sup>. Equation 3 and Equation 4 (ASHRAE, 2013) show the lower and the upper comfort limits, considering the 80% of acceptability. Tpma (out) is the average outdoor temperature of the 15 sequential days prior to the analyzed day. Consequently, the comfort range is established by the lower and upper limits and the adaptive comfort temperature is determined by the sum or subtraction from those tolerances of 3.5°C. The adaptive comfort temperature is applied as set point in natural ventilation modeling and their monthly average values for each selected Brazilian city are shown in 3.1.4. Weather Analysis.

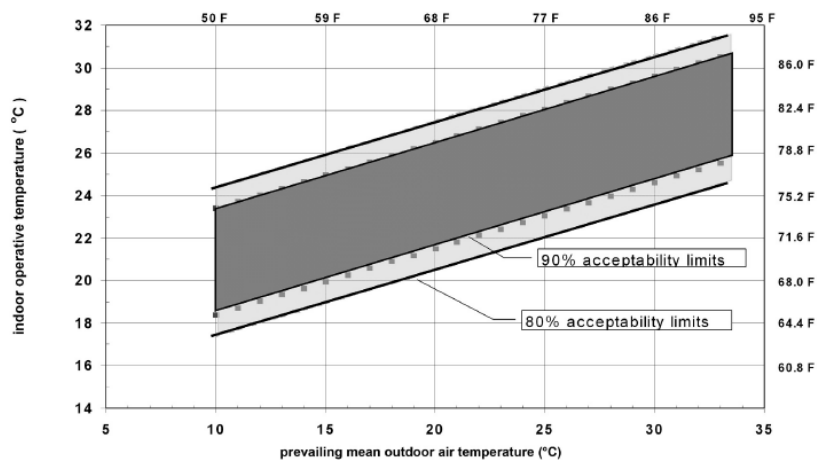


Figure 9: Relationship between the buildings' indoor operative temperature and prevailing mean outdoor air temperature proposed by Adaptive Thermal Comfort Approach of ASHRAE 55 – 2013 for naturally conditioned spaces. Source: ASHRAE, 2013.

- Lower 80% acceptability limit (°C) = 0.31 tpma (out) + 14.3                      Equation 3
- Upper 80% acceptability limit (°C) = 0.31 tpma (out) + 21.3                      Equation 4

<sup>17</sup> Arithmetic average between Air Temperature and Radiant Temperature.

<sup>18</sup> Simple arithmetic average of mean daily outdoor air temperature (tpma (out)) according the sequential days prior to the analyzed day. This sequence needs to be no fewer than 7 and no greater than 30 days (ASHRAE, 2013).

### 3.1.4 Weather Analysis

The selection of Brazilian cities for where the regression models were developed followed these criteria:

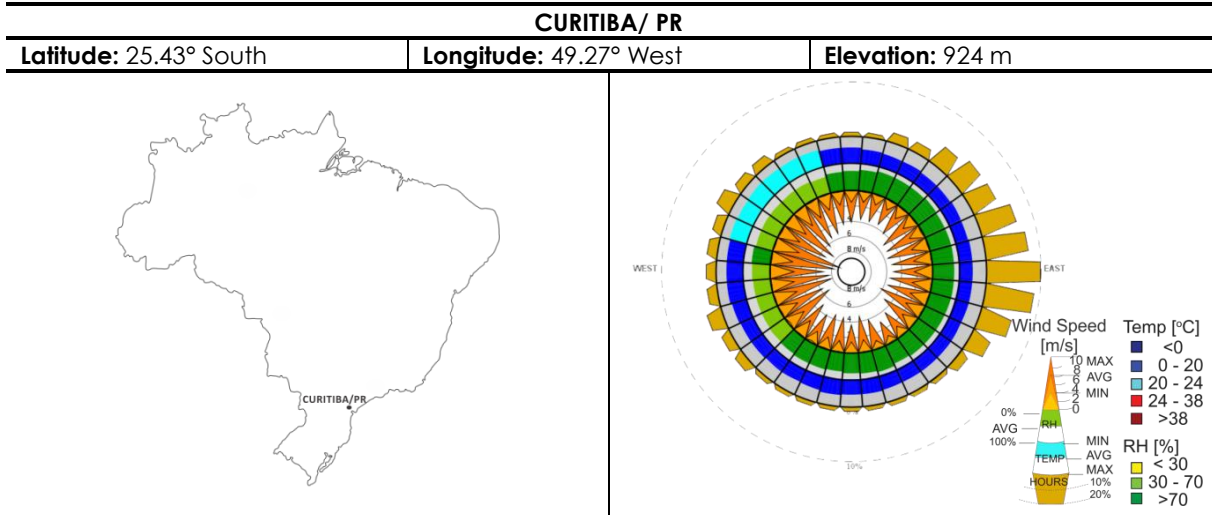
- a) The cities must belong to different states and bioclimatic zones, according to the Brazilian standard NBR 15 220: Thermal Performance in Buildings (ABNT, 2005).
- b) They must be capitals.
- c) They must be one of the 411 Brazilian cities with an available EPW weather file (RORIZ, 2013c).

As a result, three capitals were selected: Curitiba/PR (bioclimatic zone - 01), São Paulo/SP (bioclimatic zone - 03) and Manaus/AM (bioclimatic zone - 08). Therefore, the Brazilian climate variety was covered by the inclusion of one of the coldest (Curitiba/PR), the intermediate (São Paulo/SP) and the warmest (Manaus/AM) climates.

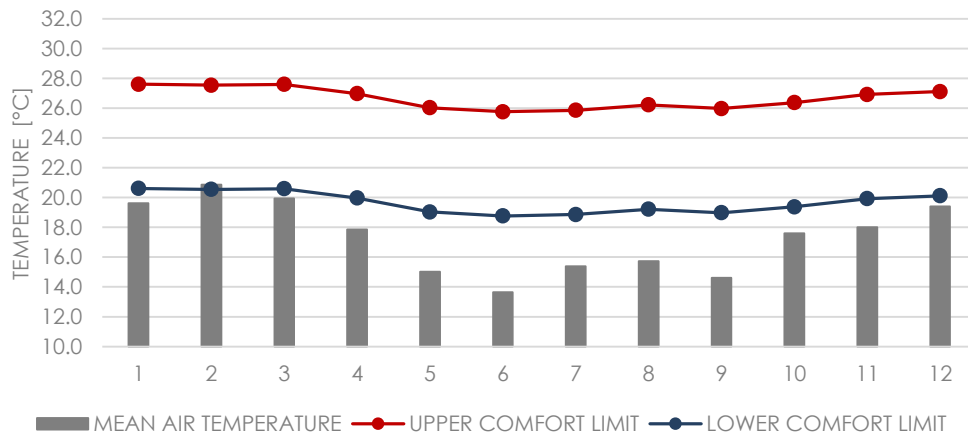
Table 6, Table 7, and Table 8 show the climate characteristics of each analyzed location and the prevailing wind direction. The annual wind wheels were generated by Climate Consultant 6.0 software (UCLA, 2015) after the input of the weather file (RORIZ, 2013c) and the selection of the ASHRAE Standard 55-2004 adaptive thermal comfort approach.

3.1.4.1 Curitiba/Paraná (Bioclimatic Zone - 01)

Table 6: Overview of Curitiba/PR climate.



COMPARISON BETWEEN COMFORT RANGE AND MEAN AIR TEMPERATURE OF CURITIBA/PR



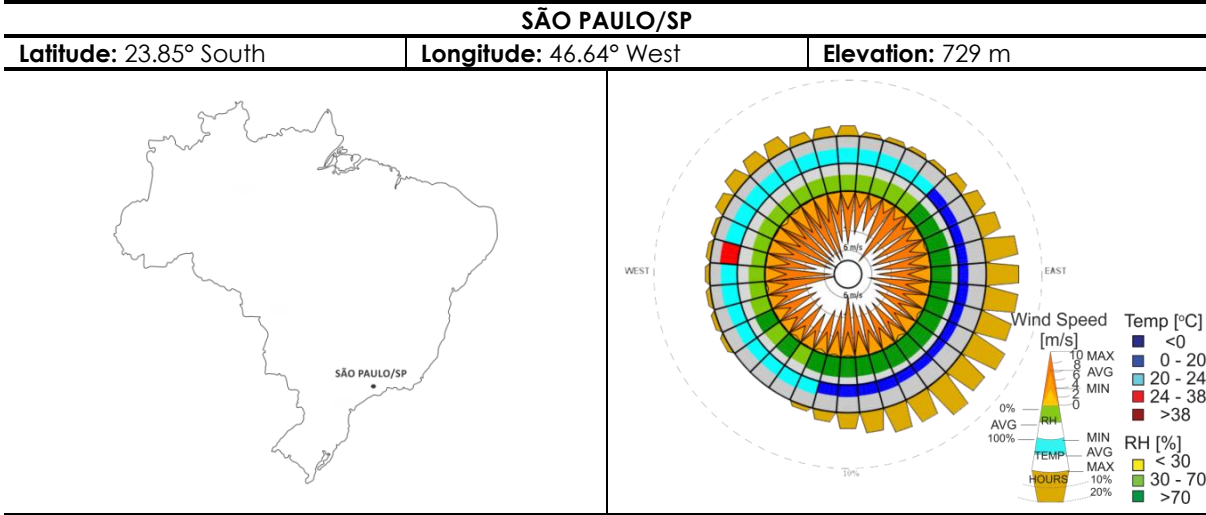
MONTH	RELATIVE HUMIDITY (%)	MEAN AIR TEMPERATURE (°C)	LOWER COMFORT LIMIT (°C)	COMFORT TEMPERATURE (°C)	UPPER COMFORT LIMIT (°C)
1	80.8	19.6	20.6	24.1	27.6
2	77.1	20.9	20.5	24.0	27.5
3	77.3	19.9	20.6	24.1	27.6
4	80.9	17.9	20.0	23.5	27.0
5	78.1	15.0	19.0	22.5	26.0
6	79.2	13.6	18.8	22.3	25.8
7	71.1	15.4	18.9	22.4	25.9
8	77.5	15.7	19.2	22.7	26.2
9	78.3	14.6	19.0	22.5	26.0
10	82.7	17.6	19.4	22.9	26.4
11	82.0	18.0	19.9	23.4	26.9
12	76.0	19.4	20.1	23.6	27.1

ANNUAL DEGREE HOURS OF DISCOMFORT (°Ch)

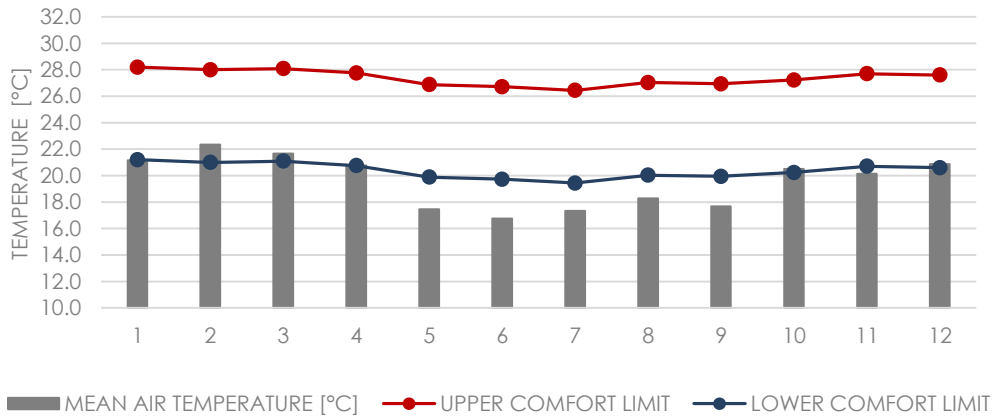
BY HEAT	239	BY COLD	28209
---------	-----	---------	-------

3.1.4.2 São Paulo/São Paulo (Bioclimatic Zone - 03)

Table 7: Overview of São Paulo/SP climate.



COMPARISON BETWEEN COMFORT RANGE AND MEAN AIR TEMPERATURE OF SÃO PAULO/SP

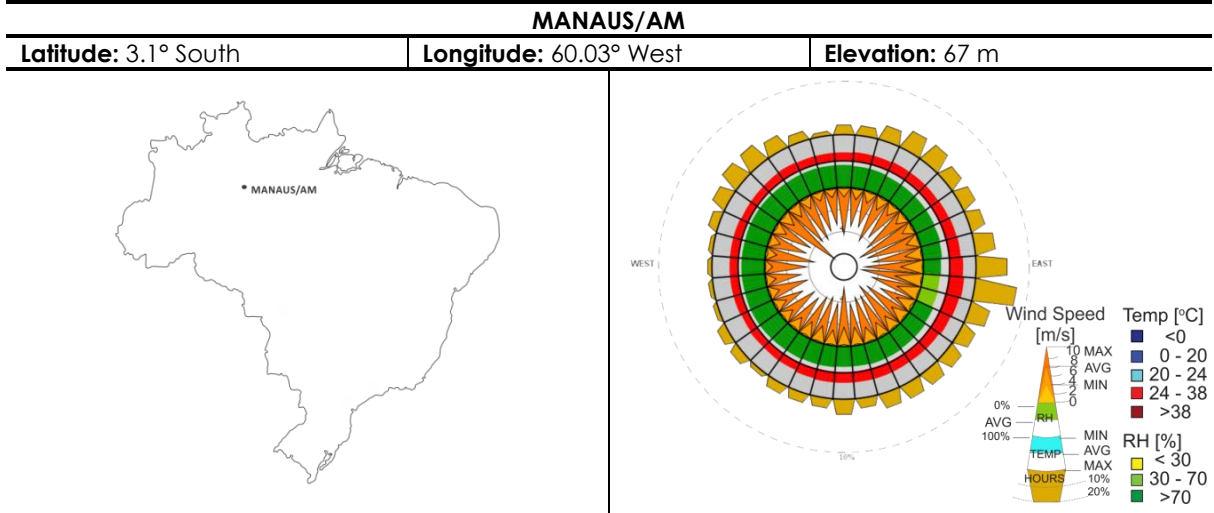


MONTH	RELATIVE HUMIDITY (%)	MEAN AIR TEMPERATURE (°C)	LOWER COMFORT LIMIT (°C)	COMFORT TEMPERATURE (°C)	UPPER COMFORT LIMIT (°C)
1	75.8	21.2	21.2	24.7	28.2
2	74.3	22.3	21.0	24.5	28.0
3	72.9	21.7	21.1	24.6	28.1
4	72.7	20.8	20.8	24.3	27.8
5	69.2	17.5	19.9	23.4	26.9
6	74.8	16.8	19.7	23.2	26.7
7	62.3	17.3	19.4	22.9	26.4
8	69.8	18.3	20.0	23.5	27.0
9	70.8	17.7	19.9	23.4	26.9
10	73.2	20.5	20.2	23.7	27.2
11	73.1	20.1	20.7	24.2	27.7
12	72.1	20.9	20.6	24.1	27.6

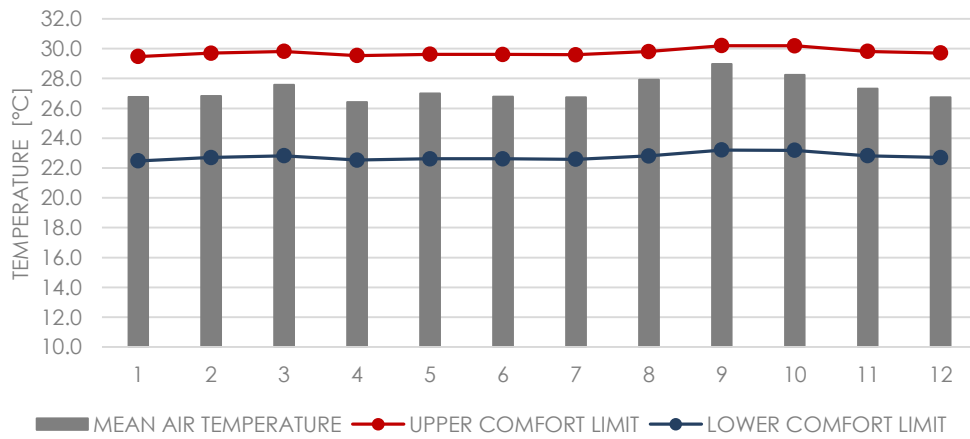
ANNUAL DEGREE HOURS OF DISCOMFORT (°Ch)			
BY HEAT	579	BY COLD	17918

3.1.4.3 MANAUS/AM (BIOCLIMATIC ZONE – 08)

Table 8: Overview of Manaus/AM climate.



COMPARISON BETWEEN COMFORT RANGE AND MEAN AIR TEMPERATURE OF MANAUS/AM



MONTH	RELATIVE HUMIDITY (%)	MEAN AIR TEMPERATURE (°C)	LOWER COMFORT LIMIT (°C)	COMFORT TEMPERATURE (°C)	UPPER COMFORT LIMIT (°C)
1	83.4	26.8	22.5	26.0	29.5
2	85.1	26.8	22.7	26.2	29.7
3	80.7	27.6	22.8	26.3	29.8
4	86.2	26.4	22.5	26.0	29.5
5	84.1	27.0	22.6	26.1	29.6
6	83.0	26.8	22.6	26.1	29.6
7	80.2	26.7	22.6	26.1	29.6
8	74.7	27.9	22.8	26.3	29.8
9	70.1	29.0	23.2	26.7	30.2
10	74.4	28.2	23.2	26.7	30.2
11	80.3	27.3	22.8	26.3	29.8
12	82.7	26.7	22.7	26.2	29.7

ANNUAL DEGREE HOURS OF DISCOMFORT (°Ch)

BY HEAT	2950	BY COLD	41
---------	------	---------	----

### 3.2 BASE MODEL SET-UP AND DESIGN PARAMETER RANGES

The base model consists in all parameter values necessary to characterize the building instance that is under consideration (HYGH et al., 2012). Some of those parameters assume fixed values, while others are varied in the Monte Carlo Simulation.

An amount of 24 parameters related to building orientation, shading devices, fenestrations, materials and constructions properties were sampled. For each parameter, minimum and maximum values establishing continuous distributions ranges were defined. Table 9 illustrates these parameters and their ranges.

All simulation inputs that compose the base model (fixed and variable) are shown in this sub item.

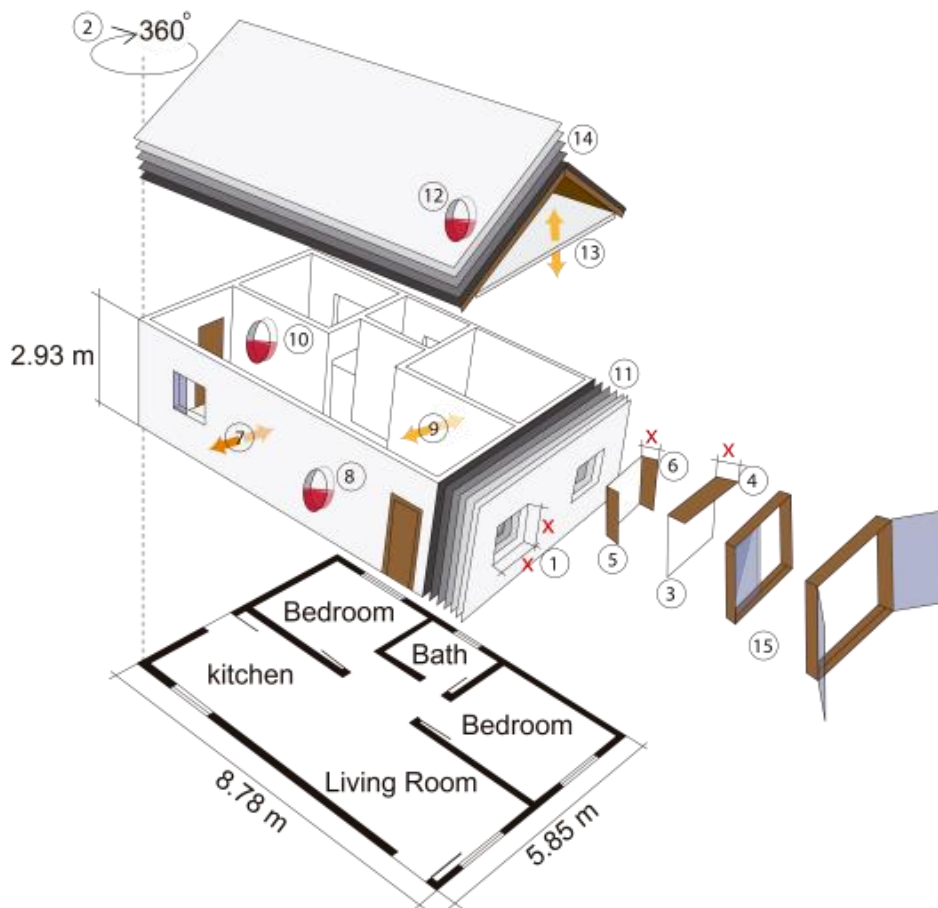


Figure 10: Base model and their variable design parameters.  
Source: ROSSI et al., 2015.



Table 9: Variable design parameters and their respectively ranges and units.

VARIABLE PARAMETERS	RANGE	UNITS
1 Bedroom_1 Window to Wall Ratio	10 to 90	%
2 Bedroom_2 Window to Wall Ratio		
3 Living room Window to Wall Ratio		
4 North Axis Direction	0 to 359	Degrees
5 Bedroom_1 Window overhang size	0.01 to 0.5	%
6 Bedroom_2 Window overhang size		
7 Living room Window overhang size		
8 Bedroom_1 Window fins position	on/off	
9 Bedroom_2 Window fins position		
10 Living room Window fins position		
11 Bedroom_1 Window fins size	0.01 to 0.5	%
12 Bedroom_2 Window fins size		
13 Living room Window fins size		
14 External Walls' U-value	0.3 to 5.0	W/(m <sup>2</sup> . K)
15 External Walls' Heat Capacity	40 to 455	KJ/ (m <sup>2</sup> . K)
16 External Walls' Solar Absorptance	0.1 to 1.0	
17 Internal Walls' U-value	0.3 to 5.0	W/(m <sup>2</sup> . K)
18 Internal Walls' Heat Capacity	40 to 455	KJ/ (m <sup>2</sup> . K)
19 Roof's U-Value	0.5 to 2.1	W/(m <sup>2</sup> . K)
20 Roof's Heat Capacity	11 to 791	KJ/ (m <sup>2</sup> . K)
21 Roof's Solar Absorptance	0.1 to 1.0	
22 Bedroom_1 Effective window ventilation area	50 to 100	%
23 Bedroom_2 Effective window ventilation area		
24 Living room Effective window ventilation area		

### 3.2.1 Geometry

In this study it was developed a fixed floor plan, focusing on detached houses. It was representative of the most commonly LCH built in Brazil. To guide the base model geometry definition, a collecting of Brazilian LCH architectural designs were made with municipal governments and funding agencies from some of the selected cities (Curitiba/PR and São Paulo/SP).

After that, these architectural designs were classified and the focus was given to items related to natural ventilation in buildings. For this reason, the main analyzed building's characteristics were: (a) shape, (b) windows distribution, (c) possibility of cross-ventilation, (d) effective window ventilation area, (e) windows types, and (f) wind permeability in surrounding of building.

The data classification occurred according to three workbook formats: (01) Workbook 01: Control, (02) Workbook 02: Collected Material, and (03) Workbook 03: Classification (geometric, thermal and openings). More details about these workbooks are presented in Appendix A.

To guide the representative floor plan definition some aspects were considered as relevant when the thermal comfort was taking under consideration, such as:

- Total of walls (internal and external), which delimitate the ambient;
- Amount and distribution of rooms in the building;
- Area;
- Building floor plan proportion;
- Window distribution.

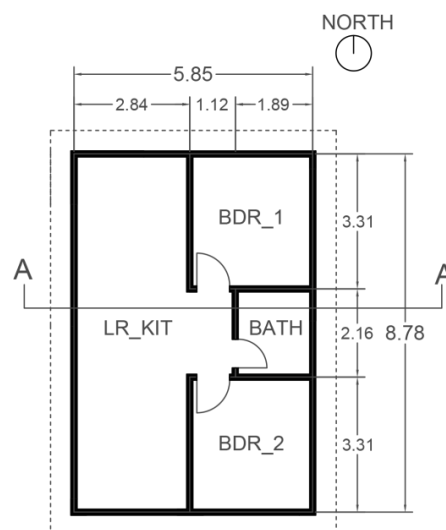
It is important to highlight that the collected samples referred to low-cost housings (Range 01) in the governmental program “Minha Casa Minha Vida” (My life My house). Considering that, it was adopted the minimum specifications for the room’s and furniture’s dimensions – published in June 2014 by the Ministry of Cities<sup>19</sup>. Consequently, the developed geometry had to meet the requirements specified in that document for a house divided into two bedrooms, a living room, a kitchen, and a bathroom.

The proposed representative low-cost house comprised several common characteristics of this building type in Brazil. It configures a rectangular-shaped detached unit with two bedrooms (BDR\_1 and BDR\_2), a living room and a kitchen (LR\_KIT), and a bathroom (BATH). The total area is about 50 m<sup>2</sup> with a non-ventilated attic under a gable roof.

Table 10 shows the base model geometry characteristics. It is worthwhile to mention it is presented with no windows, once the windows distribution definition is explained in the further item 3.2.2. Windows distribution definition.

Table 10: Base model geometry characteristics

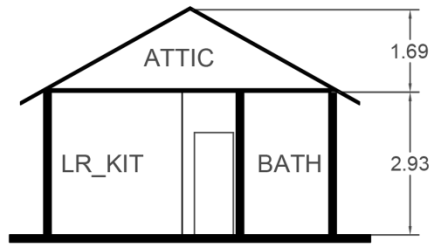
**BASE MODEL GEOMETRY**



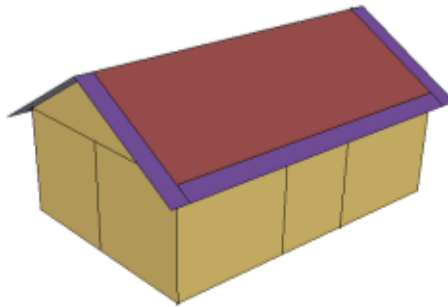
**Base Model Floor Plan**

<sup>19</sup> Available in [http://www.cidades.gov.br/images/stories/ArquivosSNH/ArquivosPDF/Especificacoes/especificacoes\\_casa\\_port168.pdf](http://www.cidades.gov.br/images/stories/ArquivosSNH/ArquivosPDF/Especificacoes/especificacoes_casa_port168.pdf)

Table10: Base model geometry characteristics (continuation)



Section AA



Base Model Perspective

**GEOMETRIC FEATURES**

<b>Type:</b> Detached	<b>Ceiling Height:</b> 2.925 m	Non-ventilated attic	<b>Geometric Proportion:</b> 1,50 *
<b>Area:</b> 51.33m <sup>2</sup>	There are eaves with 0.5 m in all facades.		

\*Ratio between the length by width of the building

**3.2.2 Windows Distribution Definition**

Three following criteria were considered to define the windows and doors positions in the base model geometry, such as (a) solar insolation; (b) prevailing wind direction; and (c) the pattern of fenestrations distributions observed in the collected architectural designs. Therefore, the objective was to define one window distribution which would expect to cover the best and the worst solutions for natural ventilation occurrence by changing the building orientation.

**(a) Solar insolation**

The best solar orientations for each location were carefully analyzed using the solar charts generated by Analysis SOL-AR software (LABEEE, 2012). The solar charts for each analyzed climate are shown in Appendix B. The summary of this verification is presented in Table 11.

Table 11: Best solar orientations for Curitiba/PR, São Paulo/SP, and Manaus/AM.

CITIES	BEST SOLAR ORIENTATIONS
CURITIBA (BIOCLIMATIC ZONE 01)	EAST AND NORTH
SÃO PAULO (BIOCLIMATIC ZONE 03)	EAST AND NORTH
MANAUS (BIOCLIMATIC ZONE 08)	NORTH AND SOUTH WITH SHADING DEVICES

### (b) Prevailing wind direction

As aforementioned the prevailing wind direction for each analyzed climate was defined based on the wind wheels generated by Climate Consultant 6.0 software. The annual wind wheels were shown in Weather Analysis section (see item 3.1.4).

Moreover, it was verified the wind pattern per seasons, regarding all selected climates. The whole year was divided into: (a) summer - from December to February; (b) fall – from March to May; (c) winter – from June to August and, (d) spring – from September to November. A figure that summarizes this analysis is shown in Appendices section (see Appendix C). For all locations, the wind wheels per seasons showed no significant changes in wind pattern when compared to the annual ones. For this reason, it was agreed to adopt the annual wind wheels as representative and then, to base the considerations of prevailing wind direction on those (see item 3.1.4).

### (c) The pattern of fenestrations distributions observed in the collected architectural designs

The input for this criterion analysis was the collected architectural designs. A single window per ambient and two exterior doors per building characterized the pattern of the great part of samples. Based on that, some sketches were elaborated to test the window distribution possibilities for each long-stay rooms (bedrooms and living-room) (see Appendix D).

As the objective of the presented analysis was to define a windows distribution that comprised the best and the worst situations for the natural ventilation occurrence by building rotation, the geometry shows in Figure 11 was selected. Since it comprised the best ( $N=270^\circ$ ) and the worst ( $N=90^\circ$ ) situations (Figure 12). However, it is very important to highlight that analysis was qualitative and based on the pre-established criteria considerations. All the geometry options developed in this analysis are summarized in Appendix D.

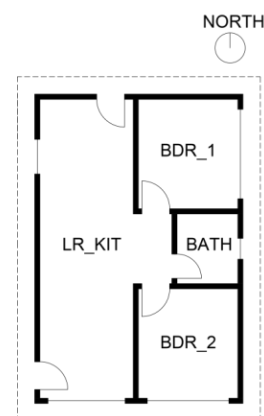


Figure 11: Base model geometry with the selected windows distribution.

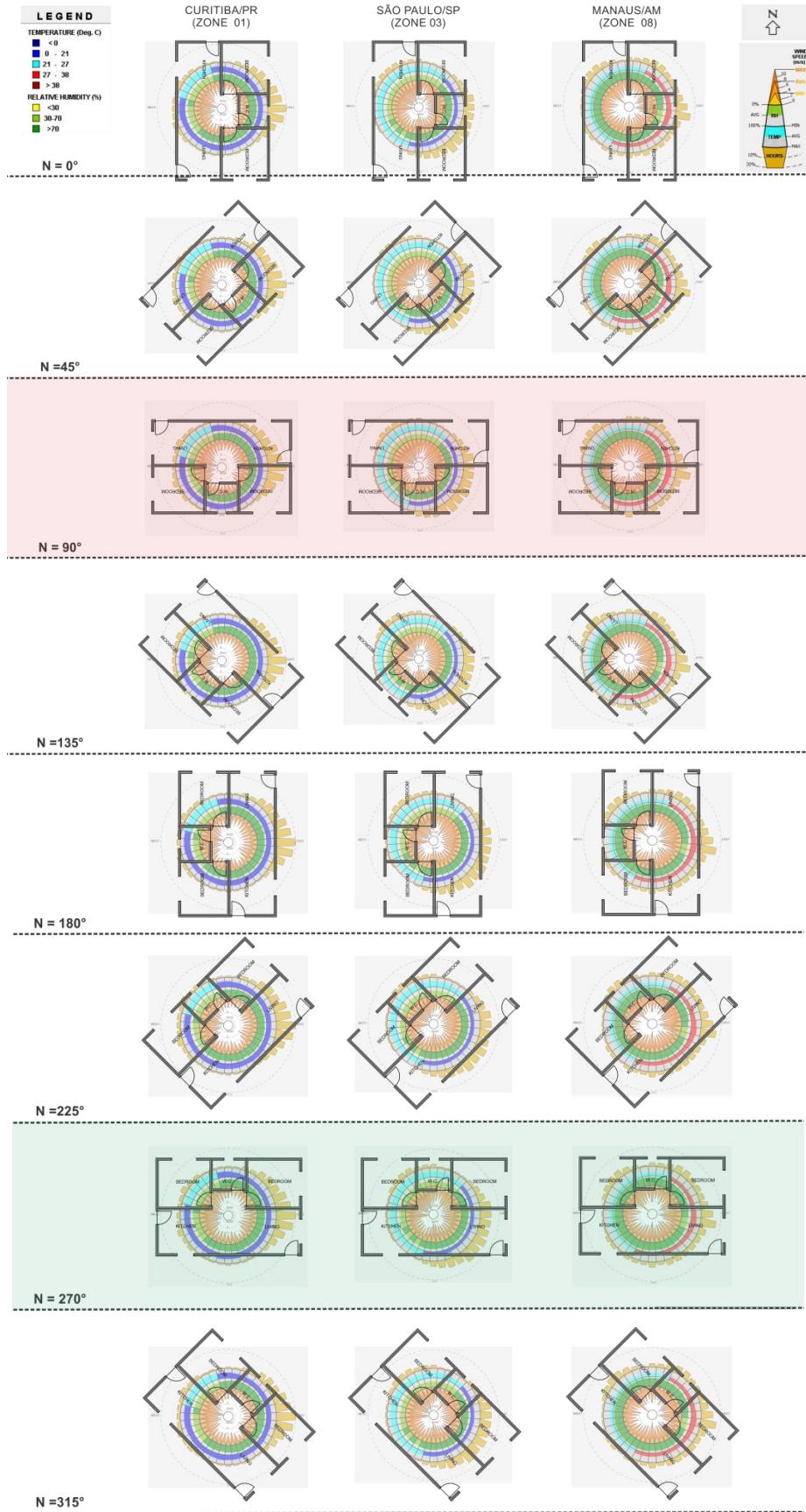


Figure 12: Qualitative analysis of the selected windows distribution, considering the natural ventilation efficacy by changing the building orientation.

### 3.2.3 Thermal Zone Definition<sup>20</sup>

The building performance simulation (BPS) is a very complex and time-consuming process, especially when it implicates in a huge number of simulations and iterations or when complex buildings are evaluated. To split the floor plan into thermal zones is the first step in simulations through BPS tools that concern zone heat balance, as for example, EnergyPlus. To better assist the decision-making process during the early design it is important to the simulation model be specific to represent the building type under consideration, but also general enough to permit changes and multiple interactions characteristics of this stage. Therefore, models with less thermal zones could better represent the definition of parameters related with conceptual design (FAVRETTO, et al., 2015).

The concept that rules zoning definition is based on thermal considerations, not in geometric concerns, once the thermal zone is a volume of air with same temperature, including all the heat transfer or storage surfaces that boundary it or are inside in this space. According to EnergyPlus documentation the number of zones is equals to the number of radiant or fan systems present in the building, not the number of rooms (EERE, 2014b).

In order to simplify the thermal zone definitions; it was performed extensive benchmark tests to evaluate if these simplifications made for the simulations were sufficiently accurate.

The base model is a representative Brazilian naturally ventilated low-cost equals to the model showed in the items "3.2.1 Geometry" and "3.2.2 Windows Distribution Definition".

Based on that, the impact on the thermal comfort predictions of such house was evaluated within three Brazilian climates: Curitiba/PR, Manaus/AM and São Paulo/SP and under three different wind and solar exposure conditions (Figure 13).

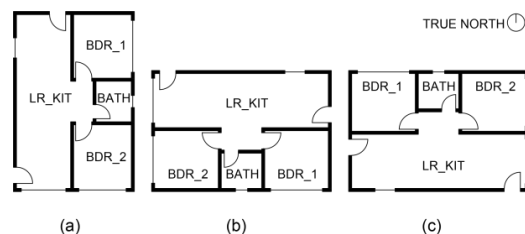


Figure 13: Building orientations.  
Source: FAVRETTO et al., 2015.



Figure 14: MZM and SZM.

The analysis considered two different zone modeling approaches: Single Zone Model [SZM] and Multi Zone Model [MZM]. While the first approach considered a single zone to characterize the whole floor plan; the second one utilized separate zones to

<sup>20</sup> The results and the complete analysis of thermal zone definitions benchmark tests were reported in the paper "Assessing the impact of zoning on the thermal comfort analysis of a naturally ventilated house during early design", submitted to Building Simulation Conference 2015.

describe each room, totalizing in four thermal zones. In both cases, the attic was considered as an independent and unconditioned thermal zone (Figure 14).

A set of 9 simulation scenarios were analyzed (Table 12). Walls and roof thermal properties as well as window-to-wall ratio were fixed parameters in simulations. Additionally, the internal gains were modeled according to values and routines established by a thermal Brazilian Regulation (INMETRO, 2012). The natural ventilation was permitted from 7 a.m. to 10 p.m., its control was per temperature, and the set point temperature was based on

Table 12: Analyzed simulation cases.

Case Number	1	2	3	4	5	6	7	8	9
Orientation	a	b	c	a	b	c	a	b	c
City	Curitiba			Manaus			São Paulo		
Wall properties	U=2.46 W/(m <sup>2</sup> .K)   HC=150 KJ/(m <sup>2</sup> .K)   α=0.4								
Roof properties	U=1.8 W/(m <sup>2</sup> .K)   HC=185 KJ/(m <sup>2</sup> .K)   α=0.7								
WWR	40% (Window-to-Wall Ratio)								

Source: FAVRETTO et al., 2015.

adaptive comfort temperatures calculated according to ASHRAE 55-2013 Adaptive Comfort Approach, for this reason vary from climate to climate. Once the geometry is rectangular-shaped the surface-average pressure coefficients automatically calculated by EnergyPlus were applied. The accuracy of such assumption will be explored in a further section of this document, "3.3.2 Impact of using surface-average instead of local wind pressure coefficients on the thermal comfort analyses".

The focus on results was in the differences observed in comparisons between the SZM and each room of MZM. Such comparisons considered the differences between the two modeling approaches ( $\Delta = SZM - MZM_{room}$ ) in the air and operative temperatures and also in the degree-hours of discomfort by heat and by cold, as demonstrate by following equations (Table 13):

Table 13: Metrics applied to evaluate the results.

<b>AIR TEMPERATURE</b>	$\Delta T_{a}^{room} = \frac{\sum_{i=1}^{8760} (T_{a,i}^S - T_{a,i}^{M,room})}{8760}$	$\Delta T_{a}^{room}$ : Average difference in air temperature prediction between SZM and each long-stay room of MZM (°C). $T_{a,i}^S$ : SZM hourly air temperature (°C). $T_{a,i}^{M,room}$ : MZM hourly air temperature for each long-stay room (°C).
<b>OPERATIVE TEMPERATURA</b>	$\Delta T_{o}^{room} = \frac{\sum_{i=1}^{8760} (T_{o,i}^S - T_{o,i}^{M,room})}{8760}$	$\Delta T_{o}^{room}$ : Average difference in operative temperature prediction between SZM and each long-stay room of MZM (°C). $T_{o,i}^S$ : SZM hourly operative temperature (°C). $T_{o,i}^{M,room}$ : MZM hourly operative temperature for each long-stay room (°C).
<b>DISCOMFORT BY COLD</b>	$\Delta D_c^{room} = \frac{\sum_{i=1}^{8760} (D_{c,i}^S - D_{c,i}^{M,room})}{8760}$	$\Delta D_c^{room}$ : Average difference in discomfort by cold prediction between SZM and each long-stay room of MZM (°Ch). $D_{c,i}^S$ : SZM hourly discomfort by cold (°Ch). $D_{c,i}^{M,room}$ : MZM hourly discomfort by cold for each long-stay room (°Ch).

Table 13: Metrics applied to evaluate the results (continuation)

<b>DISCOMFORT BY HEAT</b>	$\Delta D_h^{room} = \frac{\sum_{i=1}^{8760} (D_{h,i}^S - D_{h,i}^{M,room})}{8760}$	$\Delta D_h^{room}$ : Average difference in discomfort by heat prediction between SZM and each long-stay room of MZM (°Ch).
		$D_{h,i}^S$ : SZM hourly discomfort by heat (°Ch). $D_{h,i}^{M,room}$ : MZM hourly discomfort by heat for each long-stay room (°Ch).

Source: FAVRETTO et al., 2015.

### Air Temperature

When naturally ventilated buildings are simulated in EnergyPlus and has its ventilation control mode based on temperature, is very important to analyze the air temperature behavior.

Figure 15 illustrates small differences between the air temperature predictions from both modeling approaches. The annual average hourly air temperature differences showed a maximum value about  $-0.2^{\circ}\text{C}$ .

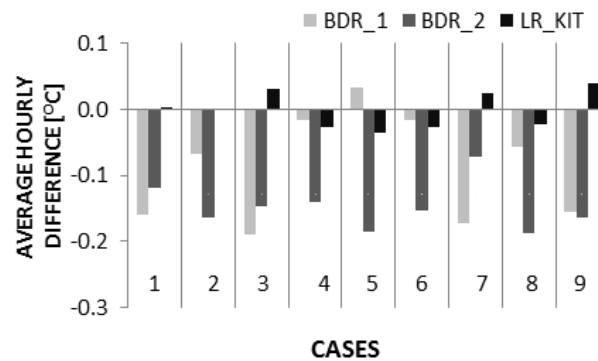


Figure 15: Annual air temperature difference between SZM and MZM (each long-stay room). Source: FAVRETTO et al., 2015.

### Operative Temperature

The operative temperature was an important output in this study, once the thermal comfort evaluation was done according to ASHRAE-55 Adaptive Comfort Approach (ASHRAE, 2013), which considers the operative temperature as an input in its analysis.

Similarly the air temperature behavior, the predictions of operative temperature regarding the two different modeling approaches indicated small differences. The Figure 16 illustrates the distribution of those discrepancies along the year. Small values, with the greatest part of differences between  $0^{\circ}\text{C}$  and  $0.3^{\circ}\text{C}$ , characterize that analysis.



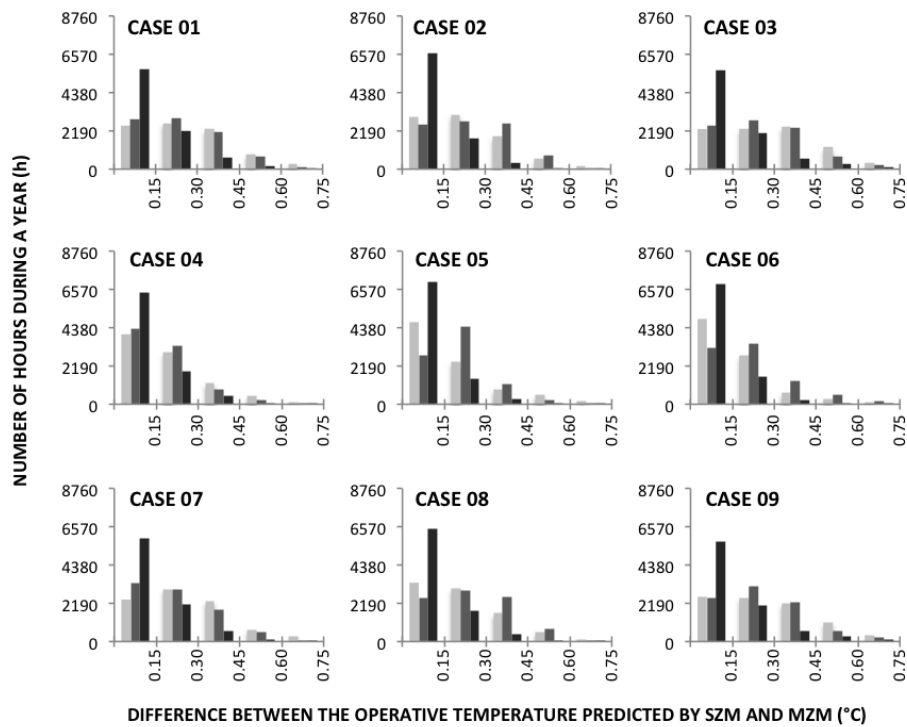


Figure 16: Distribution of hourly absolute differences between the predictions of operative temperatures by the different modeling approaches along the year. Source: FAVRETTO et al., 2015.

**Degree-Hours of discomfort by heat and by cold**

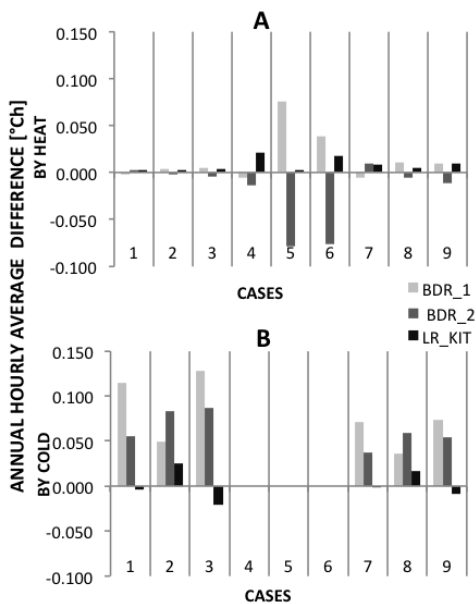


Figure 17: Average difference during the year between SPM and MPM in hourly discomfort by heat (A) and by cold (B). Source: FAVRETTO et al., 2015.

The thermal discomfort was analyzed taking under consideration, the SPM and MPM predictions and also the comfort range.

As expected due to the observations in operative temperature prediction differences, the annual average degree-hour (°Ch) of discomfort by heat and by cold calculated according to SPM and MPM hourly predictions showed very small discrepancies. When the maximum and minimum average values found were 0.086°Ch and 0.128°Ch, respectively (Figure 17).

This benchmark test confirm due to small differences presented in all standpoints: air and operative temperatures as well as thermal comfort, that is possible to use for those analyzed

cases, the SZM approach in place of MZM during early design. However, are extremely important further studies and investigations to test other parameters variations as different Window-to-Wall Ratio, building envelope thermal properties, shading devices and so on. Additionally, to investigate and guide the modeling of naturally ventilated buildings.

### 3.2.4 North Axis/ Orientation in the Terrain

The building North Axis is determined related to true North (EERE, 2014b). Based on that, the angle specified in such parameter corresponds to the angle in degrees and positive in clockwise measured between the True North and the Building North. In conclusion, the north axis direction varied continuously from  $0^\circ$  to  $359^\circ$  in order to explore all the possible building orientations tested by designers during the early design. In this research the North Axis is named **N** (Figure 18).

In addition, the field "Azimuth Angle of Long Axis of Building" (Figure 19) indicates the orientation of a rectangular-shaped building (see section 3.3. Natural ventilation modeling). In this research the Azimuth Angle of Long Axis of Building is named  **$\alpha$**

Even tough, in EnergyPlus, the North Axis allowed range is from  $0^\circ$  to  $359^\circ$ , the valid interval for Azimuth Angle of Long Axis of Building in Airflow Network group is  $0^\circ$  to  $180^\circ$ . So, a conversion factor that enabled to fit both angles intervals to the same range was necessary.

Consequently, a programming code was developed to vary this angle in a different manner in Airflow Network group, following the proposed conversion: North Axis from  $0^\circ$  to  $180^\circ \rightarrow \mathbf{N} = \alpha$ , however when Building Orientation is higher than  $180^\circ \rightarrow \mathbf{\alpha} = \mathbf{N} - 180^\circ$ . To sum up, if the building orientation is  $45^\circ$ , the input angle in Airflow Network will be  $45^\circ$ ; in contrast to that if the building is orientated to  $225^\circ$  (North Axis value), the angle describe in Azimuth Angle of Long Axis of Building will be also  $45^\circ$ .

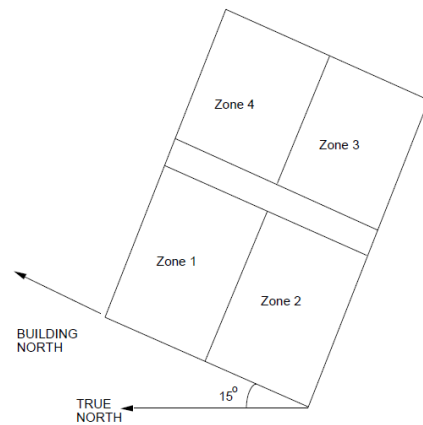


Figure 18: Building North Axis.  
Source: EERE, 2014b.

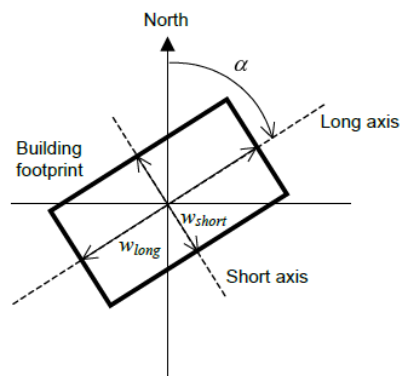


Figure 19: Azimuth Angle of Long Axis of Building. Source: EERE, 2014b.

### 3.2.5 Terrain Type

The terrain type is an important aspect to be considered especially in naturally ventilated buildings. Because this factor influences the way that wind attacks the building. The option selected for this parameter was suburb, once it is the current context of low-cost houses in Brazil, according to the architectural design collection. Table 14 summarizes the characteristics when suburb is determined as terrain type option.

Table 14: Wind Speed Coefficients and description according to terrain type definition

TERRAIN	TERRAIN DESCRIPTION	EXPONENT	BOUNDARY LAYER THICKNESS - [m]
Suburb	Rough	0.22	370

Source: Adapted from Wind Speed Profile Coefficients (ASHRAE Fundamentals 2005).

### 3.2.6 Ground Temperature

The soil figures a significant thermal inertia. Then, it is important to adjust ground temperature values properly in thermal comfort simulation. However, there are fewer accurate investigations in Brazil about this topic.

For this reason, it was defined as input data for this parameter the monthly mean air temperature values, regarding each climate. Some adjustments were necessary on those temperatures to meet the acceptable range of the simulation software (from 15°C to 25°C). The ground temperatures data adopted in simulations for each climate is shown in the Appendices section of this document (see Appendix E).

### 3.2.7 Materials Thermal Properties and Construction Systems of Building Opaque Envelope

The building materials and constructions systems characterization in EnergyPlus is highly detailed and it demands knowledge of material thermal properties that in early design stages is usually not already defined. Regarding these limitations, a virtual material structure was developed, in order to facilitate the material input data in EnergyPlus, presenting, then, a different modeling approach that better fits to architecture domain and also to the aim of this research (FAVRETTO, 2016).

The virtual material structure differs between roof and walls (internal and external) systems by the number of the layers that constitute each system. While the first one is a four-layered construction, the second is a three-layered construction (Figure 20). Such structure permitted an independently variation of the thermal transmittance (U-value) and Heat Capacity (HC)

values through the alteration in the thermal resistance field of the EnergyPlus group “Material No Mass” and the material density in the group “Material”. Table 15 and Table 16 summarize the roof’s and walls’ (external and internal) virtual material structures as well as the description of the input data in EnergyPlus and the fields in where the variance occurred in order to cover the design space options took under consideration (FAVRETTO, 2016). It is important to highlight that internal and external walls varied independently in simulation, though they have the same virtual material structure types and ranges.

The presented modelling approach was systematically tested to certify if it was representing with accuracy the thermal behavior of detailed material input data in the software. Combinations of extreme values of Heat Capacity and U-value within three selected Brazilian climates delineated the scenario of all cases tested (FAVRETTO, 2016). A good fitness was observed between the two different modeling approaches when both virtual systems (walls and roof) were analyzed together. In conclusion, those tests testified the accuracy of adopting the developed virtual material structures in place of detailed ones for parametric simulations conducted in this research. It is worthwhile to mention that tests demonstrate a good fidelity in comparisons between the operative temperatures predicted by EnergyPlus, considering the different modeling approaches for all analyzed cases and climates (FAVRETTO, 2016).

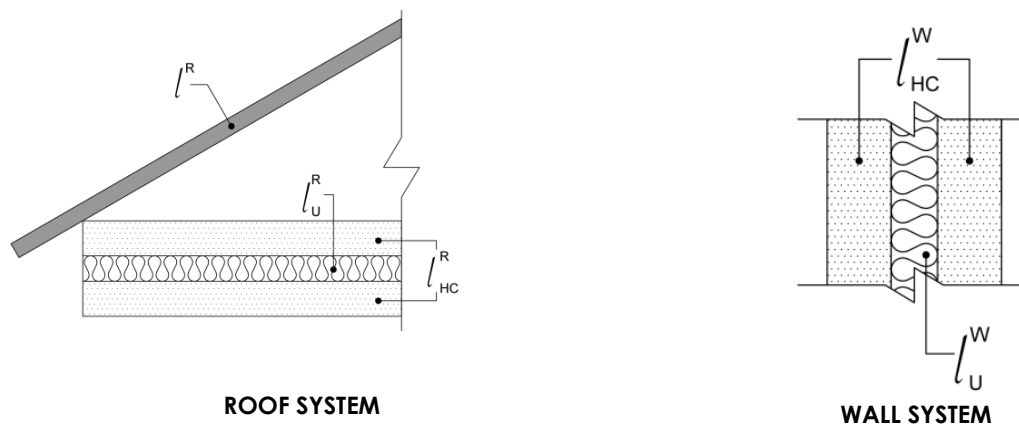


Figure 20: Roof and walls' virtual material systems structures. Source: FAVRETTO, 2016.

Table 15: Roof virtual material structures and their properties.

LAYER	EP INPUT GROUP	PROPERTIES		THERMAL RESISTANCE [m <sup>2</sup> .K/W]	HEAT CAPACITY [KJ/m <sup>2</sup> .K]	
$l^R$	MATERIAL	ROUGHNESS	MEDIUM		0.01	14
		THICKNESS [m]	0.01			
		CONDUCTIVITY [W/(m <sup>2</sup> .K)]	1			
		DENSITY [Kg/m <sup>3</sup> ]	1400			
		SPECIFIC HEAT [J/Kg.K]	1000			
		SOLAR ABSORPTANCE	0.7			
$l_{HC}^R$	MATERIAL	ROUGHNESS	MEDIUM		0.01	VARIABLE
		THICKNESS [m]	0.05			
		CONDUCTIVITY [W/(m <sup>2</sup> .K)]	5			
		DENSITY [Kg/m <sup>3</sup> ]	MIN	20		
			MAX	5560		
		SPECIFIC HEAT [J/Kg.K]	1000			
$l_U^R$	MATERIAL: NO MASS	ROUGHNESS	MEDIUM		VARIABLE	-
		THERMAL RESISTANCE [m <sup>2</sup> .K/W]	MAX	1.55		
			MIN	0.01		

Source: FAVRETTO, 2016.

Table 16: Walls (external and internal) virtual material structures and their properties.

LAYER	EP INPUT GROUP	PROPERTIES		THERMAL RESISTANCE [m <sup>2</sup> .K/W]	HEAT CAPACITY [KJ/m <sup>2</sup> .K]	
$l_{HC}^W$	MATERIAL	ROUGHNESS	MEDIUM		0.01	VARIABLE
		THICKNESS [m]	0.05			
		CONDUCTIVITY [W/(m <sup>2</sup> .K)]	5			
		DENSITY [Kg/m <sup>3</sup> ]	MIN	400		
			MAX	4450		
		SPECIFIC HEAT [J/Kg.K]	1000			
SOLAR ABSORPTANCE	0.7					
$l_U^W$	MATERIAL: NO MASS	ROUGHNESS	MEDIUM		VARIABLE	-
		THERMAL RESISTANCE [m <sup>2</sup> .K/W]	MAX	3.07		
			MIN	0.01		

Source: FAVRETTO, 2016.

The glass type as well as the floor and door materials were kept fixed in parametric simulations. Their characteristics are showed in Table 17.

Table 17: Fixed building materials and constructions systems in simulations.

BUILDING MATERIAL or CONSTRUCTION SYSTEM	DESCRIPTION
Glass	Clear, 4mm.
Floor	Ceramic floor tile (0.5 cm) + plaster (thickness = 2.5 cm) + concrete (e=8 cm) + gravel (e=3 cm)
Door	Wood, 3.5 cm.

### 3.2.8 Shading Devices

The variations of the shading devices (fins and overhangs) in simulation were related to the positions and sizes of these devices in the long-stay room's windows. The shading device's size was a function of the window's height and their ranges are presented in Table 9 (see 3.2 Base Model Set-Up and Design Parameter Ranges).

The materiality of these protections as well as the solar absorptance, and the angle formed with the opening (90°) were fixed parameters in all simulations. Finally, it is important to highlight that the base model geometry had projecting eaves around all façades of 0.5 m. Chvatal and Marques (2015) verified the impact of such elements in LCH' thermal performance. Table 18 describes the characteristics of parameters related with shading devices to be considerate in the simulations.

Table 18: Shading devices characteristics to be considered in simulations.

PARAMETERS	DESCRIPTION	VALUES/RANGES
Overhangs <sup>(1)</sup>	Position related to the window Size <sup>(A)</sup>	01 possibility <b>VARIABLE</b>
Fins <sup>(1)</sup>	Position related to the window <sup>(B)</sup> Size <sup>(A)</sup>	<b>VARIABLE</b> <b>VARIABLE</b>
Eaves <sup>(2)</sup>	0.5 m in all façades	Fixed value

(1) Both shading devices show as fixed parameters in simulations: the materiality, the solar absorptance, and the angle formed with the opening (90°). The shading devices never exceed the window's dimensions.

(2) Projecting eaves.

(A) The overhang's and fin's size is function of window's height.

(B) Eight fin positioning possibilities are considered, since there are two options (with or no shading devices) for each window side and for each long-stay room.

### 3.2.9 Internal Gains

The internal gains (lights, electric equipment, occupancy) considered in simulations of the analyzed LCH as well as their routine definitions were based on values established by Technical regulation for energy efficiency labelling of residential buildings, RTQ-R (INMETRO, 2012). The RTQ-R divides the lights, electric equipment, and occupancy routines for long-stay rooms in weekdays and weekends.

### 3.2.9.1 Occupancy

The minimum occupancy pattern<sup>21</sup> and the values of metabolic rates for each activity as recommended by RTQ-R were adopted. It is important to highlight that the values of metabolic rates presented in the Brazilian Regulation are based on ASHRAE Handbook of Fundamentals (ASHARE, 2009) and are related with the activity type developed, considering an area of skin (about 1.8 m<sup>2</sup>) equivalent to an average person. Table 19 indicates the fraction of the total of people that is using the long-stay rooms in determining days and times. Table 20 shows the metabolic rates for each activity develop by the users.

Table 19: Occupancy routine for weekdays and weekends in long-stay rooms.

HOUR	BEDROOMS*		LIVING ROOM*	
	Weekdays	Weekend	Weekdays	Weekend
1 h	1	1	0	0
2 h	1	1	0	0
3 h	1	1	0	0
4 h	1	1	0	0
5 h	1	1	0	0
6 h	1	1	0	0
7 h	1	1	0	0
8 h	0	1	0	0
9 h	0	1	0	0
10 h	0	0.5	0	0
11 h	0	0	0	0.25
12 h	0	0	0	0.75
13 h	0	0	0	0
14 h	0	0	0.25	0.75
15 h	0	0	0.25	0.5
16 h	0	0	0.25	0.5
17 h	0	0	0.25	0.5
18 h	0	0	0.25	0.25
19 h	0	0	1	0.25
20 h	0	0	0.5	0.5
21 h	0.5	0.5	0.5	0.5
22 h	1	1	0	0
23 h	1	1	0	0
24 h	1	1	0	0

\*Fraction of the total of people.

Source: Adapted from INMETRO, 2012.

Table 20: Metabolic Rates for each activity and the minimum occupation pattern per room.

ROOMS	ACTIVITY	PRODUCED HEAT PER AREA OF SKIN =180 m <sup>2</sup> (W)	OCCUPANCY PATTERN/ ROOM
Living Room	Sitting or watching TV	108	4 (2 people x 2 bedrooms)
Bedrooms	Sleeping or resting	81	2

Source: Adapted from INMETRO, 2012.

<sup>21</sup> Two people in each bedroom and the living room utilizes for all habitants.

Adjustments were realized in the occupancy pattern proposed by RTQ-R, in order to guarantee that house will be occupied during all day. Consequently, for the hours when the house was empty, a value equals the occupancy fraction in earlier or later hours was adopted. Table 21 highlights these adjustments on occupancy routine.

Table 21: Adjustments on occupancy routine for weekdays and weekends in long-stay rooms.

HOUR	BEDROOMS*		LIVING ROOM*	
	Weekdays	Weekend		Weekdays
1 h	1	1	0	0
2 h	1	1	0	0
3 h	1	1	0	0
4 h	1	1	0	0
5 h	1	1	0	0
6 h	1	1	0	0
7 h	1	1	0	0
8 h	0	1	0.25	0
9 h	0	1	0.25	0
10 h	0	0.5	0.25	0
11 h	0	0	0.25	0.25
12 h	0	0	0.25	0.75
13 h	0	0	0.25	0.75
14 h	0	0	0.25	0.75
15 h	0	0	0.25	0.5
16 h	0	0	0.25	0.5
17 h	0	0	0.25	0.5
18 h	0	0	0.25	0.25
19 h	0	0	1	0.25
20 h	0	0	0.5	0.5
21 h	0.5	0.5	0.5	0.5
22 h	1	1	0	0
23 h	1	1	0	0
24 h	1	1	0	0

\*Fraction of the total of people.

### 3.2.9.2 Electric Equipment

Electric equipment was considered only in the living room and had their power kept constant 24hs/day (Table 22).

Table 22: Electric Equipment internal gains.

ROOM	PERIOD	POWER (W/m <sup>2</sup> )
Living Room	24 h	1.5

Source: Adapted from INMETRO, 2012.

### 3.2.9.3 Lights

Similarly to the occupancy, the lights routine was described only for the long-stay rooms, and considered as different routines for weekdays and weekends. The value 0 represents the periods that the lights in the ambient are off while 1 the moments in which the lights are being



used (Table 23). The installed light power referenced in the simulations are also presented in Table 23.

Table 23: Lights routines for weekend and weekdays in long-stay rooms and the applied power.

HOUR	BEDROOMS			LIVING ROOM		
	Weekdays	Weekend	Power (W/m <sup>2</sup> )	Weekdays	Weekend	Power (W/m <sup>2</sup> )
1 h	0	0	5	0	0	6
2 h	0	0	5	0	0	6
3 h	0	0	5	0	0	6
4 h	0	0	5	0	0	6
5 h	0	0	5	0	0	6
6 h	0	0	5	0	0	6
7 h	1	0	5	0	0	6
8 h	0	0	5	0	0	6
9 h	0	1	5	0	0	6
10 h	0	0	5	0	0	6
11 h	0	0	5	0	1	6
12 h	0	0	5	0	1	6
13 h	0	0	5	0	0	6
14 h	0	0	5	0	0	6
15 h	0	0	5	0	0	6
16 h	0	0	5	0	0	6
17 h	0	0	5	1	1	6
18 h	0	0	5	1	1	6
19 h	0	0	5	1	1	6
20 h	0	0	5	1	1	6
21 h	1	1	5	1	1	6
22 h	1	1	5	0	0	6
23 h	0	0	5	0	0	6
24 h	0	0	5	0	0	6

Source: Adapted from INMETRO, 2012.

### 3.2.10 Fenestrations

The fenestrations play an important role in building thermal performance. They significant impact the natural ventilation occurrence, the air flow pattern through the indoor spaces and also the solar gains. The windows of the kitchen and bathroom as well as the exterior and interior doors had their dimensions kept fixed during the simulation. Based on the regular dimensions found in this Brazilian building type, their dimensions were defined. On the other hand, the windows dimensions of the long-stay rooms and their respectively effective window ventilation area varied parametrically during the simulations. The manner and the ranges that such parameters varied are detailed shown in the item "3.2 Base Model Set-Up and Design Parameter Ranges". Table 24 shows the dimensions of fixed fenestrations.

Table 24: Description of fixed and variable fenestrations.

FIXED FENESTRATIONS (WINDOWS and DOORS)	ROOM	WINDOW AREA (m <sup>2</sup> )	WINDOW DIMENSIONS <sup>(1)</sup> (m)	EFFECTIVE WINDOW VENTILATION AREA	DOOR DIMENSIONS (m)
	Kitchen	1.00	1.00 x 1.00/ 1.10	50%	0.8 x 2.1
	Bathroom	0.36	0.6 x 0.6 / 1.50	100%	0.7 x 2.1
VARIABLE FENESTRATIONS	Bedroom_1 Bedroom_2 Combined Living room and kitchen	VARIABLE		VARIABLE	0.8 x 2.10 0.8 x 2.10 0.8 x 2.10

<sup>(1)</sup> Window dimensions: width x height /windowsill

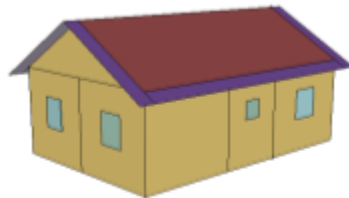
### 3.2.10.1 Window-to-Wall Ratio

Window-to-wall ratio (WWR) is the ratio (in percentage) between the window area and the facade area where it is located.

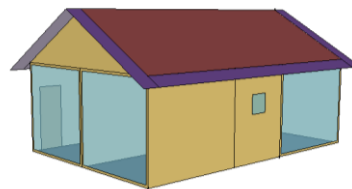
This parameter ranged continuously from 10% to 90% in simulations, only in the windows of long-stay rooms (bedrooms and living room).

Table 25 presents the base model geometry and the values correspond to some window areas, considering different WWR.

Table 25: Description of Window-to-Wall Ratios for the Long-Stay Rooms.



WWR= 10%



WWR=90%

VARIABLE WINDOWS			
LSR (LONG-STAY ROOMS)		Façade Area (m <sup>2</sup> )	Window Area (m <sup>2</sup> )
WWR=10%	Bedroom_1	9.68175	0.97
	Bedroom_2	8.80425	0.88
	Living	8.307	0.83
WWR=20%	Bedroom_1	9.68175	1.94
	Bedroom_2	8.80425	1.76
	Living	8.307	1.66
WWR=30%	Bedroom_1	9.68175	2.90
	Bedroom_2	8.80425	2.64
	Living	8.307	2.49
WWR=40%	Bedroom_1	9.68175	3.87
	Bedroom_2	8.80425	3.52
	Living	8.307	3.32
WWR=50%	Bedroom_1	9.68175	4.84
	Bedroom_2	8.80425	4.40
	Living	8.307	4.15
WWR=60%	Bedroom_1	9.68175	5.81
	Bedroom_2	8.80425	5.28
	Living	8.307	4.98

Table 25 : Description of Window-to-Wall Ratios for the Long-Stay Rooms (continuation).

<b>WWR=70%</b>	Bedroom_1	9.68175	6.78
	Bedroom_2	8.80425	6.16
	Living	8.307	5.81
<b>WWR=80%</b>	Bedroom_1	9.68175	7.75
	Bedroom_2	8.80425	7.04
	Living	8.307	6.65
<b>WWR=90%</b>	Bedroom_1	9.68175	8.71
	Bedroom_2	8.80425	7.92
	Living	8.307	7.48

### 3.2.10.2 Infiltration through Windows Cracks Analysis

The values for rectangular windows and doors established by Technical regulation for energy efficiency labelling of residential buildings, RTQ-R (INMETRO, 2012) for modeling the parameters related with the infiltration through windows cracks (Table 26) were applied.

Table 26: Values for rectangular windows and doors established by RTQ-R for modeling the parameters related with infiltration

Discharge Coefficient ( $C_D$ )	0.6
Air Mass Flow Coefficient when opening is closed ( $C_a$ )	0.001 kg/s.m
Air Mass Flow Exponent when opening is closed ( $n$ )	0.65

Source: Adapted from INMETRO, 2012.

### 3.2.10.3 Effective Window Ventilation Area

It represents the area of the window destined for ventilation. This parameter also varied continuously from 50% to 100%, symbolizing respectively a sliding and casement windows. This building feature variation occurred only in the long-stay room's windows and it was possible by ranging the field "Width Factor for Opening Factor 2" in "AirflowNetwork: Multizone: Component: DetailedOpening" group from 0.5 to 1.0 (see item 3.3 Natural ventilation modeling (d)).

## 3.3 NATURAL VENTILATION MODELING

This item comprehends all description of natural ventilation modeling as well as a benchmark test to evaluate the impact on a LCH's thermal comfort of using surface-average instead of local wind pressure coefficients.

### 3.3.1 Airflow Network Inputs

The natural ventilation was modeled in Airflow Network group in EnergyPlus, using the following objects: (a) Airflow Network: Simulation Control; (b) Airflow Network: Multizone: Zone; (c) Airflow Network: Multizone: Surface; and (d) Airflow Network: Multi Zone: Component: Detailed Opening.

#### (a) Airflow Network: Simulation Control

Table 27 summarizes the input data for this object, where parameters that control air flow calculations are defined.

Table 27: Overview of Airflow Network Inputs : Simulation Control.

FIELD	OBJECT
Name	NATURAL_VENTILATION
Airflow Network Control	Multizone Without Distribution
Wind Pressure Coefficient Type	Surface Average Calculation
Airflow Network Wind Pressure Coefficient Array Name	
Height selection for Local Wind Pressure Calculation	
Building Type	Low Rise
Maximum Number of Iterations [dimensionless]	500
Initialization Type	Zero Node Pressures
Relative Airflow Convergence Tolerance [dimensionless]	0.0001
Absolut Airflow Convergence Tolerance [kg/s]	0.000001
Convergence Acceleration Limit [dimensionless]	-0.5
Azimuth Angle of Long Axis of Building [deg]	<b>VARIABLE</b>
Ratio of Building Width Along Short Axis to Width Along Long Axis	0.67

Source: Adapted from EERE, 2014.

The building was considered as multizone without distribution, once there was no air distribution system. Surface-average pressure coefficients ( $C_p$ ) were adopted in simulations, according to the benchmark test reported in item "3.3.2 Impact of using surface-average instead of local wind pressure coefficient on thermal comfort analysis". Default values were attributed for parameters related with initialization calculation type, convergence tolerance (relative or absolute), and convergence acceleration limit. Azimuth Angle of Long Axis of Building [deg] indicates the building orientation, which is variable in simulations as function of North Axis (see section 3.2.4 North Axis/ Orientation in the terrain). Finally, the Ratio of Building Width along Short Axis to Width along Long Axis informs the building geometric proportion.

#### (b) Airflow Network: Multizone: Zone

Table 28 illustrates the adopted input data for Airflow Network: Multizone: Zone.

Table 28: Overview of Airflow Network Inputs: Multizone: Zone

FIELD	OBJECT
Name	PLAN_FLOOR
Ventilation Control Mode	Temperature
Ventilation Control Zone Temperature Setpoint Schedule Name	Setpoint_ventilation_year
Minimum Venting Open Factor [dimensionless]	
Indoor and Outdoor Temperature Difference Lower Limit For Maximum Venting Open Factor [deltaC]	
Indoor and Outdoor Temperature Difference Upper Limit for Minimum Venting Open Factor [deltaC]	100
Indoor and Outdoor Enthalpy Difference Lower Limit For Maximum Venting Open Factor [deltaJ/kg]	
Indoor and Outdoor Enthalpy Difference Upper Limit for Minimum Venting Open Factor [deltaJ/kg]	300000
Venting Availability Schedule Name	ventilation

Source: Adapted from EERE, 2014a.

The ventilation mode that ruled the ventilation occurrence in the zones and in the surfaces was **TEMPERATURE**. It means that natural ventilation will occur only if the three following requirements are met simultaneously:

- If the zone temperature is higher than outdoor air temperature (**T<sub>ZONE</sub> > T<sub>OUTDOOR</sub>**) and;
- If the zone temperature is greater than set point temperature (**T<sub>ZONE</sub> > T<sub>SET POINT</sub>**) and;
- If the venting availability schedule allows ventilation occurrence (**Schedule = 1**).

Set point temperature is equals to the adaptive comfort temperature calculated according to ASHRAE 55-2013 (ASHRAE, 2013) (see item 3.1.3 Thermal Comfort Evaluation Method) and varied among the analyzed climates. The venting availability schedule permitted the ventilation from 7 a.m. to 10 p.m. in simulations.

**(c) Airflow Network: Multizone: Surface**

Table 29 presents examples of the data considered in surfaces' modeling.

Table 29: Overview of Airflow Network Inputs: Multizone: Surface.

FIELD	OBJECT_1	OBJECT_2
Surface Name	bdr_1_Mwin_wall_b	lvrk_door_wall_a
Leakage Component Name	detail_Mwin_BDR_1	detail_door
External Node Name		
Window/Door Opening Factor, or Crack Factor [dimensionless]	1	1
Ventilation Control Mode	Temperature	Constant
Ventilation Control Zone Temperature Setpoint Schedule Name	Setpoint_ventilation_year	
Minimum Venting Open Factor [dimensionless]		

Table 29 : Overview of Airflow Network Inputs: Multizone: Surface (continuation).

Indoor and Outdoor Temperature Difference Lower Limit For Maximum Venting Open Factor [deltaC]		
Indoor and Outdoor Temperature Difference Upper Limit for Minimum Venting Open Factor [deltaC]	100	100
Indoor and Outdoor Enthalpy Difference Lower Limit For Maximum Venting Open Factor [deltaJ/kg]		
Indoor and Outdoor Enthalpy Difference Upper Limit for Minimum Venting Open Factor [deltaJ/kg]	300000	300000
Venting Availability Schedule Name	ventilation	Natural_ventilation_constant_off

Source: Adapted from EERE, 2014a.

The surface object enables an individual characterization of all leakage surfaces – associated with heat transfer surfaces as walls, roofs, or subsurfaces as doors, windows – through which the air flows. If such group is specified it can be used to override the ventilation control of the zone level (EERE, 2014b). All windows or doors opening factors were set up to 1 indicating that they are openable.

All openings (for example, detail\_Mwin\_BDR\_1) were controlled by temperature, except the exterior doors (for example, detail\_door), which presents constant controls and venting availability schedule always equals to 0 that means these doors were considered closed during all simulations. The analyzed model did not comprise internal doors, once all thermal zones were classified under the same zone, characterizing a single zone model (see section 3.2.3 Thermal Zone Definition).

#### (d) Airflow Network: Multi Zone: Component: Detailed Opening

All characteristics for this object are summarized in Table 30.

Table 30: Overview of Airflow Network Inputs: MultiZone: Component: Detailed Opening.

FIELD	OBJECT_1	OBJECT_2	OBJECT_3
Name	detail_Mwin_BDR_1	detail_door	detail_win_bth
Air Mass Flow Coefficient When Opening is Closed [kg/s.m]	0.001	0.001	0.001
Air Mass Flow Exponent When Opening Is Closed [dimensionless]	0.65	0.65	0.65
Type of Rectangular Large Vertical Opening (LVO)	NonPivoted	NonPivoted	HorizontallyPivoted
Extra Crack Length or Height of Pivoting Axis	0	0	0.3

Table 30: Overview of Airflow Network Inputs: MultiZone: Component: Detailed Opening (continuation).

Number of Sets of Opening Factor Data	2	2	2
Opening Factor 1	0	0	0
Discharge Coefficient for Opening Factor 1	0.001	0.001	0.001
Width Factor for Opening Factor 1	0	0	0
Height Factor for Opening Factor 1	0	0	0
Start Height Factor for Opening Factor 1	0	0	0
Opening Factor 2	1	1	1
Discharge Coefficient for Opening Factor 2	0.6	0.6	0.6
Width Factor for Opening Factor 2	<b>VARIABLE</b>	1	1
Height Factor for Opening Factor 2	1	1	1
Start Height Factor for Opening Factor 2	0	0	0

Source: Adapted from EERE, 2014a.

This object specifies the following openings' characteristics as well as the particularities of the air that flows through them:

- **air mass flow coefficient** and **air mass flow exponent** when the window is closed: 0.001 kg/s.m and 0.65, respectively, according to the Technical Regulation for Energy Efficiency Labelling of Residential Buildings (RTQ-R).
- There are two possibilities in EnergyPlus to describe window types: **non-pivoted** and **horizontally-pivoted**. The first option was utilized to describe the windows of kitchen and the long-stay rooms (representing sliding and casement windows situations) as well as the exterior doors. On the other hand, the second type was applied exclusively to the window of bathroom to specify a pivoted window case.
- It is necessary to model at least two **opening factor data**, for these reason it was adopted two situations, the first one when the windows were fully closed (0) and secondly when such elements were totally open (1).
- **discharge coefficients**: 0.6 for rectangular-shaped windows or doors were also used according to the Technical Regulation for Energy Efficiency Labelling of Residential Buildings (RTQ-R).
- For each open factor situations, some metrics as **width factor**, **height factor**, and **start height factor** need to be defined to characterize the effective opening area for ventilation. These factors were calculated according to the equations present in Figure 21. As the proposed windows always open their total height dimension, the effective area for ventilation was adjusted based on changes in width factor. The effective area for ventilation of long-stay rooms varied continuously from 50% to 100%,

consequently the width factor from 0.5 to 1.0. The exterior doors, the kitchen and bathroom windows had its geometric factor kept fixed during the simulations.

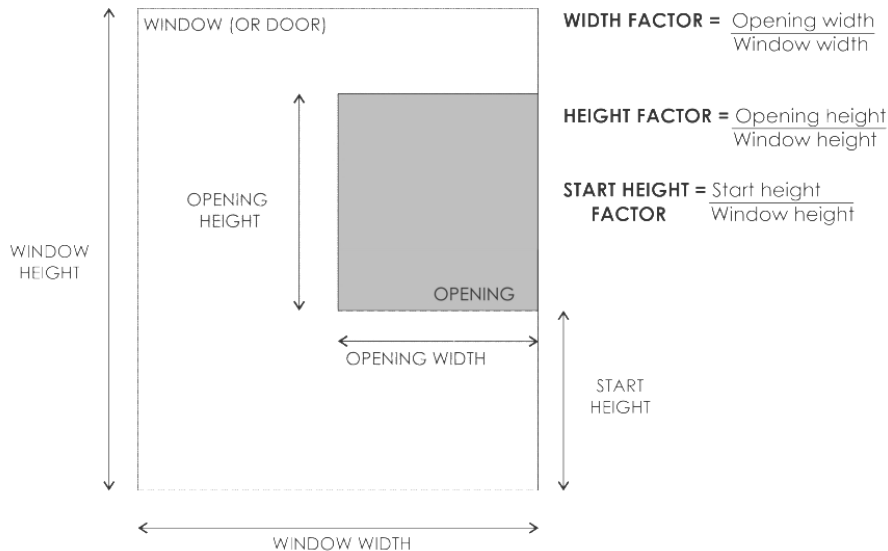


Figure 21: Geometric factors of the openings (windows and doors).  
Source: Adapted from EERE, 2014b.

### 3.3.2 Impact of Using Surface-Average Instead of Local Wind Pressure Coefficients on the Thermal Comfort Analyses

EnergyPlus has a wind pressure database only for rectangular-shaped geometries. For simulating other building shape is necessary to input such coefficients; however this task is time-consuming and hard to apply in parametric simulations. The  $C_p$  values can be obtained through wind tunnel experiments, in specific literature or using complementary computer programs. This fact is pointed out as a limitation of the natural ventilation simulation through EP, because even for rectangular geometries, the calculation provides a surface-average wind pressure coefficient value for each facade and for the roof. It is known that  $C_p$  varies along the building facade, but is unknown how the assumption of surface-average  $C_p$  impacts in simulation results.

Cóstola et al. (2010) developed a study to estimate the uncertainty due to use surface-average  $C_p$  values (AV) instead of local  $C_p$  values (LOC) in the calculation of airflow rate ( $\phi$ )<sup>22</sup>. According to those authors some studies (SWAMI; CHANDRA, 1987; WIREN, 1985) pointed out that even though the surface-average values were generated based on particular cases studies; they do not significantly reduce the accuracy of airflow rates

<sup>22</sup> The  $C_p$  data applied in this study were provided from "The Tokyo Polytechnic University (TPU) wind database" (QUAN et al., 2007).



calculations. Another one emphasized that surface-average  $C_p$  values do not correspond to the accuracy required by air-flow calculation models (FEUSTEL, 2005).

Therefore, focusing on wind-drive ventilation, 15 geometries with one internal zone and various configurations of two identical openings were tested, regarding different wind attack angles. The buoyancy was not considered. The main conclusion indicated that the uncertainty<sup>23</sup> was high ( $0.23 \phi_{AV} < \phi_{LOC} < 5.07 \phi_{AV}$ ). Additionally, the underestimation or overestimation, in cases with greatest variation of surface-averaged  $C_p$  values, was small, but it needs to be considered ( $0.52 \phi_{AV} < \phi_{LOC} < 1.42 \phi_{AV}$ ) (CÓSTOLA ET AL., 2010).

Recognizing the possible consequences due to the adoption of surface-average  $C_p$  values (AVCp) instead of local  $C_p$  values (LOCCp), the present study aims to evaluate the differences in the thermal evaluation between both approaches for a same geometry. EnergyPlus was applied to simulate the thermal performance of a representative naturally ventilated Brazilian LCH, regarding three Brazilian cities: Curitiba/PR, São Paulo/SP, and Manaus/AM (see section 3.1.4 Weather analysis).

Table 31 shows the input data of the simulations. The same base model (see sections 3.2.1 Geometry and 3.2.2 Windows Distribution Definition) were considered. Exceptions regard the roof geometry (flat instead of gable roof), thermal zone definition (multizone<sup>24</sup> instead of single zone model), and the windows distribution. The building orientation and the windows distribution were fixed in simulations. They were defined in order to achieve the highest pressure differential between windward and leeward buildings' facades (Table 31). Material construction systems and their properties as well as fenestrations' dimensions were set up according to the usual characteristics applied in Brazilian LCH. Internal gains and their routines, some natural ventilation modeling features and ground temperatures were defined as shown in items: 3.2.9, 3.2.10.2, and 3.2.6, respectively.

The wind pressure coefficients types considered were: surface-average calculation (AVCp) and input (LOCCp). AVCp was automatically calculated by the program. LOCCp were entered by the user and they are linked to external nodes. The wind data was obtained from Catavento (RORIZ; RORIZ, 2015) software that uses mainly the wind database from The Tokyo Polytechnic University (TPU) for the local  $C_p$  values generation. Natural ventilation was permitted during all day in simulations.


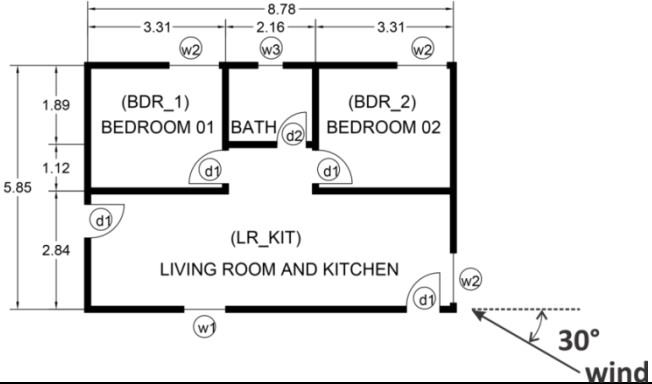
Each window displayed in the geometry was modelled as two windows. This approach made possible to include two LOCCp values for each analysed window. One LOCCp value located at the centroid of each part.

---

<sup>23</sup> The uncertainty was evaluated by comparing the airflow rate obtained due to the calculation using the surface-averaged  $C_p$  values with the airflow rate considering local  $C_p$  values. No simulations were performed. A confidence interval of 95% was applied.

<sup>24</sup> Each room was described as a separate zone in the analyzed multizone model.

Table 31: Summary of the input data.

INPUTS	
	
CLIMATE FEATURES AND BUILDING ORIENTATION	
Climates Weather File Building Orientation (North Axis Angle)	Curitiba /PR   São Paulo/SP   Manaus/AM (see item 3.1.4) EPW (Roriz, 2012 c) Curitiba /PR: 240°   São Paulo/SP: 260°   Manaus/AM: 240°
MATERIALS THERMAL PROPERTIES AND CONSTRUCTION SYSTEMS OF BUILDING OPAQUE ENVELOPE	
U-value	Roof System (Roof + Ceiling) U= 1.79W/ (m <sup>2</sup> . K) External Walls U= 2.78W/ (m <sup>2</sup> . K) Internal Walls U= 2.23W/ (m <sup>2</sup> . K) Base U= 3.08 W/ (m <sup>2</sup> . K)
Heat Capacity	Roof System (Roof + Ceiling) HC= 185 KJ/ (m <sup>2</sup> . K) External Walls HC= 209 KJ/ (m <sup>2</sup> . K) Internal Walls HC= 209 KJ/ (m <sup>2</sup> . K) Base HC= 281 KJ/ (m <sup>2</sup> . K)
Solar Absorptance	External Walls 0.3 (DORNELLES, 2008) Roof 0.75 (ABNT,2005)
FENESTRATIONS DIMENSIONS (width x height / windowsill) [m]	
W1	1.0 x 1.0 / 1.1
W2	1.2 x 1.0 / 1.1
W3	0.6 x 0.6 / 1.5
D1	0.8 x 2.1
D2	0.7 x 2.1
INTERNAL GAINS and ROTINES	
Electric Equipment/ People/Lights	See item 3.2.9
NATURAL VENTILATION MODELING	
Ventilation Control Mode Venting Availability Schedule Set point Temperature Discharge Coefficient (C <sub>D</sub> ) / Air Mass Flow Coefficient C <sub>Q</sub> / Air Mass Flow Exponent (n) Terrain type	Temperature for windows and Constant for interior (always opened) and exterior doors (always closed). 24hs/day Variable according to climate, equals to Comfort Temperature See item 3.2.10.2 See item 3.2.5
WIND PRESSURE COEFFICIENTS TYPE	<b>VARIABLE:</b> SURFACE-AVERAGE CALCULATION (EnergyPlus data) or INPUT (Catavento software data).
ADDITIONAL DATA	
Ground Temperature	Variable according to the climate. See item 3.2.6

Only the simulation results of long-stay rooms (bedrooms and living-room) are shown. The complete investigation will be showed in ROSSI et al. (2016) in elaboration<sup>25</sup>.

Figure 22 summarizes the distribution during a year, regarding the three analyzed cities, of three cases: (A) when both models (LOCCp and AVCp) are venting; (B) when none models are venting; and (C) when one model is venting and other is not.

Overall, the coldest and the intermediate climates showed the greater amount of hours concentrated on case B (about 8200 hours in Curitiba). It occurs probably because the restriction established by the ventilation control mode by temperature that did not allow ventilation during many hours. On the other hand, in Manaus it was possible to verify more hours in which both models are venting (about 5600 hours for bedrooms and 5200 for LR\_KIT). All Brazilian locations showed very small values for case C.

The results also compared the differences in predictions between each long-stay room of LOCCp and AVCp models ( $\Delta = LOCCp_{ROOM} - AVCp_{ROOM}$ ). Based on that, a positive value shows that LOCCp model overestimates the predictions of AVCp and a negative value indicates an opposite situation. The comparisons considered three standpoints: (a) the air changes per hour, (b) the air temperature, and finally (c) the operative temperature. All analyses considered only the moments that the referred zone is venting in both models.

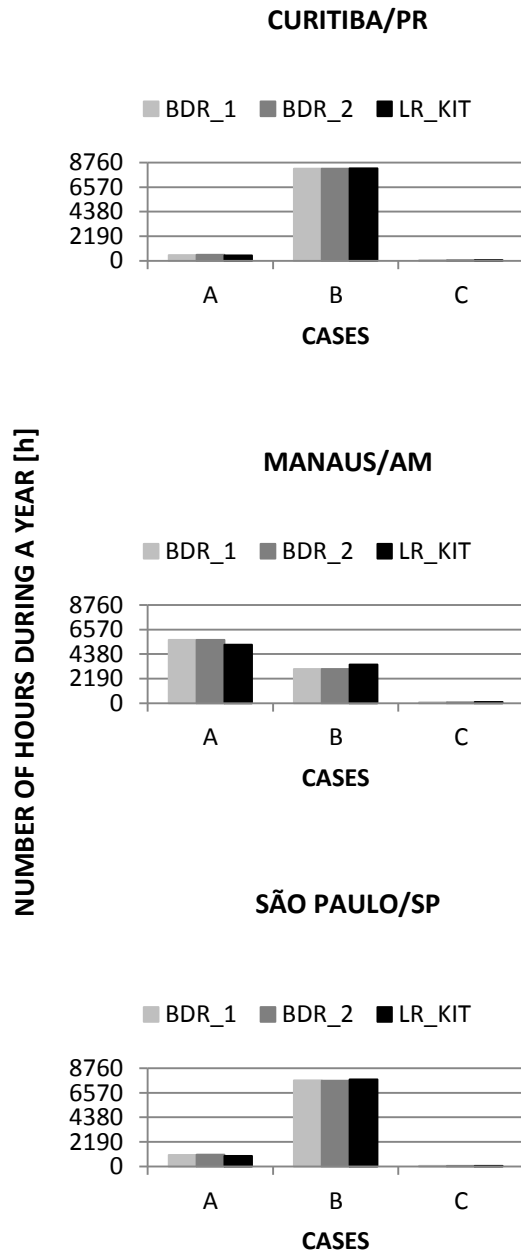


Figure 22: Distribution of number of hours along the year that both models (LOCCp and AVCp) are venting (Case A), none is venting (Case B) and when one is venting and other is not (Case C).

<sup>25</sup> ROSSI, M.M. et al. **Impact of using surface-average instead of local wind pressure coefficients on the thermal comfort analysis of a naturally ventilated Brazilian low-cost house.** In elaboration. 2015.

## Air Changes per Hour

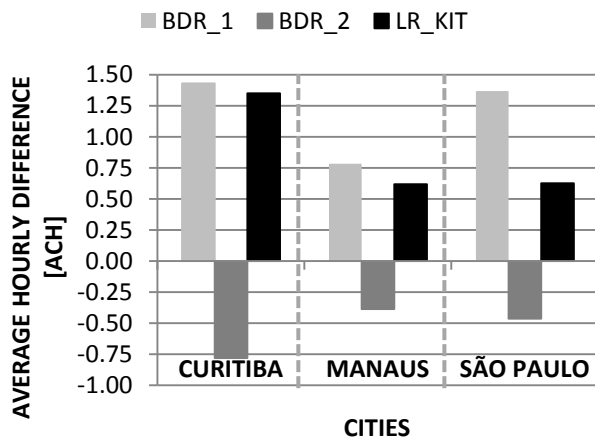


Figure 23: Annual average hourly air changes per hour rate differences between each long-stay room of LOCCp and AVCp models.

Figure 23 shows the average annual hourly difference in air changes per hour rates between LOCCp and AVCp models. For all analyzed climates the greater differences were shown for BDR\_1, with the maximum value being 1.43 ach for Curitiba. The BDR\_2 presents for all locations an overestimate pattern of AVCp model. In contrast to that LR\_KIT showed positive values for all cities

To sum up, average hourly differences in air changes per hour rates were observed in all climates. However, it is important to verify how much such differences impact on the thermal comfort analysis, for this reason the same analysis were conducted for air and operative temperatures.

## Air Temperature

Figure 24 shows the air temperature average hourly differences between LOCCp and AVCp models. Besides the previous analysis compared differences in air change per hour rates between the two modeling approaches, such discrepancies were not enough to impact in air temperature. Both climates shows very small values, with the minimum and the maximum differences being  $-0.005^{\circ}\text{C}$  for BDR\_2 and  $-0.062^{\circ}\text{C}$  for BDR\_1 both in Curitiba, respectively.

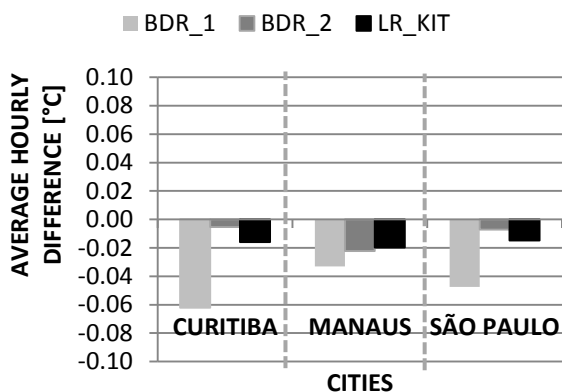


Figure 24: Annual average hourly air temperature differences between each long-stay room of LOCCp and AVCp models.

The higher differences occurred in BDR\_1 for all analyzed cities. This information agreed with the greater differences observed in air change per hour analysis. In all cities the AVCp model overestimates the LOCCp model when air temperature predictions were observed.

**Operative Temperature**

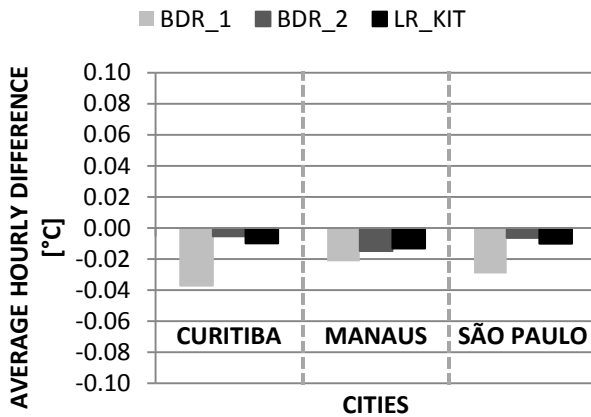


Figure 25: Annual average hourly operative temperature differences between each long-stay room of LOCCp and AVCp models.

Figure 25 presents the average hourly operative temperature differences. The same pattern identified in air temperature analysis was also shown on it. The greater differences were in BDR\_1 and the lower in some cases for BDR\_2 (for Curitiba and São Paulo) and for LR\_KIT in Manaus. The maximum difference value observed was -0.037°C and the minimum value was -0.005°C for BDR\_1 and BDR\_2 in Curitiba, respectively.

Besides the differences in air change per hour rates considering the both modeling approaches (LOCCp and AVCp models), the results showed very small differences in comparisons for air and operative temperatures. Due to the small differences found, it is possible to conclude that for the analyzed geometry and cities, the AVCp could be applied in place of LOCCp to simplify the simulation during early design, when the thermal comfort analysis is considered. However, further studies need to be conducted to verify the accuracy of such simplification in simulation process when airflow rates are studied.

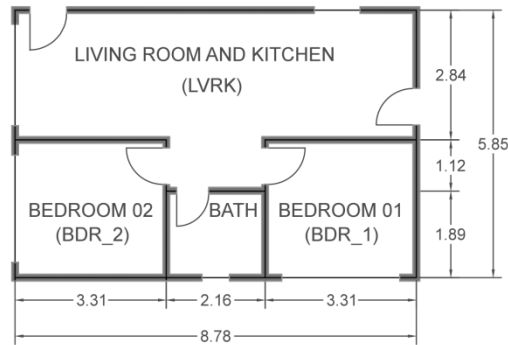
**3.4 INPUT AND OUTPUT DATA SUMMARY**

Table 32 summarizes the main input data in simulation. Detailed information about each parameter was already described in its specific subitem in this section.

Table 32: Input data summary.

INPUTS			
CLIMATE FEATURES AND BUILDING ORIENTATION			
Climates	Curitiba /PR   São Paulo/SP   Manaus/AM		
Weather File	EPW (Roriz, 2012 c)		
Building Orientation	<b>Variable</b> in function of North Axis (from 0° to 359°)		
BUILDING GEOMETRIC FEATURES			
<b>Type:</b> Detached unit	<b>Ceiling Height:</b> 2.925 m	<b>Area:</b> 51.33 m <sup>2</sup>	<b>Geometric Proportion <sup>(1)</sup>:</b> 0.67

Table 32: Input data summary (continuation).



Floor Plan

MATERIALS THERMAL PROPERTIES AND CONSTRUCTION SYSTEMS OF BUILDING OPAQUE ENVELOPE		
U-value	Roof System (Roof + Ceiling)	<b>Variable</b> U= from 0.5 to 2.1 W/ (m <sup>2</sup> . K)
	External Walls Internal Walls	<b>Variable</b> U= from 0.3 to 5.0 W/ (m <sup>2</sup> . K)
	Base	U= 3.08 W/ (m <sup>2</sup> . K)
Heat Capacity	Roof System (Roof + Ceiling)	<b>Variable</b> HC= from 11 to 791 KJ/ (m <sup>2</sup> . K)
	External Walls Internal Walls	<b>Variable</b> HC= from 40 to 455 KJ/ (m <sup>2</sup> . K)
	Base	HC= 281 KJ/ (m <sup>2</sup> . K)
Solar Absorptance	External Walls and Roof	<b>Variable</b> (from 0.1 to 1)
FENESTRATIONS <sup>(2)</sup>		
Glass	Thickness	4 mm
	Color	Clear
Door	Thickness	3.5 cm
	Material	Wood
Window-to-Wall Ratio	<b>Variable</b> (from 10% to 90%)	
SHADING DEVICES		
Eaves of 0.5 m in all building facades		
Overhangs	<b>Variable</b> sizes (see Table 19)	
Fins	<b>Variable</b> sizes and positions (see Table 19)	
OCCUPANCY <sup>(3)</sup>		
4 people		
INTERNAL GAINS <sup>(3)</sup>		
Electronic Equipments	1.5 W/m <sup>2</sup> (living-room)	
People	108 W (sitting) or 81 W (sleeping)	
Lighting	4 W/m <sup>2</sup> (bedrooms)/ 5 W/m <sup>2</sup> (living-room)	
ROTINES <sup>(3)</sup>		
Electronic Equipments	Only for living-room: 24 hs/day	
Occupancy	See table 22	
Lights	See table 24	
NATURAL VENTILATION <sup>(4)</sup>		
Ventilation Control Mode	Temperature	
Venting Availability Schedule	From 7 a.m. to 10 p.m.	
Ventilation Control Zone Temperature	<b>Variable</b> according to climate (equals to Comfort Temperature calculated based on ASHRAE 55-2013)	
Setpoint		

Table 32: Input data summary (continuation).

ADDITIONAL DATA	
Ground Temperature	Variable according to the climate
(1) Ratio of Width and Length of the analyzed building.	
(2) The Window-to-Wall Ratio (WWR) is calculated only for long-stay rooms' windows.	
(3) The routines and values used to describe the internal gains of the analyzed building was according to RTQ-R (INMETRO, 2012) values. Detailed information about these assumptions is presented in the item 3.2.9 – Internal Gains of this document section.	
(4) Detailed information about Natural Ventilation is described in the item 3.3 – Natural Ventilation Modeling of this document section.	

The all required outputs are listed below in Table 33. The highlighted rows refer to the outputs considered in the result analysis process.

Table 33: Output data summary.

OUTPUTS
Site Outdoor Air Drybulb Temperature [C](Hourly)
Site Outdoor Air Relative Humidity [%](Hourly)
Site Wind Speed [m/s](Hourly)
Site Wind Direction [deg](Hourly)
Site Outdoor Air Density [kg/m3](Hourly)
Zone People Total Heating Rate [W](Hourly)
Zone Lights Total Heating Rate [W](Hourly)
Zone Electric Equipment Total Heating Rate [W](Hourly)
Zone Windows Total Heat Gain Rate [W](Hourly)
Zone Windows Total Heat Loss Rate [W](Hourly)
Surface Inside Face Conduction Heat Transfer Rate [W](Hourly)
Surface Heat Storage Gain Rate [W](Hourly)
Surface Heat Storage Loss Rate [W](Hourly)
Zone Mean Air Temperature [C](Hourly)
Zone Operative Temperature [C](Hourly)
Zone Mean Air Humidity Ratio [kgWater/kgDryAir](Hourly)
Zone Air Heat Balance Outdoor Air Transfer Rate [W](Hourly)
AFN Node Total Pressure [Pa](Hourly)
AFN Node Total Pressure [Pa](Hourly)
AFN Node Wind Pressure [Pa](Hourly)
AFN Surface Venting Window or Door Opening Factor [] (Hourly)
AFN Surface Venting Window or Door Opening Modulation Multiplier [] (Hourly)
AFN Surface Venting Inside Setpoint Temperature [C](Hourly)
AFN Surface Venting Availability Status [] (Hourly)
AFN Zone Infiltration Sensible Heat Gain Rate [W](Hourly)
AFN Zone Infiltration Sensible Heat Loss Rate [W](Hourly)
AFN Zone Infiltration Air Change Rate [ach](Hourly)
Zone Air Relative Humidity [%](Hourly)
Schedule Value [] (Hourly)





## 4 MONTE CARLO SIMULATION

---

### 4.1 INTRODUCTION

The Monte Carlo method is applied to capture the global sensitivity in model predictions (LOMAS; EPPEL, 1992). This computational method performs statistical sampling experiments to estimate simulation output uncertainty that is sensitive to model input and parameter values.

When building performance simulation is applied as a decision support tool to assist in the design process, sensitivity analysis assists the design team to identify with more security the alternatives and parameters that most impact on building energy consumption or thermal performance. It also contributes to verify the accuracy of simulation outputs (WESTPHAL, 2007). This analysis may present different sensitivity levels, considering an individual study of each parameter or a global of all variables involved (LOMAS; EPPEL, 1992).

Once the inputs are altered simultaneously, the uncertainty related to the individual input parameter cannot be measured. The global sensitivity analysis assesses the evaluation of: (a) the accuracy of the adopted simulation program; (b) the significance of uncertainties due the input data, different algorithms or modelling approaches; and (c) the probability of results distribution (LOMAS; EPPEL, 1992).

The Monte Carlo simulation accuracy does not depend on the number of input variables. Otherwise, it is related with the simulations' number, which should be greater than 60 to 80 simulations (LOMAS; EPPEL, 1992). Macdonald (2002) points out 80 simulations as a typical value when this method is applied. Hygh et al. (2012), using Monte Carlo coupled with EnergyPlus, performed 20000 simulations to cover significantly the sample space. However, the notable decreased was observed in prediction error, considering the interval of 50 to 200 samples and it became imperceptible after about 500 samples.

### 4.2 MONTE CARLO SIMULATION APPLICATION

The Monte Carlo Simulation was applied to randomly sample the building design space to be explored, to quantify the global uncertainties, and to generate a statistically representative set of design cases for EnergyPlus simulations. Consequently, the base model, the key parameters relevant to conceptual design, and their selected ranges were the input for this stage. In parallel, a cluster of computer processors enabled the Monte Carlo Simulation runs.

A developed programming code promoted the sampling and the substitution routines derived from Monte Carlo Simulations in the appropriate places in the base models. Therefore, it allowed parametric simulations on EnergyPlus, – by randomly testing

combinations of parameters values within their previously established ranges and replacing such values for the defaults in the base model – generating a number of input data files (IDFs) equals to the Monte Carlo Simulation set. Annual EnergyPlus simulations considered all samples for each analyzed location.

A performance metric was implemented in EnergyPlus simulation outputs through other programming code, in order to calculate the monthly and annual degree-hours of discomfort by heat and by cold for each analyzed case. Two different CSV files, the “Parameter Domains” and the “Performance Metric”, summarized the EnergyPlus inputs and outputs, respectively. These files were the input for the following stage, Multivariate Regression.

This Monte Carlo Simulation is divided in sub parts: (a) Parameter Files; (b) Sampling and substitution routines and EnergyPlus Simulations; (c) Parameter Domains and (e) Performance Metric, which are explained in details below.

#### 4.2.1 Parameter Files

The delineation of the key design parameters and their ranges during the Design Problem Definition stage supported the development of the files for each analyzed city with minimum and maximum values, totalizing six IDF files (Figure 26).

These files comprised the minimum and maximum correspondent values for each variable parameter,

and also the fixed values to geometry, schedules, internal gains, among others. In conclusion, the IDF files for each climate were exactly the same, except for the ground temperature, natural ventilation set point temperature, and the weather file used for running the simulation.

After the IDF files generation, the variable parameter domains were identified. These domains consist in text files, which describe the EnergyPlus object name, the group, the location lines in the base files, and also the acceptable interval values associated with each parameter (Figure 27). In conclusion, a total of 27 domain files were created.

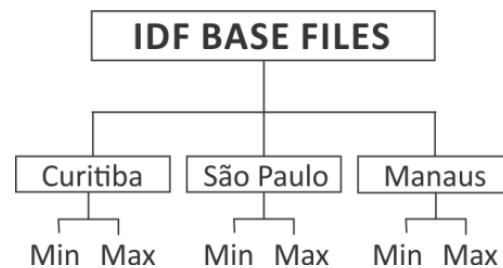


Figure 26: Generated IDF files.

#vary the Bdr\_1 Window-to-Wall Ratio in function of the edges coordinates

```
Type=FenestrationSurface:Detailed
Name.1=bdr_1_Mwin_wall_b
field=10
min=-6.59620983892095
max=-5.55462425394262
field=12
min=1.92536592784174
max=2.84580031940115
field=13
min=-6.59620983892095
max=-5.55462425394262
field=15
min=0.999634072158254
max=0.0791996805988478
field=16
min=-7.64379016107902
max=-8.68537574605736
field=18
min=0.999634072158254
max=0.0791996805988477
field=19
min=-7.64379016107902
max=-8.68537574605736
field=21
min=1.92536592784174
max=2.84580031940115
```

Figure 27: Example of a domain file.

#### 4.2.2 Sampling and Substitution Routines and EnergyPlus Simulations

Monte Carlo Simulation sampling thoroughly considered each parameter and their defined range and then, replaced these values in the base model files. The IDF files were updated by Python scripts (YANG; 2015a), which were developed to include some expressions that identified the EnergyPlus objects (by name and type) and replaced them.

Several tests certified the programming code was modifying the IDF properly. Two hundred IDF files were manually revised with aiding of a computational tool, Diff Marge, which recognizes the differences between the IDF files generated by code from the IDF files (minimum and maximum). After testifying the code accuracy, an amount of 30000 IDF files (10000 for each climate) were generated to be simulated on EnergyPlus. In parallel on 656 cores, 21nodes Linux cluster, a full annual EnergyPlus iteration was performed for each model instance.

### 4.2.3 Parameter Domains

The Parameter Domains (CSV file) summarized the input values considered in each EnergyPlus run. The columns describe the key design parameters and the rows the simulation cases (Table 34). Three Parameter Domains files were generated, one for each analyzed Brazilian location.

Table 34: Parameter Domain file example.

idf #	detail_Mwin_BDR_1/AirflowNetwork:MultiZone:Component:DetailedOpening/detail_Mwin_BDR_1/13	detail_Mwin_BDR_2/AirflowNetwork:MultiZone:Component:DetailedOpening/detail_Mwin_BDR_2/13	detail_Mwin_LVRK/AirflowNetwork:MultiZone:Component:DetailedOpening/detail_Mwin_LVRK/13
0	0.650977	0.823429	0.537996
1	0.982739	0.796357	0.624508
2	0.968553	0.862398	0.566524
3	0.865212	0.622676	0.938664
4	0.684847	0.780641	0.659679
5	0.681139	0.951002	0.599367

### 4.2.4 Performance Metric

As aforementioned, a programming code (YANG, 2015b) captured the results that were used to calculate the building thermal discomfort from EnergyPlus outputs and also performed the metric to compute it.

In the present study, the degree-hours ( $^{\circ}\text{Ch}$ ) were based on the comfort range bounded by upper and lower comfort limits (Figure 28) defined by the Adaptive Approach from ASHRAE 55-2013 (ASHRAE, 2013). Therefore, the number of degrees when the hourly average operative temperature was above the upper comfort limit indicates the degree-hour ( $^{\circ}\text{Ch}$ ) of discomfort by heat, DHH (Equation 5). When below the lower limit, the  $^{\circ}\text{Ch}$  of discomfort by cold, DHC, was calculated (Equation 6).

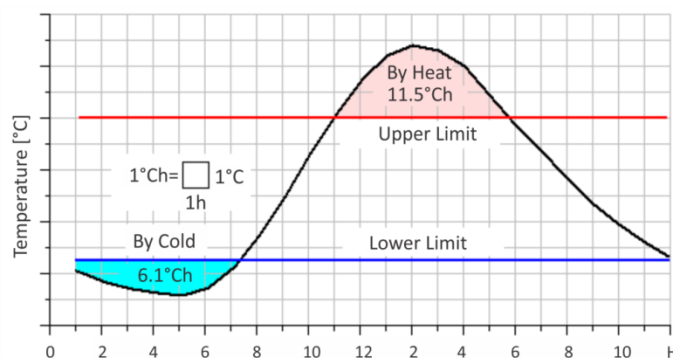


Figure 28: Degree hours of discomfort. Source: Adapted from RORIZ; CHVATAL; CAVALCANTI, 2009.

$$DHH = \sum_{i=1}^{8760} \{if\ To > Up | (Up - To)if\ To < Up | (0)\} \tag{Equation 5}$$

$$DHC = \sum_{i=1}^{8760} \{if\ To < Low | (Low - To)if\ To > Low | (0)\} \tag{Equation 6}$$

Source: Adapted from SILVA; ALMEIDA; GHISI, 2015.

Where:

**DHH:** Degree-hours of discomfort by heat [°Ch];

**DHC:** Degree-hours of discomfort by cold [°Ch];

**To:** hourly operative temperature [°C];

**Up:** Upper comfort limit calculated according ASHRAE 55-2013 [°C];

**Low:** Lower comfort limit calculated according ASHRAE 55-2013 [°C].

Finally, the Performance Metric files report monthly and annual discomfort by heat and by cold for the outdoor and indoor environments for each model instance (Table 35).

The Parameter Domains (EnergyPlus inputs) and the Performance metric (EnergyPlus outputs) composed the inputs for the next stage, Multivariate Regression.

Table 35: Performance Metric file example.

idf#	Year_HeatDisc Outdoor	Year_ColdDisc Outdoor	Year_HeatDisc Indoor	Year_ColdDisc Indoor
0	579.186	17917.56	0	1889.387
1	579.186	17917.56	148.208	2531.24
2	579.186	17917.56	162.911	3293.732
3	579.186	17917.56	55.39344	2018.425
4	579.186	17917.56	0	2369.178
5	579.186	17917.56	2.139482	3284.381



## 5 MULTIVARIATE REGRESSION

---

### 5.1 INTRODUCTION

The results from Monte Carlo Simulation were the input for the Multivariate Regression. They composed a rich set of 10000 samples for each analyzed city. From this large database, 60% was used to develop the regression models and the remaining 40% to validate them. Multivariate linear regression was applied with aid of Matlab® tool (MATHWORKS, 2013a) in order to provide approximate equations that can assess the thermal performance of a Brazilian LCH as function of design parameters, regarding the three climates. Therefore, the ultimate goal of this work is to apply such models as a support tool in place of robust simulations during early design. Decisions about the number of samples and also the proportion applied in the generated database were based on previous studies (AL GHARABLY; DECAROLIS; RANJITHAN, 2015; HYGH et al., 2012).

Multivariate Regression is divided in three sub items: (a) Regression models' development, (b) Regression models' validation and, (c) Regression models' application. Each item is explained in details below.

### 5.2 REGRESSION MODELS' DEVELOPMENT

The stepwise regression was used to systematically add or remove the design parameters from the regression model, based on their statistical significance (MATHWORKS, 2013b). This technique starts with an initial model and at each step a term is added or removed from the model after its p-value was computed. The p-value demonstrates the potential of the term in explaining the predictable variable. The adopted p-enter and p-remove values were 0.05 and 0.10, respectively. Therefore, if a term is included in the regression model (p-value < 0.05) a coefficient value will be determined for it, however if it is not included (p-value > 0.10) a 0 value will be designated.

The regression models were developed by applying two functions of stepwise regression in Matlab® (MATHWORKS, 2013a): *stepwisefit* and *stepwiselm*. While the first one tries to fit the model in a function, the second allows more flexibility in the initial model and checks the cross-terms automatically.

The development of the regression models were characterized by many steps: 1° step: Initial model, 2° step: Adding cross-terms, 3° step: Adding inverse terms, and 4° step: Expanding the upper bounds from "Interactions" to "quadratic", 5° step: Installing a Floor, and 6° step: Removing zero values (Non-zero models). The last two steps were adopted in order to solve some challenges that were identified during the regression models' development process.

Overall, the several steps indicated that the models' accuracy increased according to their complexity. Improvements on modeling results were shown by R<sup>2</sup> values<sup>26</sup>. Below, each step is described in details.

### 1° step: Initial model

Using *Stepwisefit* in Matlab® two regression models for each Brazilian location, were generated. One to predict discomfort by heat and the other to assess the discomfort by cold. The initial models comprised only the individual effects of the 24 original key design parameters (Table 36). Additionally, they were in the form indicated in Equation 7 to predict discomfort by heat or discomfort by cold ( $y$ ) in function of variations in original key design parameters ( $x_1, x_2, \dots, x_n$ ). In all cases, no good fits were achieved.

$$y(x_1, x_2, \dots, x_n) = \beta_0 + \sum_{j=1}^n \beta_j x_j \quad \text{Equation 7}$$

Source: Adapted from HYGH et al., 2012

Table 36: Original key design parameters.

COEFFICIENT	MEANING
x1	Bedroom_1 Effective window ventilation area
x2	Bedroom_2 Effective window ventilation area
x3	Living room Effective window ventilation area
x4	External Walls' Solar Absorptance
x5	Bedroom_1 Left Fin size
x6	Bedroom_2 Left Fin size
x7	Living room Left Fin size
x8	Bedroom_1 Right Fin size
x9	Bedroom_2 Right Fin size
x10	Living room Right Fin size
x11	Bedroom_1 Overhang size
x12	Bedroom_2 Overhang size
x13	Living room Overhang size
x14	Roof's Solar Absorptance
x15	North Axis/ Orientation in the terrain
x16	Bedroom_1 Window to Wall Ratio (WWR)
x17	Bedroom_2 Window to Wall Ratio (WWR)
x18	Living room Window to Wall Ratio (WWR)
x19	External Walls' U-value
x20	Internal Walls's U-Value
x21	Roof's U-Value
x22	External Walls' Heat Capacity
x23	Internal Walls' Heat Capacity
x24	Roof's Heat Capacity

<sup>26</sup> The R<sup>2</sup> values during the regression models' development considered only the 6000 data points. Once the R<sup>2</sup> values for model development and validation were normally very close, no validations were conducted for all the previous step to build the models.



### **2° step: Adding cross terms**

In order to increase the accuracy of the initial models, the inclusion of cross terms (as for example “external walls’ solar absorptance” multiplied by “external walls’ U-value”) was considered using the *Stepwiselm* function in Matlab®. The initial model was set up as a constant. In addition, forward and backward stepwise regression checked all cross terms, including or removing them according to p-value. This process recognized important combinations of the key design parameters and also their effect on the discomfort by heat and by cold in the analyzed geometry. As a result, greatly improvements on the models’ accuracy were achieved by adding cross terms in all climates, except of the models that predict discomfort by heat for Curitiba and São Paulo. They were improved, but not enough.

To sum up, the models with such interactions had between 38-72 terms while the ones without interactions had between 9-20 terms. The comparison of the complexity of the two models was evaluated by the number of non-zero parameter coefficients. Using this approach, most  $R^2$  values jumped over 0.80.

### **3° step: Adding inverse terms**

It was recognized that some key design parameters also influence the thermal comfort predictions as an inverse. Therefore, to further increase the accuracy of the regression models the key design parameters varied in Monte Carlo Simulation were expanded in order to include the inverse of each value. Therefore,  $x_{25}$  is the inverse of  $x_1$  and so on. A new database for each analyzed climate was generated and it was used to develop new regression models. Then, new regression models were generated applying the *Stepwiselm* function in Matlab®. They comprised between 85-152 terms, which included the original design parameters, their inverse values and cross terms. Except of Curitiba and São Paulo discomfort by heat, in almost all climates the  $R^2$  values were about 0.95.

### **4° step: Expanding the upper bounds from “interactions” to “quadratic”**

By expanding the upper bounds of the model from “interactions” to “quadratic”, squared terms were allowed in each model. On the whole, the models achieved the highest accuracy when compared with the previous ones, but did not significantly increase their complexity, with between 101-171 predictor terms in each. It is worthwhile to mention that the models generally improved in fit, but such improvements were less marked than what observed in the inclusion of inverse terms, for example.

As aforementioned some challenges were identified in the regression models’ development process. As the post processing EnergyPlus output is degree-hours of discomfort, a

comfortable environment is characterized as 0, thus no negative values are shown. Because of that, many simulations could result in a zero output value. Previous modeling exercises (AL GHARABLY; DECAROLIS; RANJITHAN, 2015; HYGH et al., 2012) were able to predict positive and negative values, once they were dealing with heating and cooling loads. Such exercises were important to address two main conclusions: 1) negative value predictions by regression model should not be interpreted as negative, but rather zero, and 2) when the regression models are trying to fit various data sets to an unique output value, the generated model may not result in accurate fit. Therefore, in order to solve the identified problems, two more steps were proposed: 5° step: Installing a Floor, and 6° step: Removing zero values (Non-zero models).

### **5° step: Installing a Floor**

Degree-hours of discomfort can not be negative. For this reason, a “floor” to the regression models was added, in order to disallow them to provide negative values. This action was done with an Excel® if statement<sup>27</sup>. This step was applied to Curitiba and São Paulo data and it increased the accuracy of each model as measured by R<sup>2</sup> values.

### **6° step: Removing zero values (Non-zero models)**

In São Paulo and Curitiba were observed a large preponderance of zero values in degree-hours of discomfort by heat, about 60% and 81% respectively. Regression models generated by standard regression methods could not accurately predict when various combinations of input data result in zero values. The application of such methods in those climates resulted in unsatisfactory R<sup>2</sup> values, being equal 0.61 for Curitiba and 0.74 for São Paulo.

Facing that, it was decided to train new regression models for such scenarios using only non-zero (NZ) output values. Therefore, the original data for each analyzed city (6000 data points) had all zero output values removed. Following, 75% of that new non-zero data set was used to develop the regression models, while the remaining 25% to validate them. After the models were created, they showed good fits in predicting the remaining non-zero values, with R<sup>2</sup> values upper than 0.83. However, when trying to fit the whole data set to the non-zero models the R<sup>2</sup> values decreased significantly. They dropped from 0.908 to 0.375 in São Paulo and from 0.832 to 0.05 in Curitiba. In conclusion, the non-zero model could not accurately predict when EnergyPlus output is negative or zero.

---

<sup>27</sup> (if regression result value < 0, result = 0, else result = regression result value).

### 5.3 REGRESSION MODELS' RESULTS AND VALIDATION

On the whole, the regression models for predicting discomfort by heat and by cold showed good fits for all climates. Exceptions were regarded to Curitiba and São Paulo in regression models that assess the discomfort by heat. The identified limitation is derived from situation with so many zero in degree-hours of discomfort by heat. And even NZ models had no good fits in predicting low or zero values.

Appendices from F to L show the linear regression coefficients and also their p-values for all generated regression models.

After developing the regression models, the remaining samples (4000 data points) enabled their validation based on the analyzed error. The results obtained from regression models' applications were compared with the ones resulted from the EnergyPlus simulations, regarding the same input data. The accuracy of each model was measured by the coefficient of determination ( $R^2$ ).

Table 37 summarizes the information of final linear regression models for Curitiba (CTB), Manaus (MN) and São Paulo (SP). The root mean square error (RMSE) and its coefficient of variation (CV (RMSE)), the normalized mean bias error (NMBE), the average percent error (Avg % Error), and also the coefficient of determination ( $R^2$ ), are shown. Once there was no discomfort by cold in Manaus, the model to predict this data was not generated. Besides good fits in terms of  $R^2$  values could be verified, the still significant average percent errors demonstrate positive or negative bias.

Table 37: Result Error Analysis.

		Curitiba	Manaus	São Paulo
Discomfort by COLD	RMSE	569.37		149.48
	CV(RMSE)	0.0651		0.0436
	NMBE	1.3103E-05		4.2195E-04
	Avg % Error	0.11%		0.11%
	$R^2$	0.9515		0.982
Discomfort by HEAT	RMSE	13.46	167.09	30.12
	CV(RMSE)	4.2409	0.4098	1.7853
	NMBE	-0.700	-0.080	-0.363
	Avg % Error	804.14%	5517.61%	2162.68%
	$R^2$	0.6107	0.9505	0.7464
Discomfort by HEAT (NZ)	RMSE	58.26		67.56
	CV(RMSE)	18.3563		4.0049
	NMBE	-9.537		-1.815
	Avg % Error	1592.74%		1112.14%
	$R^2$ (NZ/all)	0.8323/0.0529		0.9078/0.3749

Figure 29 illustrates the validation of the models that predict discomfort by cold and by heat for all analyzed locations. Lines show the agreement between the EnergyPlus outputs (vertical axis) and the regression models predictions (horizontal axis).

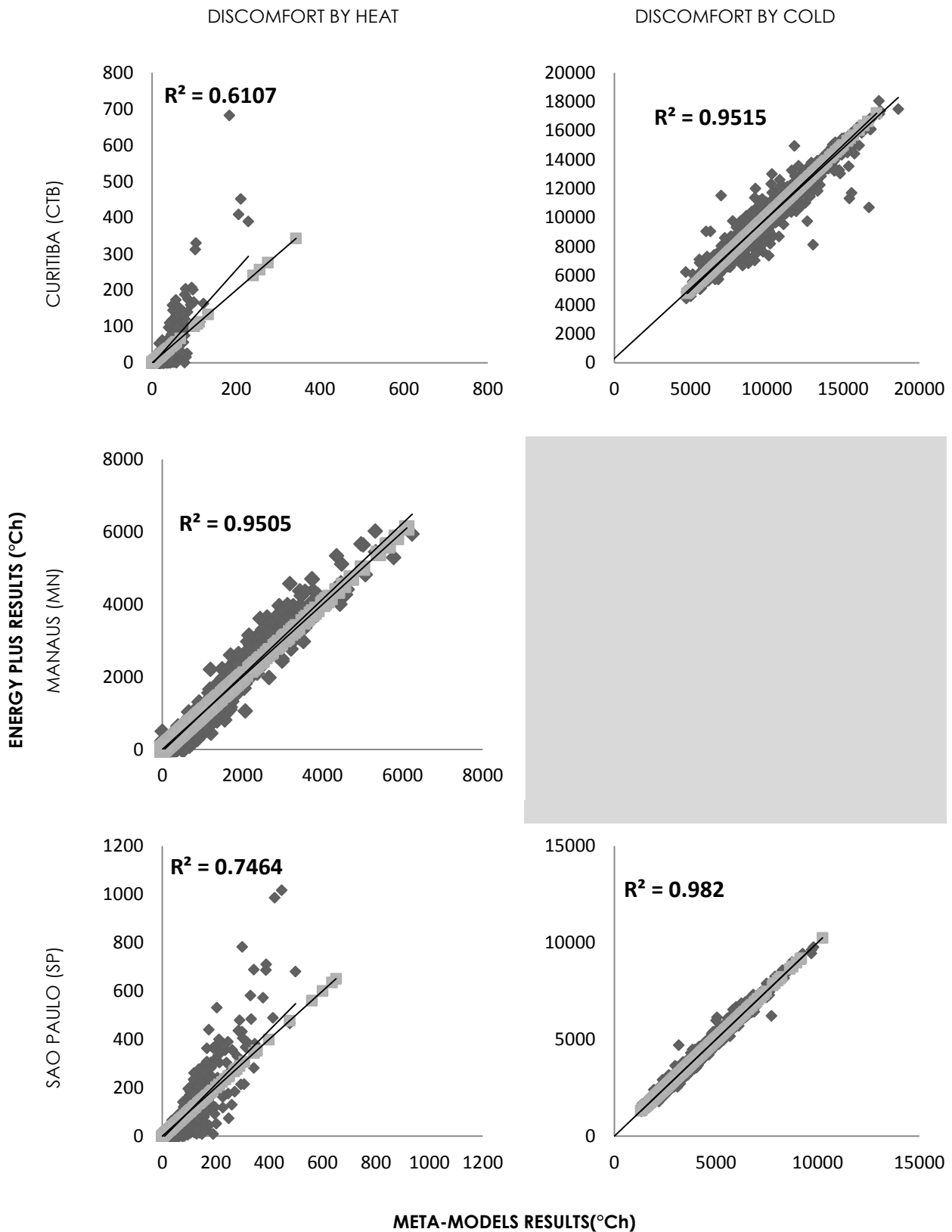


Figure 29: Validation of the regression models to predict discomfort by heat and by cold for three Brazilian locations.

NZ models' validations utilize all data points (10000). Otherwise, the NZ regression models were not accurate as can be verified in the Figure 30. For this reason, it was decided to consider the regression models that included the zero values in their development (Figure 30).

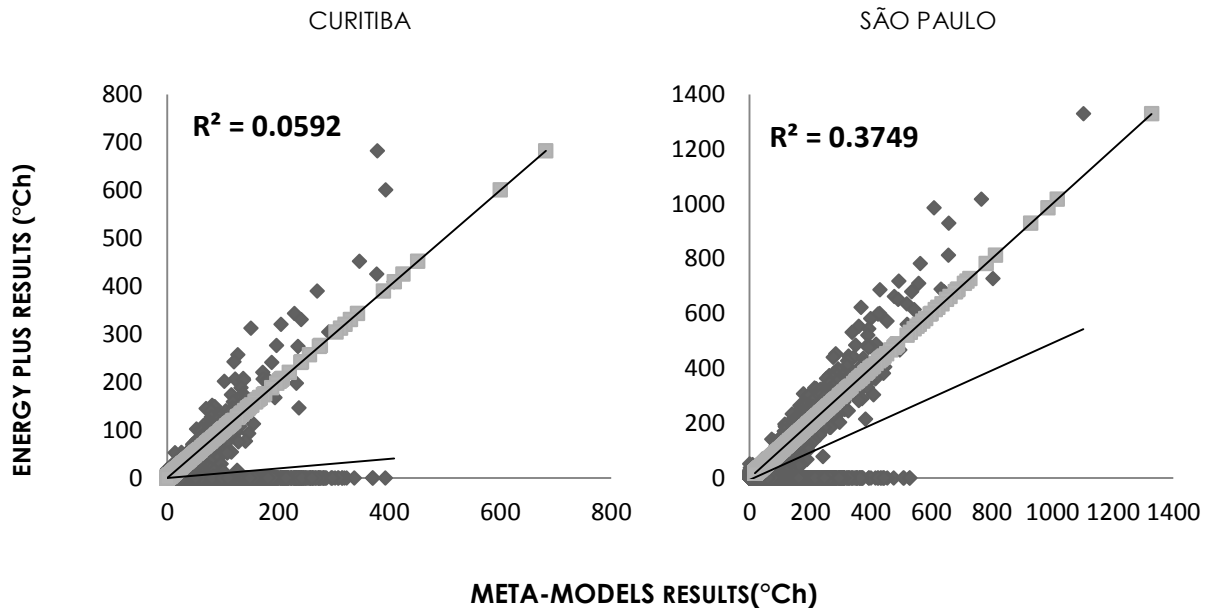


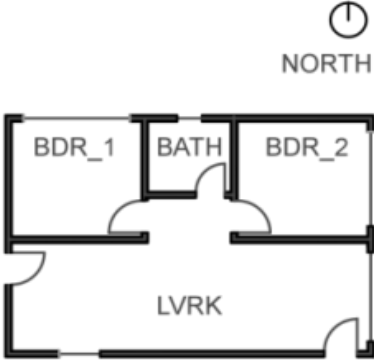
Figure 30: Validation of the NZ regression models to predict discomfort by heat for Curitiba and São Paulo, considering all 10 000 data points.

#### 5.4 REGRESSION MODELS' APPLICATION

The regression models were set up in Excel® spreadsheets. In order to test their potential as support tools during the decision-making, the LCH's discomfort by heat and by cold was obtained using them. The analyzed scenarios comprised the common characteristics observed in this Brazilian type of house. They were performed for all analyzed climates. Envelope thermal properties such as thermal transmittance, solar absorptance and heat capacity for external and internal walls and roof systems were kept fixed and represent current constructions for this type of building (MARQUES, 2013). Building north orientation also did not change. It was chosen to provide cross ventilation in the long-stay rooms, considering that prevailing wind directions in the three climates are east-southeast. No shading devices were applied, so the minimum range values were specified for this item. Only the parameters related to buildings' fenestrations, and consequently with natural ventilation strategies were varied. The effective window ventilation area (ewva) considered a sliding window (ewva=50%) and a casement window (ewva=100%) situations. The window-to-wall ratio varied from 10% to 90%, increasing in intervals of 10%. Both parameters (ewva and WWR) can vary independently in the regression models, considering the different windows' rooms. However, in this test they were the same for all long-stay rooms (living room and bedrooms). A

total of **108 tests** were done by applying the regression models. Table 38 summarizes the variable and fixed parameters considered in such tests.

Table 38: Fixed and variable parameters for meta-models' application.



COEFFICIENT	MEANING	VALUE
x1	Bedroom_1 Effective window ventilation area	<b>VARIABLE</b> 50% or 100%. All windows with the same EWVA.
x2	Bedroom_2 Effective window ventilation area	
x3	Living room Effective window ventilation area	
x4	External Walls' Solar Absorptance	0.4
x5	Bedroom_1 Left Fin size	0.01 (No shading devices)
x6	Bedroom_2 Left Fin size	
x7	Living room Left Fin size	
x8	Bedroom_1 Right Fin size	
x9	Bedroom_2 Right Fin size	
x10	Living room Right Fin size	
x11	Bedroom_1 Overhang size	
x12	Bedroom_2 Overhang size	
x13	Living room Overhang size	0.75
x14	Roof's Solar Absorptance	
x15	North Axis/ Orientation in the terrain	270°
x16	Bedroom_1 Window to Wall Ratio (WWR)	<b>VARIABLE</b> From 10% to 90% (intervals of 10%). All windows with the same WWR.
x17	Bedroom_2 Window to Wall Ratio (WWR)	
x18	Living room Window to Wall Ratio (WWR)	
x19	External Walls' U-value	2.76 W/m <sup>2</sup> .K
x20	Internal Walls's U-Value	2.27 W/m <sup>2</sup> . K
x21	Roof's U-Value	1.78 W/m <sup>2</sup> . K
x22	External Walls' Heat Capacity	266 KJ/m <sup>2</sup> . K
x23	Internal Walls' Heat Capacity	206 KJ/m <sup>2</sup> . K
x24	Roof's Heat Capacity	189 KJ/m <sup>2</sup> . K

In general, Curitiba and São Paulo showed a very similar pattern of results. For this reason, their results are shown together. Finally, the results for Manaus are presented.

Figure 31 and Figure 32 show the discomfort by heat in degree-hours, for all cases, in Curitiba and São Paulo. Overall, by increasing the window-to-wall ratio, higher values of discomfort

were obtained. Two effects happen when WWR is increased: higher solar gains during the day and higher heat losses, mainly at night, due to the low thickness of the glass. In these results, the first effect surpasses the second one.

When the effective window ventilation area (ewva) is elevated from 50% to 100% the discomfort by heat in Curitiba decreased, indicating that heat loss through ventilation is increased due to a higher airflow rate. However, the same trend could not be observed in São Paulo results. Such climate shows higher values of discomfort by heat when the windows were fully opened. This indicates that the building gains heat by ventilation. But according to the ventilation modeling, windows are automatically closed in moments that outside temperature is higher than indoor. Therefore, further investigations may be conducted in order to refine the natural ventilation modeling in EnergyPlus or also to analyze the reasons that the building is gaining heat in such situations. The lower magnitude of discomfort by heat in both cities indicates that the building operative temperatures do not reach often the upper comfort limit.

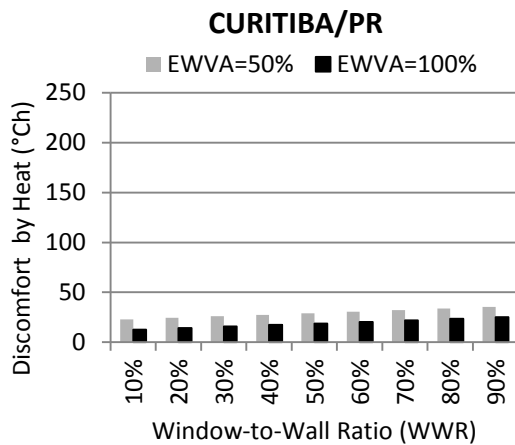


Figure 31: Impact of variation in Window-to-Wall ratios and Effective window ventilation area (ewva) in discomfort by heat in a LCH in Curitiba.

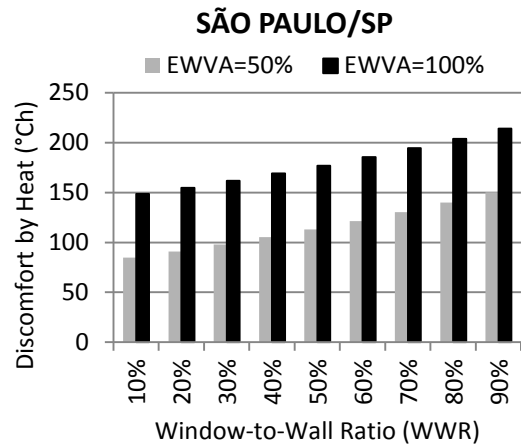


Figure 32: Impact of variation in Window-to-Wall ratios and Effective window ventilation area (ewva) in discomfort by heat in a LCH in São Paulo.

Figure 33 and Figure 34 illustrate the discomfort by cold, in degree-hours, for Curitiba and São Paulo, for all analyzed cases. Generally, both climates show a decrease of degree-hours of discomfort by cold as the window-to-wall ratios are increased. As aforementioned higher window areas permit higher solar gains during the day and higher heat losses at night. In these results, the first effect surpasses the second one and then, the discomfort by cold decreased. Otherwise, the ewva do not impact the results in both cities. Same values are shown for ewva=50% and ewva=100%. This occurs because windows are not opened during

greater part of the hours for that cities, once the building operative temperature is lower than comfort temperature used as set point in natural ventilation modeling. Both cities show a higher magnitude of discomfort by cold, which means that building operative temperatures were often below the lower comfort limit.

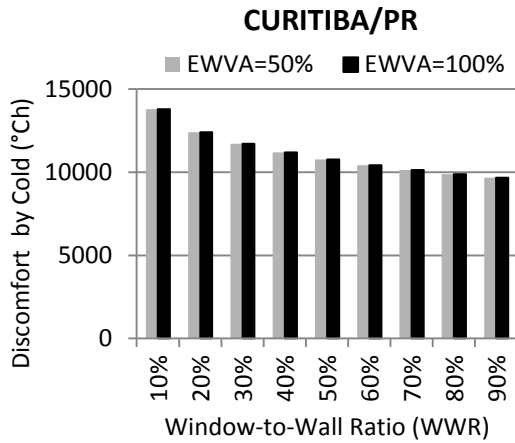


Figure 33: Impact of variation in Window-to-Wall ratios and Effective window ventilation area (ewva) in discomfort by cold in a LCH in Curitiba.

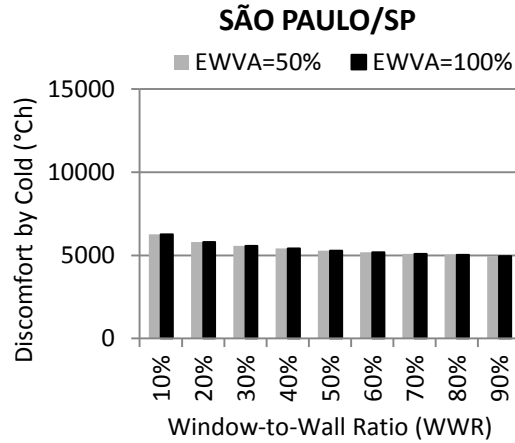


Figure 34: Impact of variation in Window-to-Wall ratios and Effective window ventilation area (ewva) in discomfort by cold in a LCH in São Paulo.

Finally, the Figure 35 and Figure 36 show the total discomfort (Total discomfort = Discomfort by Heat + Discomfort by Cold). The same trend from discomfort by cold is observed in both climates, due to its much higher values, when compared to discomfort by heat.

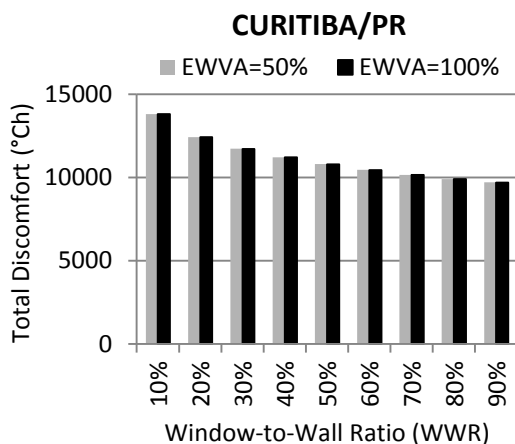


Figure 35: Impact of variation in Window-to-Wall ratios and Effective window ventilation area (ewva) in total discomfort in a LCH in Curitiba.

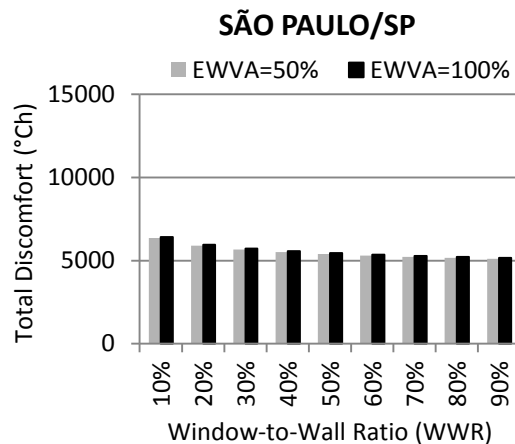


Figure 36: Impact of variation in Window-to-Wall ratios and Effective window ventilation area (ewva) in total discomfort in a LCH in São Paulo.

Figure 37 shows the discomfort by heat, in degree hours, for Manaus, for all considered cases. The higher number of discomfort by heat in this location demonstrates that most of the year



the building operative temperature is upper than comfort limit. The discomfort goes up as window-to-wall ratio is increased. Manaus is the warmer analyzed climate, at 3.1° South latitude, so window solar gain is considerable. Almost the same amount of discomfort was found for both ewva situations.

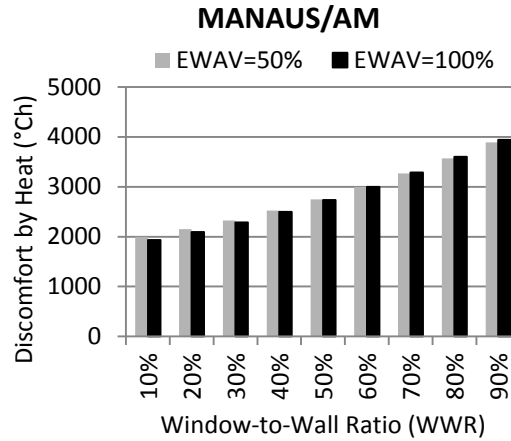


Figure 37: Impact of variation in Window-to-Wall ratios and Effective window ventilation area (ewva) in discomfort by heat in Manaus.

Table 39 summarizes the frequency that parameters (original terms and inverse terms) related with natural ventilated appeared in the final regression models, regarding the analyzed climates.

Table 39: Frequency of parameters related with natural ventilation in the final regression models.

	São Paulo		Manaus		Curitiba
	Discomfort by Heat Model	Discomfort by Cold Model	Discomfort by Heat Model	Discomfort by Heat Model	Discomfort by Cold Model
<b>Total of terms in the equation</b>	<b>76</b>	<b>127</b>	<b>142</b>	<b>64</b>	<b>151</b>
Bedroom_1 WWR	9	0	12	0	8
Bedroom_2 WWR	6	13	15	0	13
Living room WWR	7	10	16	6	8
Inverse of Bedroom_1 WWR	0	16	0	0	0
Inverse of Bedroom_2 WWR	0	0	0	0	16
Inverse of Living room WWR	0	0	0	0	0
Bedroom_1 EWVA	0	0	0	0	0
Bedroom_2 EWVA	0	0	0	0	0
Living room EWVA	0	0	0	5	0
Inverse of Bedroom_1 EWVA	0	0	3	0	0
Inverse of Bedroom_2 EWVA	0	0	0	0	0
Inverse of Living room EWVA	5	0	0	0	0

The small differences observed in the results when the ewva was increased from 50% to 100% could be explained by the lower presence of such parameters (as original terms or as inverse terms) in the equations. Therefore, the regression models may have in general less sensitivity for these parameters and because of that no significant changes could be observed when they were varied in the application tests.

That unexpected behavior, observed in São Paulo case, could be also explained by the windows modulation that rules the effective window ventilation area in EnergyPlus in function of a temperature differential between outside and inside environments. In conclusion, the value specified in the equation may be not the exactly value utilized during all hours of the year in the simulation calculation by the EnergyPlus and a noise may be generated in the meta-models, regarding this parameter.

## 6 CONCLUSIONS

---

This research developed meta-models to assess a building's thermal discomfort in a naturally ventilated Brazilian LCH during early design. The meta-models predict thermal discomfort as function of the key design parameters' changes for three Brazilian cities: Curitiba/PR, São Paulo/SP, and Manaus/AM.

Two meta-models were developed, one meta-model to predict thermal discomfort by heat and other to assess the discomfort by cold for all climates, except for Manaus that showed no discomfort by cold. It is important to highlight that the development of just one model for each climate to predict the total discomfort was not considered, once the parameters which impact the LCH's discomfort by heat or by cold were totally different.

Many steps were executed in order to improve the meta-models' accuracy, using the  $R^2$  value as a mean for this evaluation. The final regression models' validation showed  $R^2$  values higher than 0.95 for all climates. Except for the regression models that predict discomfort by heat for Curitiba and São Paulo, which presented  $R^2$  equal to 0.61 and 0.74, respectively.

The approximated equations were set up in Excel® spreadsheets and their potential as a support design tool was tested in the analyzed LCH. The focus of this research was to develop the meta-models and to evaluate the impact of the parameters related to natural ventilation strategies in thermal comfort for LCH. Therefore, only the window-to-wall ratio (WWR) and effective window ventilation area (EWVA) were varied in these tests. The other parameters were fixed at values that represented the common characteristics of LCH in Brazil.

By increasing the WWR in intervals of 10% for all climates, consistent predictions were given. While the discomfort by heat reached high values as the WWR's were incremented, the discomfort by cold decreased in the same situations for all climates. A higher increase in discomfort by heat could be observed in Manaus (warmer climate) and greater decreases in discomfort by cold in Curitiba (colder climate). This illustrated that there are greater heat gains during the day through windows as the WWR increased that surpassed the heat losses during the night in both situations.

It was possible to verify consistent predictions considering changes in EWVA only for discomfort by heat in Curitiba. The discomfort by heat values decreased with the increment in EWVA from 50% to 100%, showing heat losses due to ventilation as the airflow rates increased. For São Paulo, an unexpected situation was presented. The discomfort by heat increased with the modifications in EWVA rates, indicating a heat gain, what was not supposed to happen due to the ventilation control mode by temperature. Further investigations need to be conducted in order to solve this issue and some suggestions are pointed out in the item "6.1 Further Work".

The ewva changes did not impact the results in São Paulo and Curitiba for discomfort by cold, since most of the hours the windows were closed by ventilation control mode, not allowing natural ventilation to occur then. The same pattern could be observed in Manaus when the discomfort by heat values were taken under consideration. Finally, the lower value of the EWVA parameters in the meta-models could also explain these results, once maybe the developed models are not sensitive to such parameter changes. Sensitivity analysis was also indicated in the Further Work section to overcome this issue.

## 6.1 FURTHER WORK

The representative low-cost Brazilian house is a simple geometry to be modeled in EnergyPlus. However, further investigations or refinements could be employed to improve the base-model and also some EnergyPlus modeling approaches, considering the following points:

Ground temperature values. It is known that the soil has a higher thermal inertia, therefore, adjustments in this parameter are required, especially for tropical climates. However, few accurate studies embrace this topic in Brazil.

Natural ventilation modeling on EnergyPlus Airflow Network group. Items as windows modulation and effective window ventilation area demand more investigation. Additionally, the accuracy of using surface-average instead of local wind pressure coefficients could be verified for different building types, internal partition configurations, and windows distribution. The local pressure coefficient values could be obtained by wind tunnel experiments in order to validate the results.

Adaptive comfort temperature based on ASHRAE 55 (ASHRAE, 2013) as set point temperature for ventilation. Such temperatures show high values for some climates, avoiding natural ventilation to be allowed in moments that it is supposed to happen.

Comfort limits from ASHRAE-55 Thermal Comfort Adaptive Approach (ASHRAE, 2013) to quantify the degree-hours of discomfort is within the same topic. The upper and the lower comfort limits can increase the thermal discomfort values if they are not representing real temperature situations. This thermal comfort evaluation method is the only one aimed at naturally ventilated spaces; however it did not include Brazilian data in its development.

The meta-models can only be applied for the geometry assumed in their creation. In order to allow a real support for designers during the decision-making process, the theoretical framework already developed could be used to explore design variations not yet contemplated in such models. The inclusion of all Brazilian climates, shape factor, different windows' distribution, among others variations, could represent a first step towards generalizing the created regression models.

Finally, sensitivity analysis could be conducted to verify how influential the parameters related with natural ventilation strategies are. It is already pointed out in Multivariate Regression and Conclusions sections the small influence of the effective window ventilation area in meta-models for all climates.



## 7 REFERENCES

---

- ABCI- Associação Brasileira de Construção Industrializada. **Manual Técnico de Caixilhos/janelas**. PINI Editora. São Paulo, 1991.
- ABNT - ASSOCIAÇÃO BRASILEIRA DE NORMAS TÉCNICAS. **NBR 15220**: Desempenho Térmico de edificações. Rio de Janeiro, 2005.
- ABNT - ASSOCIAÇÃO BRASILEIRA DE NORMAS TÉCNICAS. **NBR 15575**: Edificações habitacionais – Desempenho. Rio de Janeiro, 2013.
- AL GHARABLY, M.; DECAROLIS, J. F.; RANJITHAN, S. R. An enhanced linear regression-based building energy model (LRBEM+) for early design. **Journal of Building Performance Simulation**, n. 2012, p. 1–19, 2015.
- ALLARD, F. **Natural ventilation in buildings**: a design handbook. Londres: James & James Science Publishers, 2002.
- ALLARD, F.; ALVEREZ, S. (Eds.). Fundamentals of natural ventilation. In: **Natural ventilation in buildings**: a design handbook. London, 2002.
- ALLARD, F.; GHIAUS, C.; MANSOURI, Y. Natural ventilation for health, comfort and energy efficiency. In: VIII Encontro Nacional sobre Conforto no Ambiente Construído e III Conferência Latino-americana sobre Conforto e Desempenho Térmico de Edificações, 2003, Curitiba/ PR. **Anais...** Curitiba/ PR: ANTAC, 2003.
- ASADI, S.; AMIRI, S. S.; MOTTAHEDI, M. On the development of multi-linear regression analysis to assess energy consumption in the early stages of building design. **Energy and Buildings**, v. 85, p. 246–255, 2014.
- ASHRAE - AMERICAN SOCIETY OF HEATING, REFRIGERATING AND AIR CONDITIONING ENGINEERS. **ANSI/ASHRAE Standard 55**: Thermal Environmental Conditions for Human Occupancy. Atlanta, 2013.
- ASHRAE - AMERICAN SOCIETY OF HEATING, REFRIGERATING AND AIR CONDITIONING ENGINEERS. **ANSI/ASHRAE Standard 140**: Standard method of test for the evaluation of building energy analysis computer programs. Atlanta, 2014.
- ASHRAE - AMERICAN SOCIETY OF HEATING, REFRIGERATING AND AIR CONDITIONING ENGINEERS. **ASHRAE Handbook of Fundamentals**. Atlanta, 2001.
- ASHRAE - AMERICAN SOCIETY OF HEATING, REFRIGERATING AND AIR CONDITIONING ENGINEERS. **ASHRAE Handbook of Fundamentals**. Atlanta, 2005.
- ASHRAE - AMERICAN SOCIETY OF HEATING, REFRIGERATING AND AIR CONDITIONING ENGINEERS. **ASHRAE Handbook of Fundamentals**. Atlanta, 2009.
- ATTIA, S. et al. Simulation-based decision support tool for early stages of zero-energy building design. **Energy and Buildings**, v. 49, p. 2–15, 2012.
- BASTOS, L.E.G.; BARROSO-KRAUSE, C.; BECK, L. Estratégias da ventilação natural em edificações de interesse social e a norma ABNT 15220-3: zoneamento bioclimático x potencial eólico brasileiro. In: IX Encontro Nacional e V Encontro Latino Americano de

Conforto no Ambiente Construído, 2007, Ouro Preto/MG. **Anais...** Ouro Preto/MG: ANTAC, 2007.

BITTENCOURT, L.; CÂNDIDO, C. **Introdução à ventilação natural**. 3a. edição ed. Maceió: edUFAL, 2008.

BOGO, A. J. Limitações quanto aos parâmetros de desempenho térmico e estratégias bioclimáticas recomendadas pela norma brasileira de desempenho térmico de habitações de interesse social. In: Seminário Internacional: O espaço sustentável – Inovações em edifícios e cidades, 7, 2008, São Paulo. **Anais...**São Paulo:NUTAU, 2008.

BRASIL. **Lei n. 10.295, de 17 de outubro de 2001**. Dispõe sobre a Política Nacional de Conservação e Uso Racional de Energia. Brasília, DF, 2001.

CAMPOLONGO, F. et al. Hitchliker's Guide to Sensitivity Analysis. In: **Sensitivity Analysis**. Chichester, England: John Wiley & Sons,Ltd., 2001.

CARLO, J. C. **Desenvolvimento de metodologia de avaliação da eficiência energética do envoltório de edificações não-residenciais**. 2008. 196 f. Tese (Doutorado em Engenharia Civil) – Centro Tecnológico, Universidade Federal de Santa Catarina, 2008.

CARLO, J. C.; LAMBERTS, R. Parametros e metodos adotados no regulamento de etiquetagem da eficiencia energetica de edificios – parte 1: metodo prescritivo. **Ambiente Construido**, Porto Alegre, v. 10, n. 2, p. 7-26, 2010.

CATALINA, T.; IORDACHE, V.; CARACALEANU, B. Multiple regression model for fast prediction of the heating energy demand. **Energy and Buildings**, v. 57, p. 302–312, 2013.

CATALINA, T.; VIRGONE, J.; BLANCO, E. Development and validation of regression models to predict monthly heating demand for residential buildings. **Energy and Buildings**, v. 40, n. 10, p. 1825–1832, jan. 2008.

CHVATAL, K. M. S.; MARQUES, T. H. T. Avaliação de diferentes alternativas de modelagem de habitações de interesse social no programa de simulação de desempenho térmico EnergyPlus. **Revista Tecnológica - no prelo**, 2015.

CHVATAL, K. M. S; RORIZ, V.F. Avaliação do desempenho térmico de habitações segundo a ABNT NBR 15575. In: **Avaliação de desempenho de tecnologias construtivas inovadoras: manutenção e percepção dos usuários /organizadores**. Porto Alegre: ANTAC, 2015. ISBN 978-85-89478-42-75. Disponível em: [http://media.wix.com/ugd/d804db\\_603f57d0b3b74e9d8f5ac32f1ba4deff.pdf](http://media.wix.com/ugd/d804db_603f57d0b3b74e9d8f5ac32f1ba4deff.pdf)

CÓSTOLA, D. et al. Uncertainty in airflow rate calculations due to the use of surface-averaged pressure coefficients. **Energy and Buildings**, v. 42, n. 6, p. 881–888, 2010.

CÓSTOLA, D. **Ventilação por ação do vento no edifício**: procedimentos para quantificação. Dissertação (Mestrado – Pós-graduação em Arquitetura e Urbanismo). Universidade de São Paulo, São Paulo, 2006.

CÓSTOLA, D.; BLOCKEN, B.; HENSEN, J. L. M. Overview of pressure coefficient data in building energy simulation and airflow network programs. **Building and Environment**, v. 44, n. 10, p. 2027–2036, 2009.



CUI, C. et al. A Recommendation System for Meta-modeling: A Meta-learning based Approach. **Expert Systems with Applications**, v. 46, p. 33–44, 2015.

DE DEAR, R. J.; BRAGER G. S. Thermal comfort in naturally ventilated buildings: revisions to ASHRAE Standard 55. **Energy and Buildings**, v.34, p. 549- 561, 2002.

DORNELLES, K. A. **Absortância solar de superfícies opacas**: métodos de determinação e base de dados para tintas látex acrílica e PVA. 2008. 160p. Tese (Doutorado) - Faculdade de Engenharia Civil, Arquitetura e Urbanismo, Universidade Estadual de Campinas, Campinas, 2008.

EERE - DEPARTMENT OF ENERGY EFFICIENCY AND RENEWABLE ENERGY. **EnergyPlus**. Version 8.1.0. US: Department of Energy Efficiency and Renewable Energy, Office of Building Technologies, 2013a. Disponível em: <[http://apps1.eere.energy.gov/buildings/energyplus/energyplus\\_about.cfm](http://apps1.eere.energy.gov/buildings/energyplus/energyplus_about.cfm)>. Acesso em: 08 de janeiro de 2014.

EERE - DEPARTMENT OF ENERGY EFFICIENCY AND RENEWABLE ENERGY. **Input-Output Reference**: the encyclopedic reference to *EnergyPlus* input and output. Version 8.1.0. US: Department of Energy Efficiency and Renewable Energy, Office of Building Technologies, 2013b. Disponível em: <[http://apps1.eere.energy.gov/buildings/energyplus/energyplus\\_about.cfm](http://apps1.eere.energy.gov/buildings/energyplus/energyplus_about.cfm)>. Acesso em: 08 de janeiro de 2014.

EISENHOWER, B. et al. A methodology for meta-model based optimization in building energy models. **Energy and Buildings**, v. 47, p. 292–301, 2012.

ETHERIDGE D. **Natural Ventilation of Buildings**: theory, measurement and design . John Wiley & Sons,Ltd, 2012.

FAVRETTO, A. P. O. **Regression models to assess the thermal performance of Brazilian low-cost houses**: consideration of opaque envelope. 2016. Thesis (Master) – Instituto de Arquitetura e Urbanismo de São Carlos, Universidade de São Paulo, São Carlos, 2016.

FAVRETTO, A. P. O. et al. Assessing the Impact of Zoning on the Thermal Comfort Analysis of a Naturally Ventilated House during Early Design. In: 14th International Conference of the International Building Performance Simulation Association, 2015, Hyderabad. **Proceedings**, 2015.

FEUSTEL H.E. et al, **COMIS 3.2—User Guide**, Empa, Dubendorf, 2005.

FIGUEIREDO, C. M. de; FROTA, A. B. **Ventilação Natural para Conforto Térmico em Edifícios de Escritórios** – Avaliação com Modelos Adaptativos. NUTAU (CD), s/d. Disponível em: <<http://www.usp.br/nutau/CD/149.pdf>>. Acesso em 28/09/2012.

FROTA, A.B.; SCHIFFER, S.R. **Manual de Conforto Térmico**. 5 ed. São Paulo. Studio Nobel, 2001.

GIVONI, B. **Man, climate and architecture**. 2 ed. London: Applied Science.Publishers, 1976.

HENSEN, J. et al. Building performance simulation for better design: some issues and solutions. In: PLEA Interational Conference, 21.,2004, Eindhoven, Netherlands. **Proceedings...** Eindhoven, the Netherlands: Technische Universiteit Eindhoven, 2004.

HYGH, J. S. **Implementing energy simulation as a design tool in conceptual building design with regression analysis**. Master thesis. North Carolina State University, Raleigh, North Carolina, 2011.

HYGY, J.S. et al. Multivariate regression as an energy assessment tool in early building design. **Building and Environment**, v. 57, p. 165-175. November 2012.

INMETRO - INSTITUTO NACIONAL DE METROLOGIA, NORMALIZAÇÃO E QUALIDADE INDUSTRIAL. **RTQ-R** - Regulamento técnico da qualidade para o nível de eficiência energética em edificações residenciais. Rio de Janeiro, 2012. Available in: <http://www.inmetro.gov.br/legislacao/rtac/pdf/RTAC001788.pdf>. Accessed: march-2013.

INMETRO. Instituto Nacional de Metrologia, Normalização e Qualidade Industrial. **RTQ-C** - Regulamento Técnico da Qualidade do Nível de Eficiência Energética de Edifícios Comerciais, de Serviços e Públicos. Rio de Janeiro, 2009. Available in: <http://www.inmetro.gov.br/legislacao/rtac/pdf/RTAC001462.pdf>. Accessed: march-2013.

INMETRO. Instituto Nacional de Metrologia, Normalização e Qualidade Industrial. **Anexo geral v – catálogo de propriedades térmicas de paredes, coberturas e vidros**. Anexo da portaria INMETRO nº 50 / 2013.

KLEIJNEN, J. P. C.; BURG, A. J. van den; HAM, R. Th. van der. Generalization of simulation results practicality of statistical methods. **European Journal of Operational Research**, v. 3, n. 1, p. 50–64, 1979.

KLEIJNEN, J. P. C. Sensitivity analysis of simulation experiments: regression analysis and statistical design. **Mathematics and computers in simulation**, v. 34, p. 297–315, 1992.

KLEIVEN, T. **Natural ventilation in buildings: architectural concepts, consequences and possibilities**. Thesis (Doctor of Philosophy in architecture\_). Norwegian University of science and technology. Trondheim, 2003.

KOWALTOWSKI, D. C. C. K. ; LABAKI, L. C.; PINA, S. M. G.; BERTOLLI, S. R. A visualização do conforto ambiental no projeto arquitetônico. IN: VII Encontro Nacional de Tecnologia do Ambiente Construído, 1998, Florianópolis/SC. **Anais...** Florianópolis/SC:ANTAC, 1998.

KOWALTOWSKI, D. C. C. K.; LABAKI, L. C.; PINA, S. M. G.; GUTIERRES, G. C. R. e GOMES, V.S. The Challenges of Teaching bioclimatic architectural design, IN: International Conference: Passive and low energy cooling for the built environment, 2005, Santorini, Grécia, **Anais...**Santorini, Grécia, 2005.

LABEEE - LABORATORIO DE EFICIENCIA ENERGETICA EM EDIFICACOES. **Analysis SOL-AR**. Versão 6.2. Florianopolis: LabEEE, 2012. Disponível em: <http://www.labeee.ufsc.br/downloads/software/analysis-sol-ar>. Acesso em 14 agosto de 2014.

LAM, J. C. et al. Multiple regression models for energy use in air-conditioned office buildings in different climates. **Energy Conversion and Management**, v. 51, n. 12, p. 2692–2697, 2010.

LAM, J. C.; HUI, S. C. M.; CHAN, A. L. S. Regression analysis of high-rise fully air-conditioned office buildings. **Energy and Buildings**, v. 26, n. 2, p. 189–197, 1997.

- LECHNER, N. **Heating, cooling, lighting**: Sustainable design methods for architects. Wiley: New York, 2009.
- LIDDAMENT, M. W. **A guide to energy efficient ventilation**. AIVC. Coventry:Oscar Faber, 1996.
- LOMAS, K. J.; EPPEL, H. Sensitivity analysis techniques for building thermal simulation programs. **Energy and Buildings**, v. 19, n. 1, p. 21–44, 1992.
- MACDONALD, I. A. **Quantifying the effects of uncertainty in building simulation**. PhD Thesis. University of Strathclyde, Glasgow, UK, 2002.
- MAHDAVI, A. Reflections on computational building models. **Building and Environment**, v. 39, n. 8 SPEC. ISS., p. 913–925, 2004.
- MARQUES DA SILVA, F. Aplicação da ventilação natural e mista em edifícios: as acções introdutoras da ventilação natural. In: **Cadernos Edifícios**, n.6, p. 7-26, 2010.
- MARQUES DA SILVA, F. V. **Ventilação Natural de Edifícios turbulência atmosférica**. Dissertação (Doutorado – Pós-graduação em Engenharia Mecânica). Universidade Técnica de Lisboa, Lisboa, 2003.
- MARQUES, T. H. T. **Influencia das propriedades termicas da envolvente opaca no desempenho de habitações sociais em São Carlos, SP**. Dissertação de Mestrado. Instituto de Arquitetura e Urbanismo, IAU/USP. Sao Carlos, SP, 2013.
- MARQUES, T. H. T.; REGOLÃO, R.; CHVATAL, K. M. S. Aplicação de ferramentas simplificadas de projeto voltadas ao desempenho térmico em uma habitação de interesse social. In: 2º Simpósio Brasileiro de Qualidade do Projeto no Ambiente Construído e X Workshop Brasileiro de Gestão do Processo de Projeto na Construção de Edifícios, Rio de Janeiro/RJ, 2011. **Anais...** Rio de Janeiro/RJ: ANTAC, 2011.
- MASCARÓ, L. **Energia na edificação**. Estratégia para minimizar seu consumo. São Paulo: Projeto, 1991.
- MATHWORKS INC. **Matlab Documentation R2013b - institutional**, 2013.
- MATHWORKS INC. **Matlab R2013a - institutional**, 2013.
- MATSUMOTO, E.; LABAKI, L. C.; CARAM, R. M. A aplicação de ensaios em túnel de vento no processo de projeto. In: **O processo de projeto em arquitetura: da teoria à tecnologia**. São Paulo: Oficina dos textos, 2011.
- MONTEIRO, V.M.L.; VELOSO, M.F.D; PEDRINI, A. Conforto térmico e habitação de interesse social: uma proposta adequada à realidade do município de Macaíba/RN. In: Encontro da Associação Nacional de Pesquisa e Pós-graduação em Arquitetura e Urbanismo,2, 2012, Natal/RN. **Anais...**Natal/RN: ENANPARQ, 2012.
- MORBITZER, C.A. **Towards the Integration of Simulation into the Building Design Process**. Thesis; University of Strathclyde, Energy System Research Unit, Department of Mechanical Engineering; 2003.
- NEVES, L.O. **Arquitetura bioclimática e a obra de Severiano Porto**: Estratégias de ventilação natural. Dissertação (Mestrado-Programa de Pós-graduação em Arquitetura e Urbanismo.

Área de Concentração: Arquitetura, Urbanismo e Tecnologia). Escola de Engenharia de São Carlos da Universidade de São Paulo, São Carlos, 2006.

OLGYAY, V. **Arquitectura y clima**: manual de diseño bioclimático. Barcelona: Gustavo Gili, 1998.

PEDRINI, A.; SZOKOLAY, S. Recomendações para o desenvolvimento de uma ferramenta de suporte às primeiras decisões projetuais visando ao desempenho energético de edificações de escritórios em clima quente. **Ambiente Construído**. v. 5, n. 1, p. 39-54, jan./mar. 2005.

PETERSEN, S.; SVENDSEN, S. Method and simulation program informed decisions in the early stages of building design. **Energy and Buildings**, v. 42, n. 7, p. 1113–1119, 2010.

QUAN, Y et al. TPU aerodynamic database for low-rise buildings, in: 12th International Conference on Wind Engineering, 2–6 July, Cairns, 2007.

QUEIROZ, N. et al. Análises paramétricas da equação de graus hora de resfriamento da etiqueta residencial do Procel para zonas bioclimáticas 5 e 8. In XI Encontro Nacional de Conforto no Ambiente Construído e VII Encontro Latino Americano de Conforto no Ambiente Construído, 2011, Búzios/RJ. **Anais...Búzios/RJ: ANTAC**, 2011.

RIVERO, R. **Arquitetura e Clima**. Condicionamento Térmico Natural. Porto Alegre: Luzzato, 1985.

RORIZ, M. **Uma proposta de revisão do Zoneamento Bioclimático Brasileiro**. ANTAC – Associação Nacional de Tecnologia do Ambiente Construído. Grupo de Trabalho sobre Conforto e Eficiência Energética de Edificações. São Carlos, 2012 (a). Disponível em: <[http://www.labeeee.ufsc.br/sites/default/files/projetos/Proposta\\_Revisao\\_Zoneamento\\_Bioclimatico.pdf](http://www.labeeee.ufsc.br/sites/default/files/projetos/Proposta_Revisao_Zoneamento_Bioclimatico.pdf)>. Acesso em: 22 de março de 2013.

RORIZ, M. **Segunda proposta de revisão do Zoneamento Bioclimático do Brasil**. ANTAC – Associação Nacional de Tecnologia do Ambiente Construído. Grupo de Trabalho sobre Conforto e Eficiência Energética de Edificações. São Carlos, 2012 (b). Disponível em: [http://roriz.dominiotemporario.com/doc/Zoneamento\\_Bioclimatico\\_Prop2.pdf](http://roriz.dominiotemporario.com/doc/Zoneamento_Bioclimatico_Prop2.pdf) . Acesso em: 22 março de 2013.

RORIZ, M. **Arquivos Climáticos de Municípios Brasileiros**. ANTAC – Associação Nacional de Tecnologia do Ambiente Construído. Grupo de Trabalho sobre Conforto e Eficiência Energética de Edificações. Relatório Interno, 2012 (c). Disponível em: <<http://www.labeeee.ufsc.br/downloads/arquivos-climaticos>>. Acesso em: 22 de março de 2013.

RORIZ, M.; RORIZ, V.F. **Catavento**. 2015

RORIZ, M.; CHVATAL, K. M. S.; CAVALCANTI, F. S. Sistemas construtivos de baixa resistência térmica podem proporcionar mais conforto. In: X ENCAC e VI Elacac- Encontros Nacional e Latino Americano de Conforto no Ambiente Construído, 2009, Natal. **Anais... do X ENCAC e VI ELACAC**, 2009.

ROSSI, M. M. et al. Assessing thermal performance of low-cost housing in Brazil during early design stages. POSTER presented In: **Water Resources, Coastal & Environmental Engineering Research Graduate Symposium**, 2015, Raleigh. WREE Graduate Symposium, 2015.

RUAS, A. C.; LABAKI, L. C. Ventilação do ambiente e o conforto térmico. In: VI Encontro Nacional e III Encontro Latino Americano de Conforto no Ambiente Construído, 2001, São Pedro/SP. **Anais...** São Pedro/SP, 2001.

SANTAMOURIS, M. Prediction Methods. In: ALLARD, F. (Ed.). **Natural Ventilation in Buildings**. London: James & James. Prediction Methods, p.63 – 156 , 2002.

SANTAMOURIS, M.; ASIMAKOPOULOS. **Passive cooling of buildings**. London: James & James (Science Publishers) Ltd. 2001.

SANTAMOURIS, M.; WOUTERS, P. **Building ventilation: the state of the art**. London: Earthscan, 2006.

SCALCO, V. A. et al. Innovations in the Brazilian regulations for energy efficiency of residential buildings. **Architectural Science Review**, v. 55, n. 1, p. 71–81, 2012.

SCHLUETER, A.; THESELING, F. Building information model based energy/exergy performance assessment in early design stages. **Automation in Construction**, v. 18, n. 2, p. 153–163, 2009.

SEBER, G. A. F.; LEE, A. J. **Linear Regression Analysis**. Second ed. Hoboken, New Jersey: John Wiley & Sons, Inc., 2003.

SIGNOR, R. Estudo do consumo de energia do edifício do Fórum. In: **IV Seminário Catarinense de Iniciação Científica**, Imprensa Universitária, Florianópolis. 1994.

SIGNOR, R.; WESTPHAL, F. S.; LAMBERTS, R. Regression analysis of electric energy consumption and architectural variables of conditioned commercial buildings in 14 Brazilian cities. In: Seventh International IBPSA Conferencen - Building Simulation, 2001, Rio de Janeiro/RJ. **Proceedings...**, Rio de Janeiro: IBPSA, 2001.

SILVA, A. S.; ALMEIDA, L. S. S.; GHISI, E. Análise de propagação de incertezas físicas em simulação computacional dinâmica de edificações residenciais. In: XIII ENCAC e IX ELACAC-Encontros Nacional e Latino Americano de Conforto no Ambiente Construído, 2015, Natal. **Anais...** do XIII ENCAC e IX ELACAC, 2015.

SORGATO, M. J. **Desempenho térmico de edificações residenciais unifamiliares ventiladas naturalmente**. Dissertação (Mestrado – Pós-graduação em Engenharia Civil). Universidade Federal de Santa Catarina, Florianópolis, 2009.

STAT TREK. **Statistics and Probability Dictionary**. Disponível em: <[http://stattrek.com/statistics/dictionary.aspx?definition=coefficient\\_of\\_determination](http://stattrek.com/statistics/dictionary.aspx?definition=coefficient_of_determination)>. Acesso em: 30 out. 2015.

STRUCK, C.; HENSEN, J.L.M. On supporting design decisions in conceptual design addressing specification uncertainties using performance simulation. In: Jiang, Yi (Ed.) 10<sup>th</sup> IBPSA Building Simulation Conference, 2007, Beijing. **Proceedings...** Beijing: Tsinghua University, 2007. pp. 1434-1439.

SWAMI M.V.; CHANDRA S. Procedures for calculating natural ventilation airflow rates in buildings, in: **Final Report FSEC-CR-163-86**, Florida Solar Energy Center, Cape Canaveral, 1987.

TOLEDO, A. M. **Avaliação do desempenho da ventilação natural pela ação do vento em apartamentos: uma aplicação em Maceió/AL**. Tese (Doutorado Engenharia Civil) -

Departamento de Engenharia Civil, UFSC, Universidade Federal de Santa Catarina, Florianópolis, 2006.

TOLEDO, A.M. Caracterização de sistemas de ventilação natural em tipologias correntes de dormitórios em Maceió-AL. In: VI Encontro Nacional e III Encontro Latino Americano sobre Conforto no Ambiente Construído. **Anais...** São Pedro. 2001.

TOLEDO, E. **Ventilação Natural das habitações**. Coordenação da publicação brasileira por Alexandre Toledo. Maceió: EDUFAL, 1999.

TORRES, N.R.– **Análise de regressão**: Notas de aula. Apostila FAUUSP, São Paulo: 2007. Disponível em: [http://www.fau.usp.br/cursos/graduacao/arq\\_urbanismo/disciplinas/aut0516/Apostila\\_Regressao\\_Linear.pdf](http://www.fau.usp.br/cursos/graduacao/arq_urbanismo/disciplinas/aut0516/Apostila_Regressao_Linear.pdf) . Acesso em 10 de março de 2016.

UCLA. **Climate Consultant 6.0**, University of California, Los Angeles, USA. 2015. Available in: <<http://www.energy-design-tools.aud.ucla.edu>>. Accessed: 01.08.2015.

VENÂNCIO, R.; PEDRINI, A. Modos projetuais de simulação térmica: conceitos, definições e aplicação. XI Encontro Nacional de Conforto no Ambiente Construído e VII Encontro Latino Americano de Conforto no Ambiente Construído, 2011, Búzios/RJ. **Anais...** Búzios/RJ: ANTAC, 2011.

VERSAGE, R. Equações prescritivas para o regulamento de etiquetagem de eficiência energética de edificações residenciais. **Relatório técnico**: RT\_Labee-2011/03, 2011.

WALTON, G. N. **AIRNET** – A Computer program for building airflow network modeling, NISTIR 89-4072, National Institute of Standards and Technology, Gaithersburg, Maryland, 1989.

WESTPHAL, F.; LAMBERTS, R. Regression analysis of electric energy consumption of commercial buildings in Brazil. **Proceedings Building Simulation 2007**, p. 1543–1550, 2007.

WESTPHAL, F.S. **Análise de incertezas e de sensibilidade aplicadas à simulação de desempenho energético de edificações comerciais**. Tese (Doutorado Engenharia Civil)- Departamento de Engenharia Civil, UFSC, Universidade Federal de Santa Catarina, Florianópolis, 2007.

WIREN, B.G. **Effects of Surrounding Buildings on Wind Pressure Distributions and Ventilation Losses for Single Family Houses—M85:19**, National Swedish Institute for Building Research, Gavle, 1985.

YANG, Y. **Python script with a Monte Carlo framework to generate the IDF input data**. Under coordination of Dr. Joseph F. DeCarolis and Dr. Ranji Ranjithan. NCSU, CCEE, Raleigh, NC, USA, 2015a.

YANG, Y. **Python script to process EnergyPlus output data calculating the degree-hour of discomfort**. Under coordination of Dr. Joseph F. DeCarolis and Dr. Ranji Ranjithan. NCSU, CCEE, Raleigh, NC, USA, 2015b.

## APPENDIX A - Collected Architectural Designs Classification

The "Workbook 01: Control" describes all the collected information, in order to facilitate the control and the organization of the data, comprising the following items: (a) CODE which identify the design; (b) the ENTERPRISE NAME; (c) the BUILDING TYPE, if it is detached, two-story or multi-storey; (d) LOCATION; (e) CONTACT, the name and telephone or e-mail of the person who gives the information, and (f) STATUS, about getting data situation (seek contact, made contact, requested material, waiting for material, classified material).

In the "Workbook 02: Collected Material" is summarized all collected materials for each enterprise and the items which composed it are: (a) CODE; (b) the ENTERPRISE NAME; (c) LOCATION; (d) the BUILDING TYPE; (e) BIOCLIMATIC ZONE in which the building is located; and (f) COLLECTED MATERIAL with the description of the obtained information as, for example, technical drawings - plans, sections and elevations - and descriptive memorials.

Finally, the "Workbook 03: Classification" resumes the data classification in three standpoints: Geometry; Thermal, and Openings. The GEOMETRY CLASSIFICATION encompasses the following building features: (a) CODE; (b) the BUILDING TYPE; (c) NUMBER OF STORIES; (d) NUMBER OR BEDROOMS; (f) ATTIC, if there is an attic in the analyzed building; (g) CEILING HEIGHT; (h) EAVES; (i) BUILDING GEOMETRY PROPORTION, ratio between the length by width; (j) AREA, useful in houses and of the story for buildings; and (k)OBSERVATIONS or extra information.

The THERMAL CLASSIFICATION includes items as (a) CODE; (b) CONSTRUCTIVE SYSTEMS with the description of constructive systems and also materials applied in roof, external and internal walls; (c) PAINTING which gives the colors of roof and external walls; and (d) OBSERVATIONS or extra information.

In conclusion, the OPENINGS CLASSIFICATION gives detailed information about the windows distribution in the analyzed buildings, reporting the following items: (a) CODE; (b) NUMBER OF STORIES; (c) NUMBER OR BEDROOMS; (d) WINDOWS POSITION in the long-stay rooms; (e) FACADES WITH WINDOWS PER TOTAL OF FACADES, this ratio intends to demonstrate the permeability of building to natural ventilation occurs; (f) WINDOW TYPES; (g) WINDOW-TO-WALL RATIO of the long-stay rooms (h) EFFECTIVE AREA FOR VENTILATION related to window area; and (i) OBSERVATIONS or extra information.



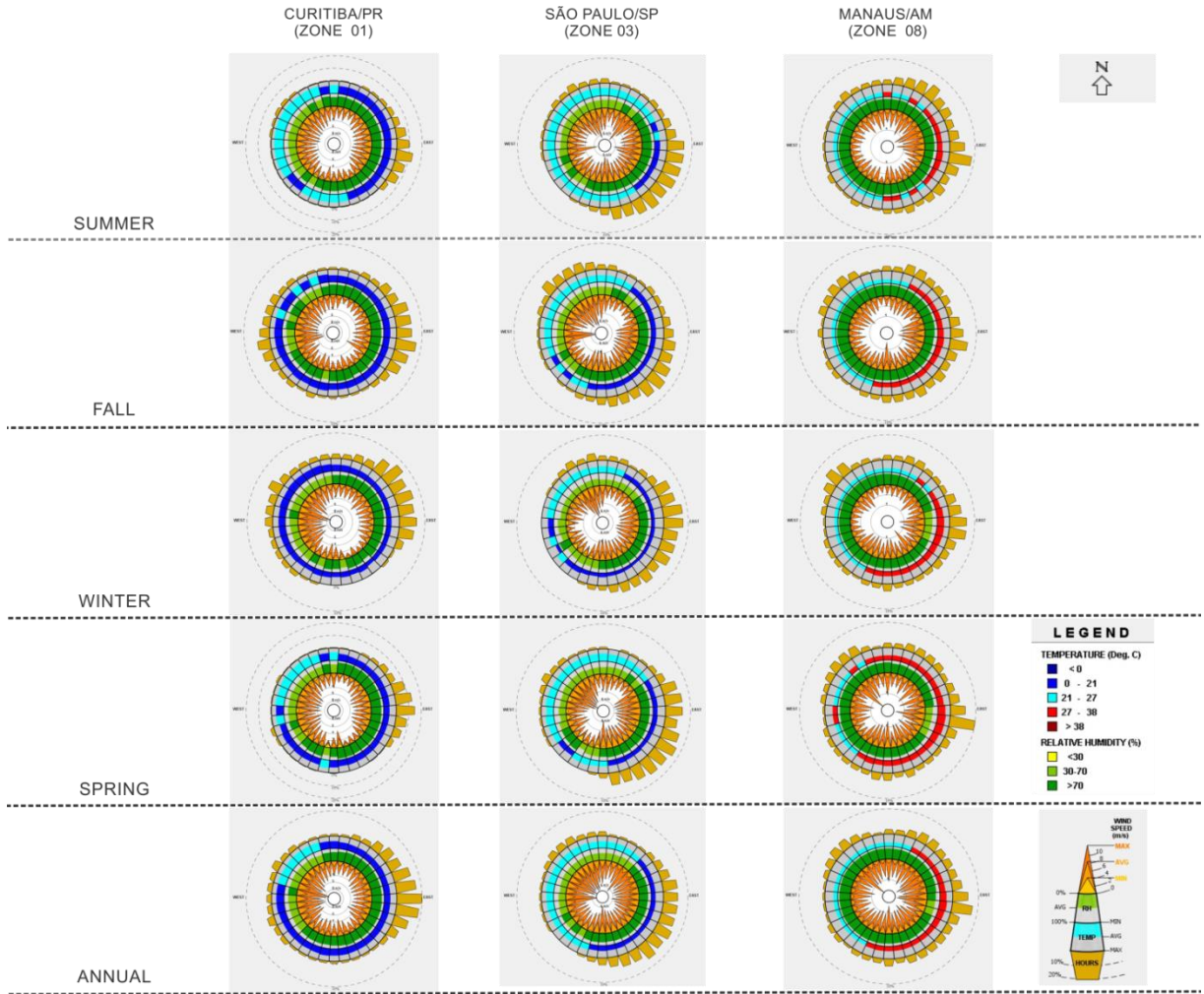


APPENDIX B - Solar Charts

SOLAR CHARTS FOR EACH ANALYZED CLIMATES		THE BEST SOLAR ORIENTATIONS
CURITIBA (BIOClimATIC ZONE 01)	<p>Latitude : -25.43 Transferidor : 0.00</p>	<b>EAST AND NORTH</b>
SÃO PAULO (BIOClimATIC ZONE 03)	<p>Latitude : -23.61 São_Paulo Transferidor : 0.00</p>	<b>EAST AND NORTH</b>
MANAUS (BIOClimATIC ZONE 08)	<p>Latitude : -3.1 Transferidor : 0.00</p>	<b>NORTH AND SOUTH WITH SHADING DEVICES</b>

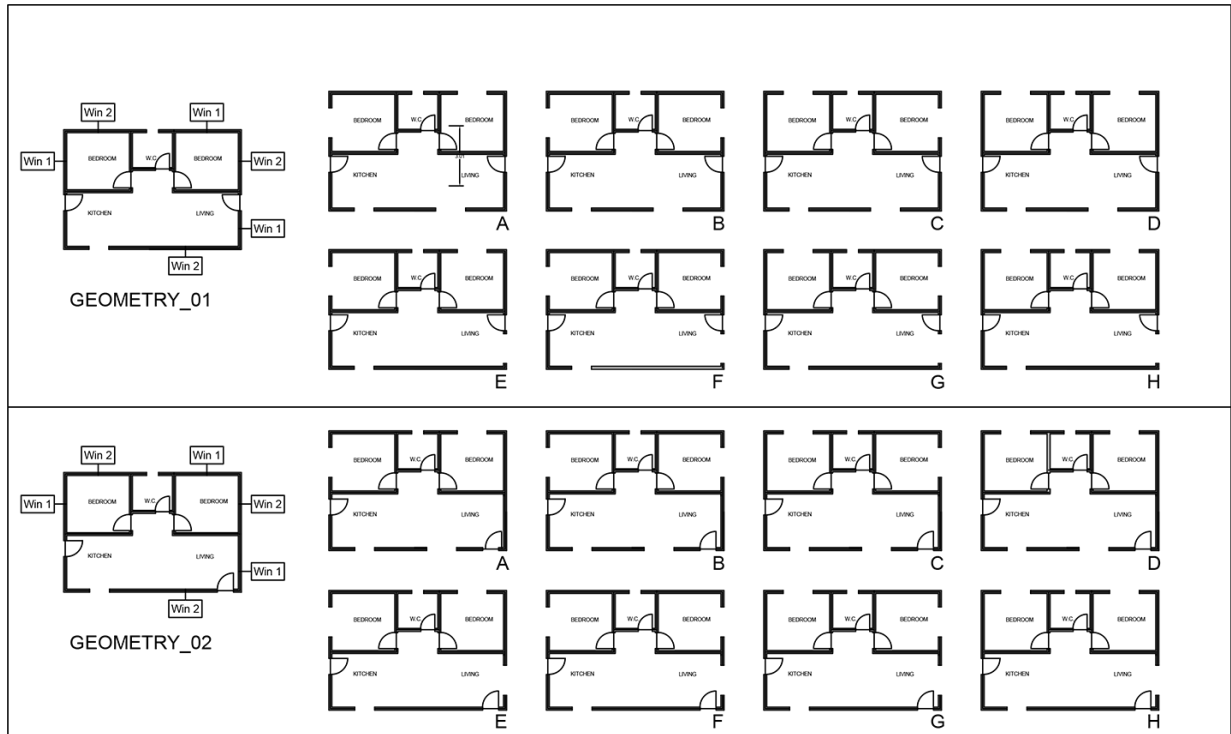


**APPENDIX C - Wind Wheels (Seasons)**





**APPENDIX D - Windows and Door Distribution Possibilities in Base Model Geometry**



GEOMETRY 02 GROUP - CASES	REASONS
A	Opaque facade to mean Wind direction (East) and a long-stay window orientated to West (high solar gains).
B	A long-stay window orientated to West (high solar gains).
C	Two long-stay rooms with windows orientated to North and East. Living room with window in South.
D	Good configuration in solar insolation standpoint to Manaus/AM (windows of long-stay rooms orientated to North and South, however an opaque facade to mean wind direction).
E	A long-stay window orientated to West and only one opening to mean wind direction.
F	Two long-stay windows in mean wind direction, allowing cross ventilation in bedrooms, however along-stay window is orientated to West.
<b>G</b>	<b>Two long-stay windows in mean wind direction and all ambients orientated to East and North (best options considering the solar insolation and ventilation standpoints).</b>
H	Long-stay rooms openings orientated to East and North (best options considering the solar insolation and ventilation standpoints). However, just one possibility of cross ventilation.



### APPENDIX E - Ground Temperatures

MANAUS/AM		
MONTH	MEAN AIR TEMPETARURE (°C)	GROUND TEMPERATURE (°C)
		(Range: 15° - 25° C)
January	26.8	25
February	26.8	25
March	27.6	25
April	26.4	25
May	27.0	25
June	26.8	25
July	26.7	25
August	27.9	25
September	29.0	25
October	28.2	25
November	27.3	25
December	26.7	25
CURITIBA/PR		
MONTH	MEAN AIR TEMPETARURE (°C)	GROUND TEMPERATURE (°C)
		(Range: 15° - 25° C)
January	19.6	19.6
February	20.9	20.9
March	19.9	19.9
April	17.9	17.9
May	15.0	15.0
June	13.6	15.0
July	15.4	15.4
August	15.7	15.7
September	14.6	15.0
October	17.6	17.6
November	18.0	18.0
December	19.4	19.4
CUIABÁ/MT		
MONTH	MEAN AIR TEMPETARURE (°C)	GROUND TEMPERATURE (°C)
		(Range: 15° - 25° C)
January	27.4	25
February	27.0	25
March	26.1	25
April	24.8	24.8
May	25.7	25
June	22.8	22.8
July	24.1	24.1
August	26.0	25
September	27.2	25
October	28.5	25
November	28.4	25
December	27.1	25
SÃO PAULO/SP		
MONTH	MEAN AIR TEMPETARURE (°C)	GROUND TEMPERATURE (°C)
		(Range: 15° - 25° C)
January	21.2	21.2
February	22.3	22.3
March	21.7	21.7
April	20.8	20.8
May	17.5	17.5
June	16.8	16.8
July	17.3	17.3
August	18.3	18.3
September	17.7	17.7
October	20.5	20.5
November	20.1	20.1
December	20.9	20.9





**APPENDIX F - Curitiba/PR Meta-model coefficients – Degree-hours of discomfort by cold (standard approach with regression floor)**

Coefficient †	Meaning	value	p-value
INTERCEPT	INTERCEPT	18385,64	3,6E-116
x4	External Walls' Solar Absorptance	-2756,91	1,13E-28
x5	Bedroom_1 Left Fin size	494,6549	5,78E-06
x6	Bedroom_2 Left Fin size	3175,784	1,3E-09
x7	Living room Left Fin size	3386,239	3,22E-07
x8	Bedroom_1 Right Fin size	-327,328	0,067332
x9	Bedroom_2 Right Fin size	-3608,49	2,48E-07
x10	Living room Right Fin size	226,1234	0,293776
x11	Bedroom_1 Overhang size	3096,869	1,68E-05
x12	Bedroom_2 Overhang size	2787,848	4,28E-09
x13	Living room Overhang size	-2377,56	1,85E-07
x14	Roof's Solar Absorptance	-4334,19	1,33E-44
x15	North Axis/ Orientation in the terrain	-20,7409	8,66E-76
x16	Bedroom_1 Window to Wall Ratio (WWR)	-961,52	0,001007
x17	Bedroom_2 Window to Wall Ratio (WWR)	-7686,31	2,33E-17
x18	Living room Window to Wall Ratio (WWR)	-1599,12	3,21E-09
x19	External Walls' U-value	2666,385	2,5E-258
x21	Roof's U-Value	2865,937	6,31E-30
x22	External Walls' Heat Capacity	-6,96385	5,64E-14
x23	Internal Walls' Heat Capacity	-11,8464	2,61E-15
x24	Roof's Heat Capacity	-6,50643	1,52E-10
x39	inverse of North Axis/ Orientation in the terrain	-1301,22	0,005534
x41	inverse of Bedroom_2 Window to Wall Ratio (WWR)	-1007,71	1,96E-20
x47	inverse of Internal Walls' Heat Capacity	-443728	9,36E-29
x48	inverse of Roof's Heat Capacity	-230452	1,49E-35
x4:x14	External Walls' Solar Absorptance x Roof's Solar Absorptance	723,4714	1,54E-08
x4:x16	External Walls' Solar Absorptance x Bedroom_1 Window to Wall Ratio (WWR)	757,6435	0,000148
x4:x17	External Walls' Solar Absorptance x Bedroom_2 Window to Wall Ratio (WWR)	707,6947	0,000482
x4:x18	External Walls' Solar Absorptance x Living room Window to Wall Ratio (WWR)	690,4265	0,000597
x4:x19	External Walls' Solar Absorptance x External Walls' U-value	-1583,65	0
x4:x22	External Walls' Solar Absorptance x External Walls' Heat Capacity	-1,39113	8,01E-07
x5:x39	Bedroom_1 Left Fin size x inverse of North Axis/ Orientation in the terrain	-1563,43	0,001514
x5:x47	Bedroom_1 Left Fin size x inverse of Internal Walls' Heat Capacity	-31719,7	0,014659
x5:x48	Bedroom_1 Left Fin size x inverse of Roof's Heat Capacity	-16085,7	0,029741
x6:x21	Bedroom_2 Left Fin size x Roof's U-Value	-303,979	0,035609
x6:x22	Bedroom_2 Left Fin size x External Walls' Heat Capacity	-0,99393	0,047843
x6:x23	Bedroom_2 Left Fin size x Internal Walls' Heat Capacity	-2,11604	0,021566

x6:x24	Bedroom_2 Left Fin size	x	Roof's Heat Capacity	-1,34206	0,007808
x6:x41	Bedroom_2 Left Fin size Wall Ratio (WWR)	x	inverse of Bedroom_2 Window to	-144,855	0,000942
x6:x47	Bedroom_2 Left Fin size Capacity	x	inverse of Internal Walls' Heat	-80661,8	0,000824
x6:x48	Bedroom_2 Left Fin size	x	inverse of Roof's Heat Capacity	-35746,7	0,000284
x7:x15	Living room Left Fin size	x	North Axis/ Orientation in the terrain	-1,28118	0,02376
x7:x17	Living room Left Fin size (WWR)	x	Bedroom_2 Window to Wall Ratio	-1550,29	0,037601
x7:x23	Living room Left Fin size	x	Internal Walls' Heat Capacity	-2,85755	0,001871
x7:x41	Living room Left Fin size Wall Ratio (WWR)	x	inverse of Bedroom_2 Window to	-275,727	0,001711
x7:x47	Living room Left Fin size Capacity	x	inverse of Internal Walls' Heat	-113778	2,43E-06
x7:x48	Living room Left Fin size	x	inverse of Roof's Heat Capacity	-38033,9	6,44E-07
x8:x15	Bedroom_1 Right Fin size	x	North Axis/ Orientation in the	1,251773	0,031419
x8:x39	Bedroom_1 Right Fin size the terrain	x	inverse of North Axis/ Orientation in	1187,851	0,002657
x8:x41	Bedroom_1 Right Fin size Wall Ratio (WWR)	x	inverse of Bedroom_2 Window to	94,34965	0,033376
x8:x48	Bedroom_1 Right Fin size	x	inverse of Roof's Heat Capacity	13754,79	0,064254
x9:x15	Bedroom_2 Right Fin size	x	North Axis/ Orientation in the	1,673533	0,003022
x9:x17	Bedroom_2 Right Fin size (WWR)	x	Bedroom_2 Window to Wall Ratio	2434,638	0,001283
x9:x23	Bedroom_2 Right Fin size	x	Internal Walls' Heat Capacity	1,85362	0,040696
x9:x24	Bedroom_2 Right Fin size	x	Roof's Heat Capacity	0,969698	0,048982
x9:x41	Bedroom_2 Right Fin size Wall Ratio (WWR)	x	inverse of Bedroom_2 Window to	350,1333	0,000117
x9:x47	Bedroom_2 Right Fin size Capacity	x	inverse of Internal Walls' Heat	83029,7	0,000513
x9:x48	Bedroom_2 Right Fin size	x	inverse of Roof's Heat Capacity	51610,01	4,08E-08
x10:x14	Living room Right Fin size	x	Roof's Solar Absorptance	-513,735	0,025839
x10:x18	Living room Right Fin size (WWR)	x	Living room Window to Wall Ratio	800,5204	0,028759
x10:x48	Living room Right Fin size	x	inverse of Roof's Heat Capacity	-16831,5	0,02117
x11:x12	Bedroom_1 Overhang size	x	Bedroom_2 Overhang size	795,0845	0,05541
x11:x14	Bedroom_1 Overhang size	x	Roof's Solar Absorptance	-504,148	0,028374
x11:x15	Bedroom_1 Overhang size terrain	x	North Axis/ Orientation in the	1,342506	0,017342
x11:x16	Bedroom_1 Overhang size (WWR)	x	Bedroom_1 Window to Wall Ratio	997,7483	0,005321
x11:x17	Bedroom_1 Overhang size (WWR)	x	Bedroom_2 Window to Wall Ratio	-1696,94	0,024549
x11:x19	Bedroom_1 Overhang size	x	External Walls' U-value	-284,195	5,88E-05
x11:x21	Bedroom_1 Overhang size	x	Roof's U-Value	-339,883	0,017539
x11:x23	Bedroom_1 Overhang size	x	Internal Walls' Heat Capacity	-2,1717	0,015469
x11:x41	Bedroom_1 Overhang size Wall Ratio (WWR)	x	inverse of Bedroom_2 Window to	-263,338	0,003379
x11:x47	Bedroom_1 Overhang size Capacity	x	inverse of Internal Walls' Heat	-88473,9	0,00013
x11:x48	Bedroom_1 Overhang size	x	inverse of Roof's Heat Capacity	-24077,2	0,000588
x12:x14	External Walls' Heat Capacity	x	External Walls' Heat Capacity	-565,314	0,014674

x12:x15	Roof's U-Value	x	Roof's U-Value	-1,17053	0,042024
x12:x17	External Walls' U-value	x	External Walls' U-value	2037,285	1,94E-08
x12:x19	Roof's Heat Capacity	x	Roof's Heat Capacity	-222,394	0,001945
x12:x23	External Walls' Solar Absorptance	x	External Walls' Solar Absorptance	-3,56782	0,000113
x12:x24	Internal Walls' Heat Capacity	x	Internal Walls' Heat Capacity	-1,41959	0,004281
x12:x39	Roof's Solar Absorptance	x	Roof's Solar Absorptance	-1458,48	0,002236
x12:x47	inverse of Roof's Heat Capacity	x	inverse of Roof's Heat Capacity	-151988	3,36E-10
x12:x48	Bedroom_2 Overhang size	x	inverse of Roof's Heat Capacity	-71942,7	4,89E-14
x13:x18	Living room Overhang size (WWR)	x	Living room Window to Wall Ratio	1118,148	0,002388
x13:x23	Living room Overhang size	x	Internal Walls' Heat Capacity	2,554241	0,006229
x13:x24	Living room Overhang size	x	Roof's Heat Capacity	1,539743	0,002327
x13:x41	Living room Overhang size (WWR)	x	inverse of Bedroom_2 Window to Wall Ratio (WWR)	131,2863	0,002459
x13:x47	Living room Overhang size	x	inverse of Internal Walls' Heat Capacity	100816,1	4,2E-05
x13:x48	Living room Overhang size	x	inverse of Roof's Heat Capacity	68930,95	4,81E-13
x14:x15	Roof's Solar Absorptance	x	North Axis/ Orientation in the terrain	1,062143	0,000999
x14:x18	Roof's Solar Absorptance (WWR)	x	Living room Window to Wall Ratio	471,3394	0,01923
x14:x19	Roof's Solar Absorptance	x	External Walls' U-value	498,219	2,26E-39
x14:x21	Roof's Solar Absorptance	x	Roof's U-Value	-3651,43	0
x14:x23	Roof's Solar Absorptance	x	Internal Walls' Heat Capacity	2,057037	5,73E-05
x14:x39	Roof's Solar Absorptance	x	inverse of North Axis/ Orientation in the terrain	1107,284	6E-06
x14:x47	Roof's Solar Absorptance	x	inverse of Internal Walls' Heat Capacity	87494,02	2,22E-11
x14:x48	Roof's Solar Absorptance	x	inverse of Roof's Heat Capacity	59679,53	2,35E-49
x15:x16	North Axis/ Orientation in the terrain	x	Bedroom_1 Window to Wall Ratio (WWR)	-4,17904	3,78E-17
x15:x17	North Axis/ Orientation in the terrain	x	Bedroom_2 Window to Wall Ratio (WWR)	2,284073	0,029372
x15:x19	North Axis/ Orientation in the terrain	x	External Walls' U-value	0,266389	0,009415
x15:x21	North Axis/ Orientation in the terrain	x	Roof's U-Value	0,474984	0,019096
x15:x23	North Axis/ Orientation in the terrain	x	Internal Walls' Heat Capacity	0,00519	3,53E-05
x15:x24	North Axis/ Orientation in the terrain	x	Roof's Heat Capacity	0,002092	0,002756
x15:x41	North Axis/ Orientation in the terrain	x	inverse of Bedroom_2 Window to Wall Ratio (WWR)	0,467003	0,000214
x15:x47	North Axis/ Orientation in the terrain	x	inverse of Internal Walls' Heat Capacity	190,3256	6,42E-09
x15:x48	North Axis/ Orientation in the terrain	x	inverse of Roof's Heat Capacity	100,1104	2,34E-13
x16:x17	Bedroom_1 Window to Wall Ratio (WWR)	x	Bedroom_2 Window to Wall Ratio (WWR)	1048,579	0,000712
x16:x18	Bedroom_1 Window to Wall Ratio (WWR)	x	Living room Window to Wall Ratio (WWR)	647,0496	0,042999
x16:x19	Bedroom_1 Window to Wall Ratio (WWR)	x	External Walls' U-value	-130,306	0,0379
x16:x22	Bedroom_1 Window to Wall Ratio (WWR)	x	External Walls' Heat Capacity	-0,93141	0,035377
x17:x21	Bedroom_2 Window to Wall Ratio (WWR)	x	Roof's U-Value	725,1015	0,006219

x17:x22	Bedroom_2 Window to Wall Ratio (WWR) Heat Capacity	x	External Walls'	2,104073	0,021782
x17:x23	Bedroom_2 Window to Wall Ratio (WWR) Heat Capacity	x	Internal Walls'	6,28843	0,00013
x17:x24	Bedroom_2 Window to Wall Ratio (WWR) Capacity	x	Roof's Heat	2,351353	0,009602
x17:x47	Bedroom_2 Window to Wall Ratio (WWR) Walls' Heat Capacity	x	inverse of Internal	233910,8	1,08E-08
x17:x48	Bedroom_2 Window to Wall Ratio (WWR) Heat Capacity	x	inverse of Roof's	127327,5	3,93E-12
x18:x39	Living room Window to Wall Ratio (WWR) Axis/ Orientation in the terrain	x	inverse of North	1813,6	0,000292
x18:x41	Living room Window to Wall Ratio (WWR) Bedroom_2 Window to Wall Ratio (WWR)	x	inverse of	-194,491	3,26E-07
x19:x21	External Walls' U-value	x	Roof's U-Value	-218,549	6,88E-20
x19:x22	External Walls' U-value	x	External Walls' Heat Capacity	-0,69686	1,66E-16
x19:x24	External Walls' U-value	x	Roof's Heat Capacity	-0,16906	0,040065
x19:x39	External Walls' U-value	x	inverse of North Axis/ Orientation in the terrain	-668,837	0,000175
x19:x41	External Walls' U-value	x	inverse of Bedroom_2 Window to Wall Ratio (WWR)	27,2388	9,63E-05
x19:x47	External Walls' U-value	x	inverse of Internal Walls' Heat Capacity	13754,08	1,04E-09
x19:x48	External Walls' U-value	x	inverse of Roof's Heat Capacity	5654,901	3,6E-05
x21:x23	Roof's U-Value	x	Internal Walls' Heat Capacity	0,812822	0,00934
x21:x24	Roof's U-Value	x	Roof's Heat Capacity	-0,42091	0,01508
x21:x39	Roof's U-Value	x	inverse of North Axis/ Orientation in the terrain	-280,024	0,018208
x21:x41	Roof's U-Value	x	inverse of Bedroom_2 Window to Wall Ratio (WWR)	121,9251	0,000127
x21:x47	Roof's U-Value	x	inverse of Internal Walls' Heat Capacity	44061,9	4,34E-08
x21:x48	Roof's U-Value	x	inverse of Roof's Heat Capacity	22642,77	8,18E-13
x22:x23	External Walls' Heat Capacity	x	Internal Walls' Heat Capacity	0,003632	0,000994
x22:x24	External Walls' Heat Capacity	x	Roof's Heat Capacity	0,003173	2,25E-12
x22:x41	External Walls' Heat Capacity	x	inverse of Bedroom_2 Window to Wall Ratio (WWR)	0,419161	0,00011
x22:x47	External Walls' Heat Capacity	x	inverse of Internal Walls' Heat Capacity	72,54738	0,012133
x23:x24	Internal Walls' Heat Capacity	x	Roof's Heat Capacity	0,004758	1,26E-05
x23:x41	Internal Walls' Heat Capacity	x	inverse of Bedroom_2 Window to Wall Ratio (WWR)	1,223949	2,32E-10
x23:x48	Internal Walls' Heat Capacity	x	inverse of Roof's Heat Capacity	186,8037	1,32E-19
x24:x39	Roof's Heat Capacity	x	inverse of North Axis/ Orientation in the terrain	-0,8409	0,065167
x24:x41	Roof's Heat Capacity	x	inverse of Bedroom_2 Window to Wall Ratio (WWR)	0,404944	0,000146
x24:x47	Roof's Heat Capacity	x	inverse of Internal Walls' Heat Capacity	151,6058	9,22E-08
x41:x47	inverse of Bedroom_2 Window to Wall Ratio (WWR)	x	inverse of Internal Walls' Heat Capacity	46847,78	1,12E-22
x41:x48	inverse of Bedroom_2 Window to Wall Ratio (WWR)	x	inverse of Roof's Heat Capacity	21864,94	2,67E-24
x47:x48	inverse of Internal Walls' Heat Capacity	x	inverse of Roof's Heat Capacity	8761530	1,16E-59
x4^2	External Walls' Solar Absorptance	x	External Walls' Solar Absorptance	527,8405	0,000248

x6^2	Bedroom_2 Left Fin size x Bedroom_2 Left Fin size	-941,356	0,043109
x14^2	Roof's Solar Absorptance x Roof's Solar Absorptance	1404,531	9,52E-23
x15^2	North Axis/ Orientation in the terrain x North Axis/ Orientation in the terrain	0,036833	3,6E-304
x19^2	External Walls' U-value x External Walls' U-value	-109,712	1,4E-43
x22^2	External Walls' Heat Capacity x External Walls' Heat Capacity	0,005532	5,52E-16
x24^2	Roof's Heat Capacity x Roof's Heat Capacity	0,001443	0,037068
x39^2	inverse of North Axis/ Orientation in the terrain x inverse of North Axis/ Orientation in the terrain	148,4513	1,64E-14
x47^2	inverse of Internal Walls' Heat Capacity x inverse of Internal Walls' Heat Capacity	1778989	0,001615
x48^2	inverse of Roof's Heat Capacity x inverse of Roof's Heat Capacity	-483967	3,11E-05



**APPENDIX G - Curitiba/PR Meta-model coefficients – Degree-hours of discomfort by heat (standard approach with regression floor)**

Coefficient	Meaning	value	p-value
INTERCEPT	INTERCEPT	56,21201	0,003227
x3	Living room Effective window ventilation area	90,89477	3,48E-08
x4	External Walls' Solar Absorptance	-58,35	5,75E-09
x13	Living room Overhang size	103,5655	9,66E-10
x14	Roof's Solar Absorptance	-157,764	1,57E-54
x18	Living room Window to Wall Ratio (WWR)	-5,06523	0,205875
x19	External Walls' U-value	-18,3262	2,11E-44
x21	Roof's U-Value	-59,9842	3,2E-07
x24	Roof's Heat Capacity	0,203004	6,31E-23
x45	inverse of Roof's U-Value	-9,31795	0,248669
x46	inverse of External Walls' Heat Capacity	-5744,54	1E-22
x47	inverse of Internal Walls' Heat Capacity	-3347,65	8,56E-09
x48	inverse of Roof's Heat Capacity	-1980,84	7,37E-07
x3:x21	Living room Effective window ventilation area x Roof's U-Value	-49,0604	5,48E-10
x3:x45	Living room Effective window ventilation area x inverse of Roof's U-Value	-30,8972	2,63E-05
x3:x46	Living room Effective window ventilation area x inverse of External Walls' Heat Capacity	-972,667	0,00025
x3:x47	Living room Effective window ventilation area x inverse of Internal Walls' Heat Capacity	-617,76	0,018928
x4:x14	External Walls' Solar Absorptance x Roof's Solar Absorptance	11,1276	2,1E-05
x4:x19	External Walls' Solar Absorptance x External Walls' U-value	13,62601	3,05E-65
x4:x21	External Walls' Solar Absorptance x Roof's U-Value	20,73743	3,07E-06
x4:x24	External Walls' Solar Absorptance x Roof's Heat Capacity	-0,02653	3,76E-10
x4:x45	External Walls' Solar Absorptance x inverse of Roof's U-Value	12,41491	0,002711
x4:x46	External Walls' Solar Absorptance x inverse of External Walls' Heat Capacity	1323,415	6,63E-19
x4:x47	External Walls' Solar Absorptance x inverse of Internal Walls' Heat Capacity	397,254	0,009521
x13:x14	Living room Overhang size x Roof's Solar Absorptance	-15,1162	0,00146
x13:x21	Living room Overhang size x Roof's U-Value	-50,0336	4,91E-10
x13:x45	Living room Overhang size x inverse of Roof's U-Value	-30,3248	6,26E-05
x13:x46	Living room Overhang size x inverse of External Walls' Heat Capacity	-1100,82	2,66E-05
x13:x47	Living room Overhang size x inverse of Internal Walls' Heat Capacity	-1045,1	0,000123
x13:x48	Living room Overhang size x inverse of Roof's Heat Capacity	-375,549	0,00856
x14:x19	Roof's Solar Absorptance x External Walls' U-value	4,912302	1,62E-10
x14:x21	Roof's Solar Absorptance x Roof's U-Value	75,7089	2,74E-65
x14:x24	Roof's Solar Absorptance x Roof's Heat Capacity	-0,02123	0,000188
x14:x45	Roof's Solar Absorptance x inverse of Roof's U-Value	40,51501	1,66E-22
x14:x46	Roof's Solar Absorptance x inverse of External Walls' Heat Capacity	1773,623	6,39E-34

x14:x47	Roof's Solar Absorptance Capacity	x	inverse of Internal Walls' Heat Capacity	925,5288	5,65E-10
x14:x48	Roof's Solar Absorptance Capacity	x	inverse of Roof's Heat Capacity	1433,689	5,55E-39
x18:x19	Living room Window to Wall Ratio (WWR) U-value	x	External Walls' U-value	3,131024	0,013169
x18:x21	Living room Window to Wall Ratio (WWR)	x	Roof's U-Value	6,445681	0,014365
x18:x24	Living room Window to Wall Ratio (WWR) Capacity	x	Roof's Heat Capacity	-0,03225	1,15E-06
x18:x46	Living room Window to Wall Ratio (WWR)	x	inverse of External Walls' Heat Capacity	896,7809	0,000131
x18:x47	Living room Window to Wall Ratio (WWR)	x	inverse of Internal Walls' Heat Capacity	682,4573	0,00453
x19:x21	External Walls' U-value	x	Roof's U-Value	1,579005	0,001159
x19:x24	External Walls' U-value	x	Roof's Heat Capacity	-0,01408	4,74E-17
x19:x46	External Walls' U-value	x	inverse of External Walls' Heat Capacity	845,1039	3,41E-80
x19:x47	External Walls' U-value	x	inverse of Internal Walls' Heat Capacity	309,437	1,17E-11
x19:x48	External Walls' U-value	x	inverse of Roof's Heat Capacity	62,09573	0,022655
x21:x24	Roof's U-Value	x	Roof's Heat Capacity	-0,07346	2,43E-14
x21:x46	Roof's U-Value	x	inverse of External Walls' Heat Capacity	2721,857	2,57E-28
x21:x47	Roof's U-Value	x	inverse of Internal Walls' Heat Capacity	1794,206	1,2E-12
x21:x48	Roof's U-Value	x	inverse of Roof's Heat Capacity	1372,534	2,08E-14
x24:x45	Roof's Heat Capacity	x	inverse of Roof's U-Value	-0,04596	2,72E-07
x24:x46	Roof's Heat Capacity	x	inverse of External Walls' Heat Capacity	-1,96853	1,33E-09
x24:x47	Roof's Heat Capacity	x	inverse of Internal Walls' Heat Capacity	-1,36258	2,27E-05
x45:x46	inverse of Roof's U-Value	x	inverse of External Walls' Heat Capacity	1323,99	2,01E-08
x45:x47	inverse of Roof's U-Value	x	inverse of Internal Walls' Heat Capacity	865,682	0,000234
x45:x48	inverse of Roof's U-Value	x	inverse of Roof's Heat Capacity	515,4849	0,002303
x46:x47	inverse of External Walls' Heat Capacity	x	inverse of Internal Walls' Heat Capacity	96581,18	9,64E-30
x46:x48	inverse of External Walls' Heat Capacity	x	inverse of Roof's Heat Capacity	57558,36	4,23E-21
x47:x48	inverse of Internal Walls' Heat Capacity	x	inverse of Roof's Heat Capacity	24868,09	3,91E-05
x4^2	External Walls' Solar Absorptance	x	External Walls' Solar Absorptance	7,359847	0,012301
x14^2	Roof's Solar Absorptance	x	Roof's Solar Absorptance	18,52881	1,94E-10
x19^2	External Walls' U-value	x	External Walls' U-value	1,641649	2,12E-24
x21^2	Roof's U-Value	x	Roof's U-Value	16,13522	5,97E-10
x48^2	inverse of Roof's Heat Capacity	x	inverse of Roof's Heat Capacity	-17056,6	4,48E-24



**APPENDIX H-Curitiba/PR Meta-model coefficients – Degree-hours of discomfort by heat (Non-zero approach with regression floor)**

Coefficient	Meaning	value	p-value
INTERCEPT	INTERCEPT	358,3747	3,02E-12
x4	External Walls' Solar Absorptance	-176,567	5,93E-18
x9	Bedroom_2 Right Fin size	-52,0469	0,000224
x11	Bedroom_1 Overhang size	-8,72256	0,035275
x12	Bedroom_2 Overhang size	-2,7608	0,844729
x13	Living room Overhang size	45,81751	0,000384
x14	Roof's Solar Absorptance	-336,754	3,26E-12
x16	Bedroom_1 Window to Wall Ratio (WWR)	47,6327	0,000125
x17	Bedroom_2 Window to Wall Ratio (WWR)	-14,7976	0,214369
x18	Living room Window to Wall Ratio (WWR)	26,97337	0,001166
x19	External Walls' U-value	-44,9846	1,21E-13
x21	Roof's U-Value	-249,298	6,01E-14
x22	External Walls' Heat Capacity	0,004138	0,951917
x24	Roof's Heat Capacity	0,586081	1,33E-16
x30	inverse of Bedroom_2 Left Fin size	-0,07762	0,812395
x43	inverse of External Walls' U-value	-6,28239	0,166167
x45	inverse of Roof's U-Value	-59,1857	0,000447
x46	inverse of External Walls' Heat Capacity	-14492,7	4,43E-14
x47	inverse of Internal Walls' Heat Capacity	-6040,44	2,4E-10
x4:x12	External Walls' Solar Absorptance x Bedroom_2 Overhang size	-42,2659	0,017261
x4:x14	External Walls' Solar Absorptance x Roof's Solar Absorptance	92,14922	3,08E-10
x4:x17	External Walls' Solar Absorptance x Bedroom_2 Window to Wall Ratio (WWR)	31,99793	0,036676
x4:x19	External Walls' Solar Absorptance x External Walls' U-value	41,88045	1,48E-56
x4:x21	External Walls' Solar Absorptance x Roof's U-Value	52,73584	2,29E-19
x4:x24	External Walls' Solar Absorptance x Roof's Heat Capacity	-0,21619	6,66E-24
x4:x46	External Walls' Solar Absorptance x inverse of External Walls' Heat Capacity	5883,885	1,23E-29
x4:x47	External Walls' Solar Absorptance x inverse of Internal Walls' Heat Capacity	2729,927	2,68E-07
x9:x14	Bedroom_2 Right Fin size x Roof's Solar Absorptance	42,82548	0,019203
x9:x24	Bedroom_2 Right Fin size x Roof's Heat Capacity	0,065345	0,020128
x12:x43	Bedroom_2 Overhang size x inverse of External Walls' U-value	10,66446	0,021182
x13:x21	Living room Overhang size x Roof's U-Value	-34,7	5,53E-05
x13:x47	Living room Overhang size x inverse of Internal Walls' Heat Capacity	-2777,92	0,001667
x14:x16	Roof's Solar Absorptance x Bedroom_1 Window to Wall Ratio (WWR)	-50,6403	0,001423
x14:x19	Roof's Solar Absorptance x External Walls' U-value	18,58297	7,43E-11
x14:x21	Roof's Solar Absorptance x Roof's U-Value	191,2808	1,26E-30
x14:x22	Roof's Solar Absorptance x External Walls' Heat Capacity	-0,15364	0,004051
x14:x24	Roof's Solar Absorptance x Roof's Heat Capacity	-0,29456	2,21E-35
x14:x45	Roof's Solar Absorptance x inverse of Roof's U-Value	56,254	0,000841

x14:x46	Roof's Solar Absorptance Capacity	x	inverse of External Walls' Heat Capacity	3868,094	7,04E-05
x14:x47	Roof's Solar Absorptance Capacity	x	inverse of Internal Walls' Heat Capacity	3724,52	4,84E-10
x16:x43	Bedroom_1 Window to Wall Ratio (WWR)	x	inverse of External Walls' U-value	12,93459	0,001122
x16:x47	Bedroom_1 Window to Wall Ratio (WWR)	x	inverse of Internal Walls' Heat Capacity	-2115,81	0,005263
x17:x46	Bedroom_2 Window to Wall Ratio (WWR)	x	inverse of External Walls' Heat Capacity	1987,836	0,004038
x18:x24	Living room Window to Wall Ratio (WWR)	x	Roof's Heat Capacity	-0,07456	0,002555
x18:x30	Living room Window to Wall Ratio (WWR)	x	inverse of Bedroom_2 Left Fin size	-1,25358	0,002534
x18:x46	Living room Window to Wall Ratio (WWR)	x	inverse of External Walls' Heat Capacity	2890,185	6,53E-05
x19:x21	External Walls' U-value	x	Roof's U-Value	7,855186	3,9E-05
x19:x22	External Walls' U-value	x	External Walls' Heat Capacity	-0,05341	3,69E-08
x19:x24	External Walls' U-value	x	Roof's Heat Capacity	-0,06174	2,8E-41
x19:x46	External Walls' U-value	x	inverse of External Walls' Heat Capacity	1038,687	2,14E-07
x19:x47	External Walls' U-value	x	inverse of Internal Walls' Heat Capacity	1171,907	1,12E-20
x21:x22	Roof's U-Value	x	External Walls' Heat Capacity	-0,08	0,000884
x21:x24	Roof's U-Value	x	Roof's Heat Capacity	-0,31627	3,4E-38
x21:x30	Roof's U-Value	x	inverse of Bedroom_2 Left Fin size	0,541511	7,41E-06
x21:x43	Roof's U-Value	x	inverse of External Walls' U-value	-5,0214	0,032584
x21:x46	Roof's U-Value	x	inverse of External Walls' Heat Capacity	4088,617	5,32E-07
x21:x47	Roof's U-Value	x	inverse of Internal Walls' Heat Capacity	3164,67	7,07E-29
x22:x24	External Walls' Heat Capacity	x	Roof's Heat Capacity	0,000571	1,7E-13
x24:x30	Roof's Heat Capacity	x	inverse of Bedroom_2 Left Fin size	-0,00124	0,000751
x24:x45	Roof's Heat Capacity	x	inverse of Roof's U-Value	-0,10499	7,38E-05
x24:x46	Roof's Heat Capacity	x	inverse of External Walls' Heat Capacity	-6,61937	6,33E-06
x24:x47	Roof's Heat Capacity	x	inverse of Internal Walls' Heat Capacity	-11,3061	1,69E-32
x30:x47	inverse of Bedroom_2 Left Fin size	x	inverse of Internal Walls' Heat Capacity	26,18306	0,028809
x45:x46	inverse of Roof's U-Value	x	inverse of External Walls' Heat Capacity	1511,287	0,046572
x46:x47	inverse of External Walls' Heat Capacity	x	inverse of Internal Walls' Heat Capacity	225123,5	6,97E-20
x14^2	Roof's Solar Absorptance	x	Roof's Solar Absorptance	62,80359	2,98E-06
x19^2	External Walls' U-value	x	External Walls' U-value	3,785869	4,54E-08
x21^2	Roof's U-Value	x	Roof's U-Value	47,31777	1,5E-09
x22^2	External Walls' Heat Capacity	x	External Walls' Heat Capacity	0,000288	0,004714
x24^2	Roof's Heat Capacity	x	Roof's Heat Capacity	0,000526	6,42E-59
x30^2	inverse of Bedroom_2 Left Fin size	x	inverse of Bedroom_2 Left Fin size	0,005166	0,017999

### APPENDIX I - São Paulo/SP: Meta-model coefficients – Degree-hours of discomfort by cold (standard approach with regression floor)

Coefficient	Meaning	value	p-value
INTERCEPT	INTERCEPT	3492,212	0
x4	External Walls' Solar Absorptance	-1805,7	2,9E-149
x5	Bedroom_1 Left Fin size	150,607	0,001339
x6	Bedroom_2 Left Fin size	181,8468	0,004163
x7	Living room Left Fin size	-4,07676	0,937628
x8	Bedroom_1 Right Fin size	-17,1501	0,538154
x9	Bedroom_2 Right Fin size	-47,8172	0,361285
x10	Living room Right Fin size	71,5257	0,254192
x11	Bedroom_1 Overhang size	313,6652	6,55E-06
x12	Bedroom_2 Overhang size	170,6565	0,000175
x13	Living room Overhang size	381,4572	6,05E-08
x14	Roof's Solar Absorptance	-1626,23	6,7E-129
x15	North Axis/ Orientation in the terrain	-8,43494	0
x17	Bedroom_2 Window to Wall Ratio (WWR)	-612,262	1,42E-15
x18	Living room Window to Wall Ratio (WWR)	-750,439	3,58E-28
x19	External Walls' U-value	1896,31	0
x21	Roof's U-Value	2671,813	0
x22	External Walls' Heat Capacity	-2,76346	1,28E-45
x23	Internal Walls' Heat Capacity	-0,82868	2,56E-12
x24	Roof's Heat Capacity	-1,04491	1,15E-10
x35	inverse of Bedroom_1 Overhang size	0,968856	6,95E-07
x39	inverse of North Axis/ Orientation in the terrain	-829,156	5,65E-10
x40	inverse of Bedroom_1 Window to Wall Ratio (WWR)	82,86173	5,41E-15
x46	inverse of External Walls' Heat Capacity	-5027,45	0,119784
x48	inverse of Roof's Heat Capacity	7326,963	0,000656
x4:x11	External Walls' Solar Absorptance x Bedroom_1 Overhang size	-115,734	0,022153
x4:x14	External Walls' Solar Absorptance x Roof's Solar Absorptance	797,5468	1,4E-167
x4:x15	External Walls' Solar Absorptance x North Axis/ Orientation in the terrain	0,333428	1,58E-06
x4:x17	External Walls' Solar Absorptance x Bedroom_2 Window to Wall Ratio (WWR)	424,3361	3,6E-22
x4:x18	External Walls' Solar Absorptance x Living room Window to Wall Ratio (WWR)	401,2784	5,98E-21
x4:x19	External Walls' Solar Absorptance x External Walls' U-value	-930,732	0
x4:x21	External Walls' Solar Absorptance x Roof's U-Value	-45,8067	0,007676
x4:x22	External Walls' Solar Absorptance x External Walls' Heat Capacity	-0,24648	0,024791
x4:x40	External Walls' Solar Absorptance x inverse of Bedroom_1 Window to Wall Ratio (WWR)	-43,0326	5,39E-17
x4:x46	External Walls' Solar Absorptance x inverse of External Walls' Heat Capacity	12010,35	2,15E-05
x5:x6	Bedroom_1 Left Fin size x Bedroom_2 Left Fin size	195,6862	0,037671
x5:x14	Bedroom_1 Left Fin size x Roof's Solar Absorptance	-121,834	0,016785

x5:x40	Bedroom_1 Left Fin size	x	inverse of Bedroom_1 Window to Wall Ratio (WWR)	-19,052	0,043601
x6:x7	Bedroom_2 Left Fin size	x	Living room Left Fin size	-202,7	0,029376
x6:x14	Bedroom_2 Left Fin size	x	Roof's Solar Absorptance	-140,855	0,005356
x6:x15	Bedroom_2 Left Fin size	x	North Axis/ Orientation in the terrain	-0,4445	0,000615
x6:x17	Bedroom_2 Left Fin size	x	Bedroom_2 Window to Wall Ratio (WWR)	242,9577	0,002577
x6:x39	Bedroom_2 Left Fin size	x	inverse of North Axis/ Orientation in the terrain	-801,063	7,8E-10
x7:x18	Living room Left Fin size	x	Living room Window to Wall Ratio (WWR)	190,2675	0,015741
x7:x21	Living room Left Fin size	x	Roof's U-Value	58,86032	0,057451
x8:x15	Bedroom_1 Right Fin size	x	North Axis/ Orientation in the terrain	0,493053	0,000154
x8:x39	Bedroom_1 Right Fin size	x	inverse of North Axis/ Orientation in the terrain	628,9143	0,000139
x9:x14	Bedroom_2 Right Fin size	x	Roof's Solar Absorptance	-99,0826	0,049068
x9:x17	Bedroom_2 Right Fin size	x	Bedroom_2 Window to Wall Ratio (WWR)	292,7451	0,000188
x9:x40	Bedroom_2 Right Fin size	x	inverse of Bedroom_1 Window to Wall Ratio (WWR)	24,63209	0,00857
x10:x18	Living room Right Fin size	x	Living room Window to Wall Ratio (WWR)	320,7788	3,53E-05
x10:x39	Living room Right Fin size	x	inverse of North Axis/ Orientation in the terrain	-381,671	0,000392
x11:x14	Bedroom_1 Overhang size	x	Roof's Solar Absorptance	-235,881	3,11E-06
x11:x15	Bedroom_1 Overhang size	x	North Axis/ Orientation in the terrain	1,047235	4,47E-16
x11:x19	Bedroom_1 Overhang size	x	External Walls' U-value	-42,7339	0,006204
x11:x22	Bedroom_1 Overhang size	x	External Walls' Heat Capacity	0,313453	0,004487
x11:x23	Bedroom_1 Overhang size	x	Internal Walls' Heat Capacity	0,267591	0,014708
x11:x40	Bedroom_1 Overhang size	x	inverse of Bedroom_1 Window to Wall Ratio (WWR)	-38,0826	6,54E-05
x11:x48	Bedroom_1 Overhang size	x	inverse of Roof's Heat Capacity	-6283,54	3,09E-05
x12:x14	Bedroom_2 Overhang size	x	Roof's Solar Absorptance	-180,868	0,000329
x12:x17	Bedroom_2 Overhang size	x	Bedroom_2 Window to Wall Ratio (WWR)	451,1494	6,97E-09
x13:x14	Living room Overhang size	x	Roof's Solar Absorptance	-173,407	0,00064
x13:x15	Living room Overhang size	x	North Axis/ Orientation in the terrain	-0,25133	0,049674
x13:x17	Living room Overhang size	x	Bedroom_2 Window to Wall Ratio (WWR)	-214,925	0,007735
x13:x18	Living room Overhang size	x	Living room Window to Wall Ratio (WWR)	475,6046	1,41E-09
x13:x19	Living room Overhang size	x	External Walls' U-value	-58,3345	0,000248
x13:x21	Living room Overhang size	x	Roof's U-Value	-71,392	0,025666
x14:x15	Roof's Solar Absorptance	x	North Axis/ Orientation in the terrain	0,159975	0,023603
x14:x17	Roof's Solar Absorptance	x	Bedroom_2 Window to Wall Ratio (WWR)	367,3323	2,54E-16
x14:x18	Roof's Solar Absorptance	x	Living room Window to Wall Ratio (WWR)	494,6006	2,02E-29
x14:x19	Roof's Solar Absorptance	x	External Walls' U-value	181,8692	8,52E-98
x14:x21	Roof's Solar Absorptance	x	Roof's U-Value	-2122,23	0
x14:x24	Roof's Solar Absorptance	x	Roof's Heat Capacity	-0,54307	2,33E-18

x14:x39	Roof's Solar Absorptance in the terrain	x	inverse of North Axis/ Orientation	-487,504	6,61E-14
x14:x40	Roof's Solar Absorptance	x	inverse of Bedroom_1 Window to Wall Ratio (WWR)	-57,3359	2,1E-27
x14:x48	Roof's Solar Absorptance	x	inverse of Roof's Heat Capacity	5720,702	2,78E-06
x15:x19	North Axis/ Orientation in the terrain	x	External Walls' U-value	0,040484	0,070059
x15:x22	North Axis/ Orientation in the terrain	x	External Walls' Heat Capacity	0,000447	0,004094
x15:x40	North Axis/ Orientation in the terrain	x	inverse of Bedroom_1 Window to Wall Ratio (WWR)	0,206795	2,89E-52
x15:x48	North Axis/ Orientation in the terrain	x	inverse of Roof's Heat Capacity	7,525179	0,001461
x17:x18	Bedroom_2 Window to Wall Ratio (WWR)	x	Living room Window to Wall Ratio (WWR)	318,7175	3,8E-06
x17:x19	Bedroom_2 Window to Wall Ratio (WWR)	x	External Walls' U-value	-100,539	3,58E-13
x17:x23	Bedroom_2 Window to Wall Ratio (WWR)	x	Internal Walls' Heat Capacity	-0,19837	0,039359
x17:x24	Bedroom_2 Window to Wall Ratio (WWR)	x	Roof's Heat Capacity	-0,3074	1,64E-05
x17:x40	Bedroom_2 Window to Wall Ratio (WWR)	x	inverse of Bedroom_1 Window to Wall Ratio (WWR)	-43,2287	8,14E-08
x17:x46	Bedroom_2 Window to Wall Ratio (WWR)	x	inverse of External Walls' Heat Capacity	6268,585	0,011145
x18:x19	Living room Window to Wall Ratio (WWR)	x	External Walls' U-value	-82,8442	1,7E-10
x18:x24	Living room Window to Wall Ratio (WWR)	x	Roof's Heat Capacity	-0,31335	7,96E-06
x18:x40	Living room Window to Wall Ratio (WWR)	x	inverse of Bedroom_1 Window to Wall Ratio (WWR)	-47,2867	3,09E-09
x19:x21	External Walls' U-value	x	Roof's U-Value	-144,395	5,1E-173
x19:x22	External Walls' U-value	x	External Walls' Heat Capacity	-0,34184	2,77E-24
x19:x23	External Walls' U-value	x	Internal Walls' Heat Capacity	-0,23263	1,53E-33
x19:x24	External Walls' U-value	x	Roof's Heat Capacity	-0,22311	5,6E-35
x19:x39	External Walls' U-value	x	inverse of North Axis/ Orientation in the terrain	-523,632	1E-29
x19:x40	External Walls' U-value	x	inverse of Bedroom_1 Window to Wall Ratio (WWR)	10,48896	5,24E-12
x19:x46	External Walls' U-value	x	inverse of External Walls' Heat Capacity	4767,008	3,6E-08
x19:x48	External Walls' U-value	x	inverse of Roof's Heat Capacity	1568,278	5,21E-06
x21:x23	Roof's U-Value	x	Internal Walls' Heat Capacity	-0,14394	0,000114
x21:x24	Roof's U-Value	x	Roof's Heat Capacity	-0,74904	2,64E-84
x21:x39	Roof's U-Value	x	inverse of North Axis/ Orientation in the terrain	-248,817	6,23E-09
x21:x46	Roof's U-Value	x	inverse of External Walls' Heat Capacity	8974,969	2,08E-21
x21:x48	Roof's U-Value	x	inverse of Roof's Heat Capacity	4216,483	1,42E-08
x22:x24	External Walls' Heat Capacity	x	Roof's Heat Capacity	0,001281	6,19E-13
x22:x39	External Walls' Heat Capacity	x	inverse of North Axis/ Orientation in the terrain	2,768684	3,9E-30
x23:x24	Internal Walls' Heat Capacity	x	Roof's Heat Capacity	0,001017	3,62E-14
x23:x39	Internal Walls' Heat Capacity	x	inverse of North Axis/ Orientation in the terrain	1,681017	7,49E-19
x23:x40	Internal Walls' Heat Capacity	x	inverse of Bedroom_1 Window to Wall Ratio (WWR)	0,03713	0,001131

x23:x46	Internal Walls' Heat Capacity x inverse of External Walls' Heat Capacity	-46,8797	1,89E-41
x23:x48	Internal Walls' Heat Capacity x inverse of Roof's Heat Capacity	-15,1352	4,83E-09
x24:x40	Roof's Heat Capacity x inverse of Bedroom_1 Window to Wall Ratio (WWR)	0,030903	0,000226
x24:x46	Roof's Heat Capacity x inverse of External Walls' Heat Capacity	-17,9343	0,000497
x35:x39	inverse of Bedroom_1 Overhang size x inverse of North Axis/ Orientation in the terrain	-17,656	5,95E-09
x39:x40	inverse of North Axis/ Orientation in the terrain x inverse of Bedroom_1 Window to Wall Ratio (WWR)	77,0011	2,38E-10
x39:x46	inverse of North Axis/ Orientation in the terrain x inverse of External Walls' Heat Capacity	52481	1,2E-26
x39:x48	inverse of North Axis/ Orientation in the terrain x inverse of Roof's Heat Capacity	-5069,76	0,072726
x40:x46	inverse of Bedroom_1 Window to Wall Ratio (WWR) x inverse of External Walls' Heat Capacity	-939,124	0,000996
x46:x48	inverse of External Walls' Heat Capacity x inverse of Roof's Heat Capacity	931757,5	6,74E-45
x4^2	External Walls' Solar Absorptance x External Walls' Solar Absorptance	559,2501	3,69E-70
x10^2	Living room Right Fin size x Living room Right Fin size	-243,027	0,017286
x14^2	Roof's Solar Absorptance x Roof's Solar Absorptance	982,538	2,2E-207
x15^2	North Axis/ Orientation in the terrain x North Axis/ Orientation in the terrain	0,017765	0
x19^2	External Walls' U-value x External Walls' U-value	-55,8444	3,5E-210
x22^2	External Walls' Heat Capacity x External Walls' Heat Capacity	0,002656	4,24E-22
x23^2	Internal Walls' Heat Capacity x Internal Walls' Heat Capacity	0,000897	2,44E-09
x24^2	Roof's Heat Capacity x Roof's Heat Capacity	0,001593	1,17E-24
x39^2	inverse of North Axis/ Orientation in the terrain x inverse of North Axis/ Orientation in the terrain	32,56589	1,82E-41
x40^2	inverse of Bedroom_1 Window to Wall Ratio (WWR) x inverse of Bedroom_1 Window to Wall Ratio (WWR)	-2,8693	7,98E-06
x48^2	inverse of Roof's Heat Capacity x inverse of Roof's Heat Capacity	-218561	2,01E-17

### APPENDIX J - São Paulo/SP: Meta-model coefficients – Degree-hours of discomfort by heat (standard approach with regression floor)

Coefficient	Meaning	value	p-value
INTERCEPT	INTERCEPT	209,0965	3,57E-54
x4	External Walls' Solar Absorptance	-142,318	3,32E-33
x11	Bedroom_1 Overhang size	11,57586	0,248043
x13	Living room Overhang size	35,13246	0,001299
x14	Roof's Solar Absorptance	-313,121	2,2E-121
x16	Bedroom_1 Window to Wall Ratio (WWR)	-58,3168	0,000395
x17	Bedroom_2 Window to Wall Ratio (WWR)	-47,5932	3,94E-07
x18	Living room Window to Wall Ratio (WWR)	-42,1278	0,000443
x19	External Walls' U-value	-47,3152	5,9E-32
x21	Roof's U-Value	-170,638	2,9E-66
x23	Internal Walls' Heat Capacity	0,187527	1,31E-11
x27	inverse of Living room Effective window ventilation area	17,42579	6,2E-05
x33	inverse of Bedroom_2 Right Fin size	0,670124	0,010185
x46	inverse of External Walls' Heat Capacity	-10970	6,84E-59
x48	inverse of Roof's Heat Capacity	-5654,8	2,48E-36
x4:x11	External Walls' Solar Absorptance x Bedroom_1 Overhang size	-25,7689	0,025528
x4:x14	External Walls' Solar Absorptance x Roof's Solar Absorptance	54,79794	1,08E-17
x4:x18	External Walls' Solar Absorptance x Living room Window to Wall Ratio (WWR)	21,50221	0,027303
x4:x19	External Walls' Solar Absorptance x External Walls' U-value	55,77705	4,5E-162
x4:x21	External Walls' Solar Absorptance x Roof's U-Value	32,08197	3,64E-16
x4:x23	External Walls' Solar Absorptance x Internal Walls' Heat Capacity	-0,05415	0,000118
x4:x46	External Walls' Solar Absorptance x inverse of External Walls' Heat Capacity	4866,426	2,07E-41
x4:x48	External Walls' Solar Absorptance x inverse of Roof's Heat Capacity	1934,396	2,15E-21
x11:x19	Bedroom_1 Overhang size x External Walls' U-value	-14,1075	7,87E-05
x11:x23	Bedroom_1 Overhang size x Internal Walls' Heat Capacity	0,066866	0,007631
x11:x48	Bedroom_1 Overhang size x inverse of Roof's Heat Capacity	-1623,67	2,8E-06
x13:x14	Living room Overhang size x Roof's Solar Absorptance	-23,8267	0,040175
x13:x16	Living room Overhang size x Bedroom_1 Window to Wall Ratio (WWR)	-36,9951	0,040171
x13:x19	Living room Overhang size x External Walls' U-value	-13,5123	0,000182
x14:x16	Roof's Solar Absorptance x Bedroom_1 Window to Wall Ratio (WWR)	44,22432	6,39E-06
x14:x17	Roof's Solar Absorptance x Bedroom_2 Window to Wall Ratio (WWR)	46,05074	6,85E-06
x14:x18	Roof's Solar Absorptance x Living room Window to Wall Ratio (WWR)	28,3489	0,004541
x14:x19	Roof's Solar Absorptance x External Walls' U-value	18,92962	2,65E-22
x14:x21	Roof's Solar Absorptance x Roof's U-Value	146,2219	1,9E-267
x14:x23	Roof's Solar Absorptance x Internal Walls' Heat Capacity	-0,12287	2,71E-18
x14:x33	Roof's Solar Absorptance x inverse of Bedroom_2 Right Fin	0,466267	0,001684

	size				
x14:x46	Roof's Solar Absorptance	x	inverse of External Walls' Heat Capacity	6190,598	2,51E-66
x14:x48	Roof's Solar Absorptance	x	inverse of Roof's Heat Capacity	6090,088	1,8E-173
x16:x21	Bedroom_1 Window to Wall Ratio (WWR)	x	Roof's U-Value	30,3961	2,57E-07
x16:x23	Bedroom_1 Window to Wall Ratio (WWR)	x	Internal Walls' Heat Capacity	-0,074	0,00058
x16:x46	Bedroom_1 Window to Wall Ratio (WWR)	x	inverse of External Walls' Heat Capacity	2535,154	2,46E-06
x16:x48	Bedroom_1 Window to Wall Ratio (WWR)	x	inverse of Roof's Heat Capacity	1360,055	1,3E-05
x17:x21	Bedroom_2 Window to Wall Ratio (WWR)	x	Roof's U-Value	20,89712	0,000575
x17:x33	Bedroom_2 Window to Wall Ratio (WWR)	x	inverse of Bedroom_2 Right Fin size	-0,5553	0,012045
x17:x46	Bedroom_2 Window to Wall Ratio (WWR)	x	inverse of External Walls' Heat Capacity	2039,182	0,000288
x17:x48	Bedroom_2 Window to Wall Ratio (WWR)	x	inverse of Roof's Heat Capacity	1533,531	1,4E-06
x18:x21	Living room Window to Wall Ratio (WWR)	x	Roof's U-Value	26,28055	1,72E-05
x18:x23	Living room Window to Wall Ratio (WWR)	x	Internal Walls' Heat Capacity	-0,057	0,008634
x18:x46	Living room Window to Wall Ratio (WWR)	x	inverse of External Walls' Heat Capacity	2040,648	0,00023
x18:x48	Living room Window to Wall Ratio (WWR)	x	inverse of Roof's Heat Capacity	1879,125	1,54E-09
x19:x21	External Walls' U-value	x	Roof's U-Value	4,114495	0,00029
x19:x23	External Walls' U-value	x	Internal Walls' Heat Capacity	-0,03756	1,15E-17
x19:x27	External Walls' U-value	x	inverse of Living room Effective window ventilation area	-4,72156	0,009332
x19:x33	External Walls' U-value	x	inverse of Bedroom_2 Right Fin size	0,206007	3,08E-06
x19:x46	External Walls' U-value	x	inverse of External Walls' Heat Capacity	2940,155	1,1E-158
x19:x48	External Walls' U-value	x	inverse of Roof's Heat Capacity	767,2884	4,3E-37
x21:x23	Roof's U-Value	x	Internal Walls' Heat Capacity	-0,04472	1,66E-07
x21:x27	Roof's U-Value	x	inverse of Living room Effective window ventilation area	-8,44865	0,021323
x21:x33	Roof's U-Value	x	inverse of Bedroom_2 Right Fin size	-0,17966	0,046587
x21:x46	Roof's U-Value	x	inverse of External Walls' Heat Capacity	3366,082	4,61E-54
x21:x48	Roof's U-Value	x	inverse of Roof's Heat Capacity	3748,863	8,3E-180
x23:x33	Internal Walls' Heat Capacity	x	inverse of Bedroom_2 Right Fin size	-0,0008	0,011919
x23:x46	Internal Walls' Heat Capacity	x	inverse of External Walls' Heat Capacity	-7,31071	1,85E-20
x23:x48	Internal Walls' Heat Capacity	x	inverse of Roof's Heat Capacity	-4,61654	8,5E-26
x27:x33	inverse of Living room Effective window ventilation area	x	inverse of Bedroom_2 Right Fin size	-0,49387	0,000127
x27:x48	inverse of Living room Effective window ventilation area	x	inverse of Roof's Heat Capacity	-735,039	4,12E-05
x33:x48	inverse of Bedroom_2 Right Fin size	x	inverse of Roof's Heat Capacity	14,26025	0,005877
x46:x48	inverse of External Walls' Heat Capacity	x	inverse of Roof's Heat Capacity	293633,9	1,7E-145
x4^2	External Walls' Solar Absorptance	x	External Walls' Solar Absorptance	28,60354	6,04E-05
x14^2	Roof's Solar Absorptance	x	Roof's Solar Absorptance	78,87161	4,51E-29



x16^2	Bedroom_1 Window to Wall Ratio (WWR) x Bedroom_1 Window to Wall Ratio (WWR)	26,923	0,036682
x19^2	External Walls' U-value x External Walls' U-value	4,881887	9,24E-35
x21^2	Roof's U-Value x Roof's U-Value	22,18825	8,19E-22
x23^2	Internal Walls' Heat Capacity x Internal Walls' Heat Capacity	0,000133	0,000115
x33^2	inverse of Bedroom_2 Right Fin size x inverse of Bedroom_2 Right Fin size	0,003711	0,008683
x46^2	inverse of External Walls' Heat Capacity x inverse of External Walls' Heat Capacity	-56791,2	0,000216
x48^2	inverse of Roof's Heat Capacity x inverse of Roof's Heat Capacity	-52405,2	1,57E-66



**APPENDIX K- São Paulo/SP: Meta-model coefficients – Degree-hours of discomfort by heat (Non-zero approach with regression floor)**

Coefficient	Meaning	value	p-value
INTERCEPT	INTERCEPT	378,9731	9,43E-15
x4	External Walls' Solar Absorptance	-205,863	6,73E-17
x5	Bedroom_1 Left Fin size	-11,5254	0,003621
x11	Bedroom_1 Overhang size	58,04928	3,77E-05
x12	Bedroom_2 Overhang size	-32,1959	0,004398
x13	Living room Overhang size	9,071032	0,366586
x14	Roof's Solar Absorptance	-671,798	6,08E-48
x16	Bedroom_1 Window to Wall Ratio (WWR)	24,80705	0,172697
x17	Bedroom_2 Window to Wall Ratio (WWR)	-23,8698	0,234426
x18	Living room Window to Wall Ratio (WWR)	-55,8355	0,012285
x19	External Walls' U-value	-55,0305	7,43E-25
x21	Roof's U-Value	-362,528	3,83E-30
x22	External Walls' Heat Capacity	0,275397	0,000188
x23	Internal Walls' Heat Capacity	0,304049	1,16E-08
x24	Roof's Heat Capacity	0,69502	5,8E-20
x33	inverse of Bedroom_2 Right Fin size	-0,04448	0,866359
x41	inverse of Bedroom_2 Window to Wall Ratio (WWR)	5,104988	0,000508
x45	inverse of Roof's U-Value	-85,2232	5,93E-09
x46	inverse of External Walls' Heat Capacity	-8705,61	9,45E-12
x48	inverse of Roof's Heat Capacity	-4156,2	1,24E-07
x4:x11	External Walls' Solar Absorptance Overhang size x Bedroom_1	-55,7242	0,000497
x4:x14	External Walls' Solar Absorptance Absorptance x Roof's Solar	194,791	2,41E-55
x4:x18	External Walls' Solar Absorptance to Wall Ratio (WWR) x Living room Window	43,68695	0,001157
x4:x19	External Walls' Solar Absorptance value x External Walls' U-	102,2987	4,9E-294
x4:x21	External Walls' Solar Absorptance x Roof's U-Value	94,48206	1,62E-63
x4:x22	External Walls' Solar Absorptance Capacity x External Walls' Heat	-0,34993	3,29E-20
x4:x23	External Walls' Solar Absorptance Capacity x Internal Walls' Heat	-0,17166	2,01E-16
x4:x24	External Walls' Solar Absorptance Capacity x Roof's Heat	-0,30419	4,44E-39
x4:x41	External Walls' Solar Absorptance Bedroom_2 Window to Wall Ratio (WWR) x inverse of	-4,87267	0,007654
x4:x46	External Walls' Solar Absorptance Walls' Heat Capacity x inverse of External	4625,35	7,72E-09
x4:x48	External Walls' Solar Absorptance Heat Capacity x inverse of Roof's	1471,436	1,81E-06
x11:x19	Bedroom_1 Overhang size x External Walls' U-value	-18,6852	7E-07
x11:x46	Bedroom_1 Overhang size Heat Capacity x inverse of External Walls'	-1926,78	0,011736
x11:x48	Bedroom_1 Overhang size Capacity x inverse of Roof's Heat	-1447,7	0,000145
x12:x18	Bedroom_2 Overhang size x Living room Window to Wall	46,07613	0,04825

x13:x19	Living room Overhang size	x	External Walls' U-value	-9,30435	0,014397
x13:x33	Living room Overhang size Fin size	x	inverse of Bedroom_2 Right	1,061089	0,012862
x13:x46	Living room Overhang size	x	inverse of External Walls' Heat Capacity	-2430,05	0,001618
x13:x48	Living room Overhang size	x	inverse of Roof's Heat Capacity	-826,618	0,034632
x14:x16	Roof's Solar Absorptance	x	Bedroom_1 Window to Wall Ratio (WWR)	60,48912	8,27E-05
x14:x17	Roof's Solar Absorptance	x	Bedroom_2 Window to Wall Ratio (WWR)	59,37387	0,000205
x14:x18	Roof's Solar Absorptance	x	Living room Window to Wall Ratio (WWR)	45,38299	0,003385
x14:x19	Roof's Solar Absorptance	x	External Walls' U-value	41,25817	7,63E-47
x14:x21	Roof's Solar Absorptance	x	Roof's U-Value	402,8104	1,7E-132
x14:x22	Roof's Solar Absorptance	x	External Walls' Heat Capacity	-0,4033	9,72E-19
x14:x23	Roof's Solar Absorptance	x	Internal Walls' Heat Capacity	-0,24136	7,18E-24
x14:x24	Roof's Solar Absorptance	x	Roof's Heat Capacity	-0,4663	5,65E-73
x14:x33	Roof's Solar Absorptance	x	inverse of Bedroom_2 Right Fin size	0,980809	0,000141
x14:x45	Roof's Solar Absorptance	x	inverse of Roof's U-Value	118,8332	3,47E-14
x14:x46	Roof's Solar Absorptance	x	inverse of External Walls' Heat Capacity	6141,33	3,98E-12
x14:x48	Roof's Solar Absorptance	x	inverse of Roof's Heat Capacity	5420,793	4,18E-50
x16:x21	Bedroom_1 Window to Wall Ratio (WWR)	x	Roof's U- Value	28,51599	8,56E-05
x16:x22	Bedroom_1 Window to Wall Ratio (WWR)	x	External Walls' Heat Capacity	-0,11861	8,43E-05
x16:x23	Bedroom_1 Window to Wall Ratio (WWR)	x	Internal Walls' Heat Capacity	-0,1004	0,000673
x16:x24	Bedroom_1 Window to Wall Ratio (WWR)	x	Roof's Heat Capacity	-0,09137	0,002248
x16:x48	Bedroom_1 Window to Wall Ratio (WWR)	x	inverse of Roof's Heat Capacity	2599,851	1,13E-08
x17:x21	Bedroom_2 Window to Wall Ratio (WWR)	x	Roof's U- Value	33,57022	1,16E-05
x17:x23	Bedroom_2 Window to Wall Ratio (WWR)	x	Internal Walls' Heat Capacity	-0,09893	0,000829
x17:x24	Bedroom_2 Window to Wall Ratio (WWR)	x	Roof's Heat Capacity	-0,06203	0,043406
x17:x46	Bedroom_2 Window to Wall Ratio (WWR)	x	inverse of External Walls' Heat Capacity	4256,2	1,23E-09
x17:x48	Bedroom_2 Window to Wall Ratio (WWR)	x	inverse of Roof's Heat Capacity	2649,202	4,41E-09
x18:x21	Living room Window to Wall Ratio (WWR)	x	Roof's U- Value	43,14944	6,09E-09
x18:x23	Living room Window to Wall Ratio (WWR)	x	Internal Walls' Heat Capacity	-0,10453	0,000308
x18:x24	Living room Window to Wall Ratio (WWR)	x	Roof's Heat Capacity	-0,12446	3,97E-05
x18:x46	Living room Window to Wall Ratio (WWR)	x	inverse of External Walls' Heat Capacity	3660,921	5,07E-08
x18:x48	Living room Window to Wall Ratio (WWR)	x	inverse of Roof's Heat Capacity	1654,549	0,000214
x19:x21	External Walls' U-value	x	Roof's U-Value	22,09194	3,51E-60
x19:x22	External Walls' U-value	x	External Walls' Heat Capacity	-0,1062	3,88E-30

x19:x23	External Walls' U-value	x	Internal Walls' Heat Capacity	-0,07222	6,1E-44
x19:x24	External Walls' U-value	x	Roof's Heat Capacity	-0,09551	1,12E-74
x19:x33	External Walls' U-value	x	inverse of Bedroom_2 Right Fin size	0,218991	2,26E-05
x19:x46	External Walls' U-value	x	inverse of External Walls' Heat Capacity	2175,135	2,64E-25
x19:x48	External Walls' U-value	x	inverse of Roof's Heat Capacity	258,3311	0,000736
x21:x22	Roof's U-Value	x	External Walls' Heat Capacity	-0,23472	1,9E-30
x21:x23	Roof's U-Value	x	Internal Walls' Heat Capacity	-0,12132	3,93E-27
x21:x24	Roof's U-Value	x	Roof's Heat Capacity	-0,40882	1,47E-66
x21:x46	Roof's U-Value	x	inverse of External Walls' Heat Capacity	1864,055	7,52E-06
x21:x48	Roof's U-Value	x	inverse of Roof's Heat Capacity	2268,019	3,55E-37
x22:x23	External Walls' Heat Capacity	x	Internal Walls' Heat Capacity	0,000335	1,18E-05
x22:x24	External Walls' Heat Capacity	x	Roof's Heat Capacity	0,000551	1,75E-10
x22:x33	External Walls' Heat Capacity	x	inverse of Bedroom_2 Right Fin size	-0,00146	0,008529
x22:x48	External Walls' Heat Capacity	x	inverse of Roof's Heat Capacity	-6,16094	2,99E-07
x23:x24	Internal Walls' Heat Capacity	x	Roof's Heat Capacity	0,000398	1,84E-18
x23:x33	Internal Walls' Heat Capacity	x	inverse of Bedroom_2 Right Fin size	-0,0021	2,98E-05
x23:x46	Internal Walls' Heat Capacity	x	inverse of External Walls' Heat Capacity	-5,87328	0,000391
x23:x48	Internal Walls' Heat Capacity	x	inverse of Roof's Heat Capacity	-5,30587	7,77E-16
x24:x33	Roof's Heat Capacity	x	inverse of Bedroom_2 Right Fin size	-0,00088	0,017034
x24:x45	Roof's Heat Capacity	x	inverse of Roof's U-Value	-0,08679	0,000156
x24:x46	Roof's Heat Capacity	x	inverse of External Walls' Heat Capacity	-11,2287	4,22E-10
x46:x48	inverse of External Walls' Heat Capacity	x	inverse of Roof's Heat Capacity	126041,4	3,8E-06
x4^2	External Walls' Solar Absorptance	x	External Walls' Solar Absorptance	64,23986	5,1E-10
x14^2	Roof's Solar Absorptance	x	Roof's Solar Absorptance	124,8602	6,76E-24
x19^2	External Walls' U-value	x	External Walls' U-value	6,95283	2,36E-47
x21^2	Roof's U-Value	x	Roof's U-Value	65,10893	1,5E-16
x22^2	External Walls' Heat Capacity	x	External Walls' Heat Capacity	0,000747	8,15E-17
x23^2	Internal Walls' Heat Capacity	x	Internal Walls' Heat Capacity	0,00032	6,93E-12
x24^2	Roof's Heat Capacity	x	Roof's Heat Capacity	0,000632	7,72E-36
x48^2	inverse of Roof's Heat Capacity	x	inverse of Roof's Heat Capacity	-42880,6	3,58E-12



### APPENDIX L- Manaus/AM: Meta-model coefficients – Degree-hours of discomfort by heat (standard approach with regression floor)

Coefficient	Meaning	value	p-value
INTERCEPT	INTERCEPT	911,8894	4,62E-13
x4	External Walls' Solar Absorptance	-1850,12	2,44E-82
x5	Bedroom_1 Left Fin size	308,6149	0,004451
x6	Bedroom_2 Left Fin size	48,42138	0,475329
x8	Bedroom_1 Right Fin size	468,2416	0,000621
x9	Bedroom_2 Right Fin size	390,6307	4,08E-05
x11	Bedroom_1 Overhang size	393,9732	1,18E-05
x12	Bedroom_2 Overhang size	155,6619	0,164865
x13	Living room Overhang size	580,1741	6,48E-12
x14	Roof's Solar Absorptance	-3010,46	2,1E-199
x15	North Axis/ Orientation in the terrain	-0,27827	0,012303
x16	Bedroom_1 Window to Wall Ratio (WWR)	-296,258	0,019323
x17	Bedroom_2 Window to Wall Ratio (WWR)	-539,48	1,65E-05
x18	Living room Window to Wall Ratio (WWR)	-666,16	2,38E-07
x19	External Walls' U-value	-216,528	3,45E-23
x21	Roof's U-Value	-1243,23	3,8E-118
x24	Roof's Heat Capacity	1,68734	2,87E-15
x25	inverse of Bedroom_1 Effective window ventilation area	67,28971	0,0075
x31	inverse of Living room Left Fin size	-5,02796	9,85E-06
x32	inverse of Bedroom_1 Right Fin size	-0,52004	0,510173
x34	inverse of Living room Right Fin size	0,52491	0,498399
x43	inverse of External Walls' U-value	235,9633	6,54E-15
x46	inverse of External Walls' Heat Capacity	-28572,8	2,28E-07
x47	inverse of Internal Walls' Heat Capacity	-20062,9	1,21E-05
x48	inverse of Roof's Heat Capacity	-39261,2	4,97E-23
x4:x6	External Walls' Solar Absorptance x Bedroom_2 Left Fin size	-161,352	0,016394
x4:x11	External Walls' Solar Absorptance x Bedroom_1 Overhang size	-155,998	0,019908
x4:x12	External Walls' Solar Absorptance x Bedroom_2 Overhang size	-197,806	0,002829
x4:x13	External Walls' Solar Absorptance x Living room Overhang size	-183,121	0,005272
x4:x14	External Walls' Solar Absorptance x Roof's Solar Absorptance	792,1097	1,1E-101
x4:x16	External Walls' Solar Absorptance x Bedroom_1 Window to Wall Ratio (WWR)	270,5399	2,58E-06
x4:x17	External Walls' Solar Absorptance x Bedroom_2 Window to Wall Ratio (WWR)	226,356	7,85E-05
x4:x18	External Walls' Solar Absorptance x Living room Window to Wall Ratio (WWR)	284,6164	7,47E-07
x4:x19	External Walls' Solar Absorptance x External Walls' U-value	907,7453	0
x4:x21	External Walls' Solar Absorptance x Roof's U-Value	253,1698	7,86E-30
x4:x24	External Walls' Solar Absorptance x Roof's Heat Capacity	-0,53998	1,1E-11

x4:x32	External Walls' Solar Absorptance Bedroom_1 Right Fin size	x	inverse of	1,868761	0,020749
x4:x43	External Walls' Solar Absorptance Walls' U-value	x	inverse of External	110,1346	8,89E-11
x4:x46	External Walls' Solar Absorptance Walls' Heat Capacity	x	inverse of External	51882,5	2,2E-124
x4:x47	External Walls' Solar Absorptance Walls' Heat Capacity	x	inverse of Internal	12085,61	7,03E-09
x4:x48	External Walls' Solar Absorptance Heat Capacity	x	inverse of Roof's	6593,142	2,66E-05
x5:x12	Bedroom_1 Left Fin size	x	Bedroom_2 Overhang size	243,9179	0,046649
x5:x14	Bedroom_1 Left Fin size	x	Roof's Solar Absorptance	-140,524	0,035856
x5:x18	Bedroom_1 Left Fin size	x	Living room Window to Wall Ratio (WWR)	-206,912	0,04961
x5:x19	Bedroom_1 Left Fin size	x	External Walls' U-value	-92,8213	0,005869
x5:x32	Bedroom_1 Left Fin size size	x	inverse of Bedroom_1 Right Fin size	-3,09938	0,039812
x5:x43	Bedroom_1 Left Fin size	x	inverse of External Walls' U- value	-66,3944	0,035854
x5:x46	Bedroom_1 Left Fin size	x	inverse of External Walls' Heat Capacity	-10676	0,007401
x6:x17	Bedroom_2 Left Fin size	x	Bedroom_2 Window to Wall Ratio (WWR)	-217,089	0,038712
x6:x24	Bedroom_2 Left Fin size	x	Roof's Heat Capacity	0,303552	0,004626
x8:x19	Bedroom_1 Right Fin size	x	External Walls' U-value	-169,982	2,95E-07
x8:x43	Bedroom_1 Right Fin size	x	inverse of External Walls' U- value	-86,3336	0,005826
x8:x46	Bedroom_1 Right Fin size	x	inverse of External Walls' Heat Capacity	11726,31	0,018486
x8:x48	Bedroom_1 Right Fin size	x	inverse of Roof's Heat Capacity	-4275,67	0,035669
x9:x14	Bedroom_2 Right Fin size	x	Roof's Solar Absorptance	-133,26	0,044852
x9:x17	Bedroom_2 Right Fin size	x	Bedroom_2 Window to Wall Ratio (WWR)	-270,203	0,009488
x9:x47	Bedroom_2 Right Fin size	x	inverse of Internal Walls' Heat Capacity	-11684,8	0,001533
x11:x14	Bedroom_1 Overhang size	x	Roof's Solar Absorptance	-300,391	6,87E-06
x11:x16	Bedroom_1 Overhang size	x	Bedroom_1 Window to Wall Ratio (WWR)	-283,935	0,007
x11:x21	Bedroom_1 Overhang size	x	Roof's U-Value	-137,172	0,000702
x11:x24	Bedroom_1 Overhang size	x	Roof's Heat Capacity	0,267408	0,01369
x11:x34	Bedroom_1 Overhang size	x	inverse of Living room Right Fin size	-3,91906	0,008649
x11:x46	Bedroom_1 Overhang size	x	inverse of External Walls' Heat Capacity	-9792,22	0,012519
x12:x14	Bedroom_2 Overhang size	x	Roof's Solar Absorptance	-272,818	5,04E-05
x12:x17	Bedroom_2 Overhang size	x	Bedroom_2 Window to Wall Ratio (WWR)	-565,38	6,28E-08
x12:x24	Bedroom_2 Overhang size	x	Roof's Heat Capacity	0,297132	0,005684
x12:x46	Bedroom_2 Overhang size	x	inverse of External Walls' Heat Capacity	-8479,82	0,030252
x12:x47	Bedroom_2 Overhang size	x	inverse of Internal Walls' Heat Capacity	-8393,31	0,028185
x13:x14	Living room Overhang size	x	Roof's Solar Absorptance	-209,114	0,001508
x13:x18	Living room Overhang size	x	Living room Window to Wall Ratio (WWR)	-421,627	5,6E-05
x13:x21	Living room Overhang size	x	Roof's U-Value	-140,294	0,000354



x13:x34	Living room Overhang size Fin size	x	inverse of Living room Right	-3,42052	0,016614
x13:x47	Living room Overhang size Heat Capacity	x	inverse of Internal Walls'	-13082,2	0,000561
x13:x48	Living room Overhang size Capacity	x	inverse of Roof's Heat	-12577,4	8,91E-10
x14:x15	Roof's Solar Absorptance terrain	x	North Axis/ Orientation in the	0,300336	0,001014
x14:x16	Roof's Solar Absorptance Ratio (WWR)	x	Bedroom_1 Window to Wall	606,2887	3,69E-26
x14:x17	Roof's Solar Absorptance Ratio (WWR)	x	Bedroom_2 Window to Wall	547,5171	1,32E-21
x14:x18	Roof's Solar Absorptance Ratio (WWR)	x	Living room Window to Wall	497,4884	4,53E-18
x14:x19	Roof's Solar Absorptance	x	External Walls' U-value	101,4124	8,63E-09
x14:x21	Roof's Solar Absorptance	x	Roof's U-Value	1926,697	0
x14:x24	Roof's Solar Absorptance	x	Roof's Heat Capacity	-1,70997	5,2E-97
x14:x43	Roof's Solar Absorptance	x	inverse of External Walls' U- value	-70,9483	2,83E-05
x14:x46	Roof's Solar Absorptance Heat Capacity	x	inverse of External Walls'	48938,73	4,7E-112
x14:x47	Roof's Solar Absorptance Heat Capacity	x	inverse of Internal Walls'	19379,41	4,61E-20
x14:x48	Roof's Solar Absorptance Capacity	x	inverse of Roof's Heat	36554,19	1,2E-121
x15:x18	North Axis/ Orientation in the terrain Window to Wall Ratio (WWR)	x	Living room	0,316551	0,026577
x15:x21	North Axis/ Orientation in the terrain	x	Roof's U-Value	0,106798	0,051286
x15:x24	North Axis/ Orientation in the terrain Capacity	x	Roof's Heat	-0,00034	0,019017
x15:x46	North Axis/ Orientation in the terrain Walls' Heat Capacity	x	inverse of External	10,23942	0,051698
x16:x17	Bedroom_1 Window to Wall Ratio (WWR) Window to Wall Ratio (WWR)	x	Bedroom_2	245,7963	0,005512
x16:x18	Bedroom_1 Window to Wall Ratio (WWR) Window to Wall Ratio (WWR)	x	Living room	266,7729	0,002918
x16:x21	Bedroom_1 Window to Wall Ratio (WWR)	x	Roof's U- Value	90,80791	0,008612
x16:x24	Bedroom_1 Window to Wall Ratio (WWR)	x	Roof's Heat Capacity	-0,38619	0,001751
x16:x25	Bedroom_1 Window to Wall Ratio (WWR) Bedroom_1 Effective window ventilation area	x	inverse of	-143,52	0,006686
x16:x46	Bedroom_1 Window to Wall Ratio (WWR)	x	inverse of	14812,75	2,11E-05
x16:x47	Bedroom_1 Window to Wall Ratio (WWR) Internal Walls' Heat Capacity	x	inverse of	8711,905	0,005764
x16:x48	Bedroom_1 Window to Wall Ratio (WWR) Roof's Heat Capacity	x	inverse of	14835,55	5,84E-11
x17:x18	Bedroom_2 Window to Wall Ratio (WWR) Window to Wall Ratio (WWR)	x	Living room	307,7179	0,000633
x17:x21	Bedroom_2 Window to Wall Ratio (WWR)	x	Roof's U- Value	188,6714	4,79E-08
x17:x24	Bedroom_2 Window to Wall Ratio (WWR) Capacity	x	Roof's Heat	-0,45313	0,000317
x17:x46	Bedroom_2 Window to Wall Ratio (WWR) External Walls' Heat Capacity	x	inverse of	14969,28	3,81E-06
x17:x47	Bedroom_2 Window to Wall Ratio (WWR) Internal Walls' Heat Capacity	x	inverse of	13441,73	5,19E-05
x17:x48	Bedroom_2 Window to Wall Ratio (WWR) Roof's Heat Capacity	x	inverse of	16297,15	2,47E-11

x18:x21	Living room Window to Wall Ratio (WWR)	x	Roof's U-Value	81,86552	0,01702
x18:x24	Living room Window to Wall Ratio (WWR)	x	Roof's Heat Capacity	-0,36643	0,003386
x18:x34	Living room Window to Wall Ratio (WWR)	x	inverse of Living room Right Fin size	3,231787	0,012141
x18:x46	Living room Window to Wall Ratio (WWR)	x	inverse of External Walls' Heat Capacity	18605,07	4,26E-08
x18:x47	Living room Window to Wall Ratio (WWR)	x	inverse of Internal Walls' Heat Capacity	12246,53	0,000138
x18:x48	Living room Window to Wall Ratio (WWR)	x	inverse of Roof's Heat Capacity	9196,268	0,000112
x19:x24	External Walls' U-value	x	Roof's Heat Capacity	-0,24571	2,47E-24
x19:x31	External Walls' U-value	x	inverse of Living room Left Fin size	2,500773	2,75E-08
x19:x46	External Walls' U-value	x	inverse of External Walls' Heat Capacity	19191,14	2,69E-83
x19:x47	External Walls' U-value	x	inverse of Internal Walls' Heat Capacity	5209,872	4,44E-18
x19:x48	External Walls' U-value	x	inverse of Roof's Heat Capacity	1689,813	0,000436
x21:x24	Roof's U-Value	x	Roof's Heat Capacity	-1,16593	2,6E-126
x21:x31	Roof's U-Value	x	inverse of Living room Left Fin size	1,126068	0,026995
x21:x46	Roof's U-Value	x	inverse of External Walls' Heat Capacity	16682,36	1,58E-38
x21:x47	Roof's U-Value	x	inverse of Internal Walls' Heat Capacity	12566,95	1E-23
x21:x48	Roof's U-Value	x	inverse of Roof's Heat Capacity	15021,79	1,7E-60
x24:x46	Roof's Heat Capacity	x	inverse of External Walls' Heat Capacity	-62,1312	4,03E-41
x24:x47	Roof's Heat Capacity	x	inverse of Internal Walls' Heat Capacity	-31,2748	2,96E-12
x25:x48	inverse of Bedroom_1 Effective window ventilation area	x	inverse of Roof's Heat Capacity	2753,509	0,006277
x31:x43	inverse of Living room Left Fin size	x	inverse of External Walls' U-value	1,076889	0,003813
x31:x48	inverse of Living room Left Fin size	x	inverse of Roof's Heat Capacity	88,7408	0,000912
x32:x46	inverse of Bedroom_1 Right Fin size	x	inverse of External Walls' Heat Capacity	256,1624	3,93E-05
x34:x48	inverse of Living room Right Fin size	x	inverse of Roof's Heat Capacity	54,14534	0,033488
x43:x46	inverse of External Walls' U-value	x	inverse of External Walls' Heat Capacity	-5646,37	1,44E-08
x46:x47	inverse of External Walls' Heat Capacity	x	inverse of Internal Walls' Heat Capacity	1493300	4,85E-32
x46:x48	inverse of External Walls' Heat Capacity	x	inverse of Roof's Heat Capacity	1628899	1,89E-77
x47:x48	inverse of Internal Walls' Heat Capacity	x	inverse of Roof's Heat Capacity	741422,3	2,46E-20
x4^2	External Walls' Solar Absorptance	x	External Walls' Solar Absorptance	286,135	3,22E-12
x8^2	Bedroom_1 Right Fin size	x	Bedroom_1 Right Fin size	-431,147	0,015436
x9^2	Bedroom_2 Right Fin size	x	Bedroom_2 Right Fin size	-336,007	0,012734
x12^2	Bedroom_2 Overhang size	x	Bedroom_2 Overhang size	326,389	0,01687
x14^2	Roof's Solar Absorptance	x	Roof's Solar Absorptance	1043,219	1,4E-136
x17^2	Bedroom_2 Window to Wall Ratio (WWR)	x	Bedroom_2 Window to Wall Ratio (WWR)	224,3875	0,003441
x18^2	Living room Window to Wall Ratio (WWR)	x	Living room Window to Wall Ratio (WWR)	193,6553	0,011336

x21^2	Roof's U-Value x Roof's U-Value	237,8337	3,07E-72
x24^2	Roof's Heat Capacity x Roof's Heat Capacity	0,002055	9,13E-24
x43^2	inverse of External Walls' U-value x inverse of External Walls' U-value	-33,5901	2,27E-09
x46^2	inverse of External Walls' Heat Capacity x inverse of External Walls' Heat Capacity	-1833500	5,88E-85
x47^2	inverse of Internal Walls' Heat Capacity x inverse of Internal Walls' Heat Capacity	-549903	2,53E-10
x48^2	inverse of Roof's Heat Capacity x inverse of Roof's Heat Capacity	-428602	1,19E-34

